Hoffman Lab Microscopes

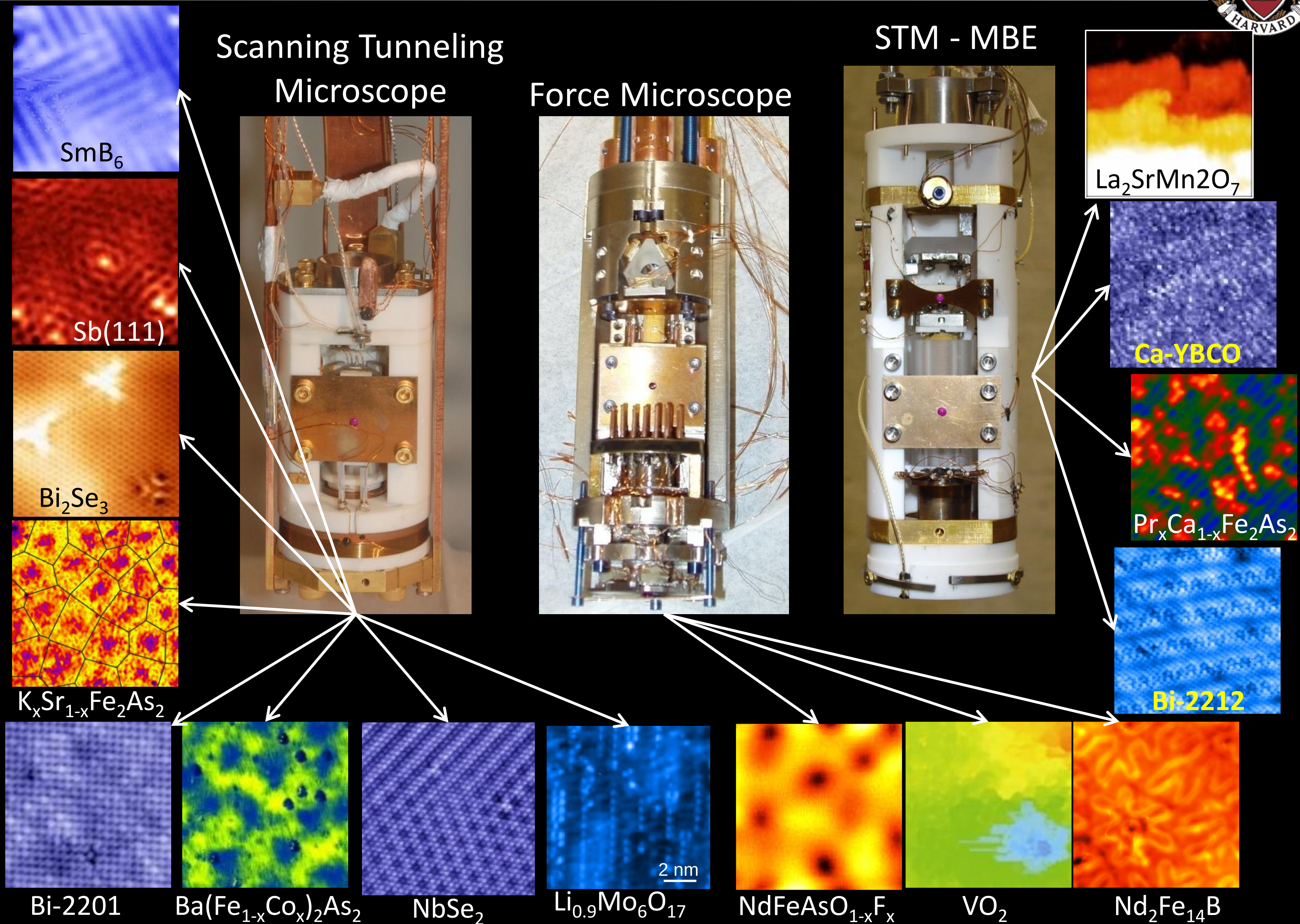

High-T_c Superconductivity

Picoscale atomic distortion

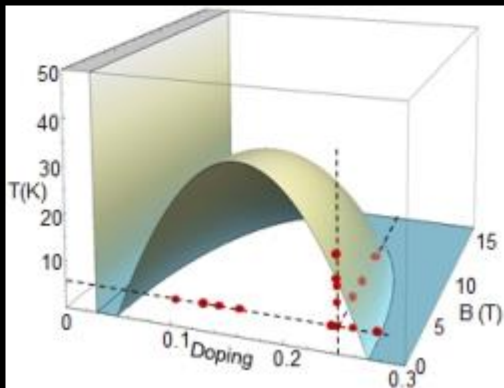

Nature Materials 11, 585 (2012)

Charge ordering

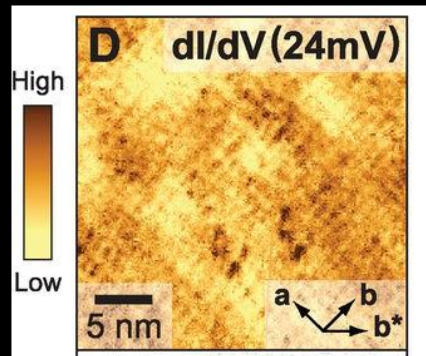

Science 343, 390 (2014)

d-wave charge ordering

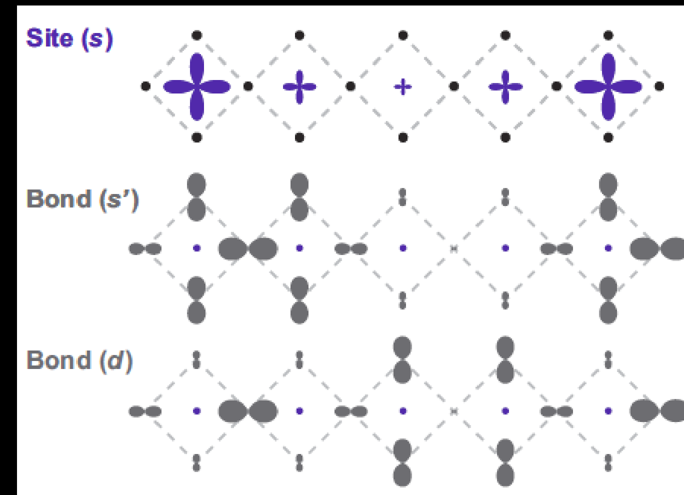

arxiv:1402.5415

Single oxygen atoms

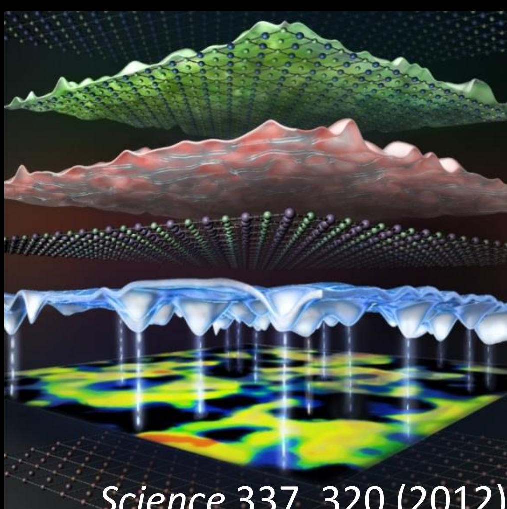

Science 337, 320 (2012)

Fermi surface transition

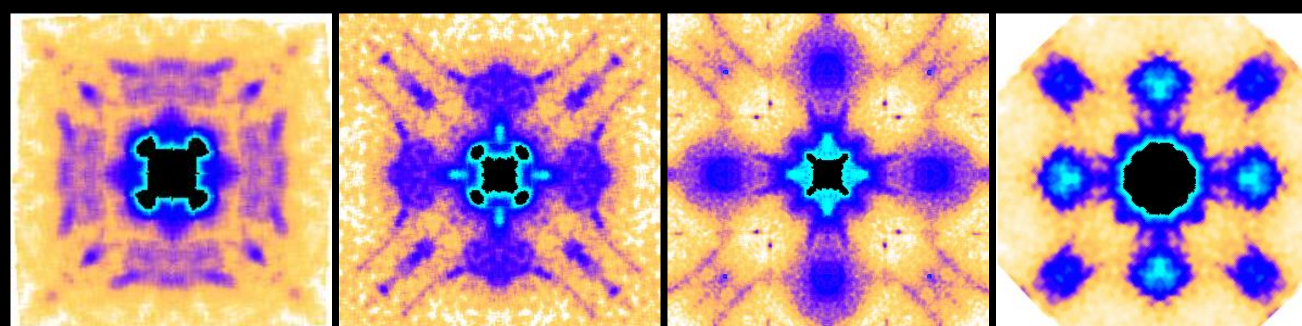

Science 344, 608 (2014)

Scanning Tunneling Microscopy

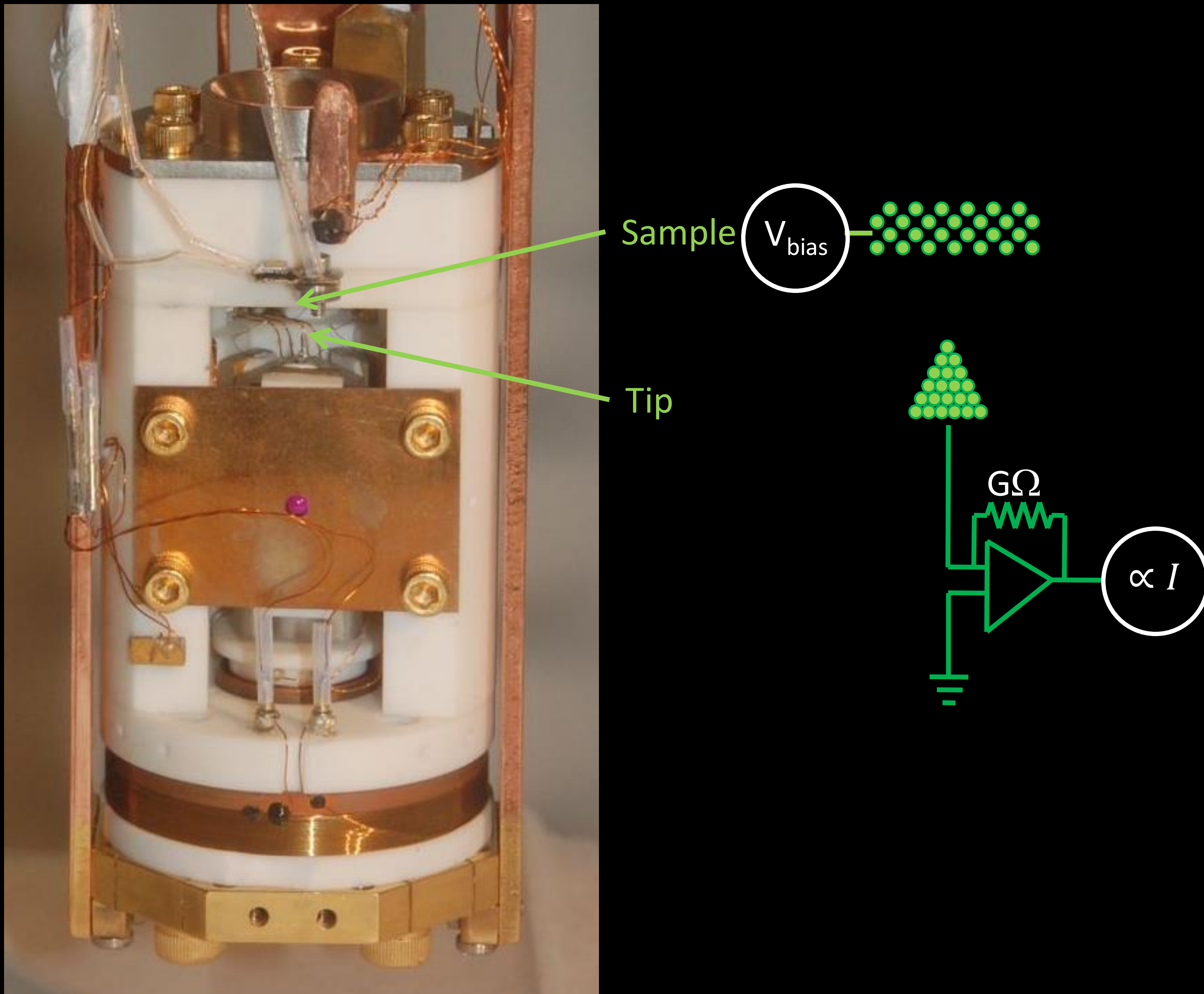

Scanning Tunneling Microscopy

Apply negative voltage to the sample:

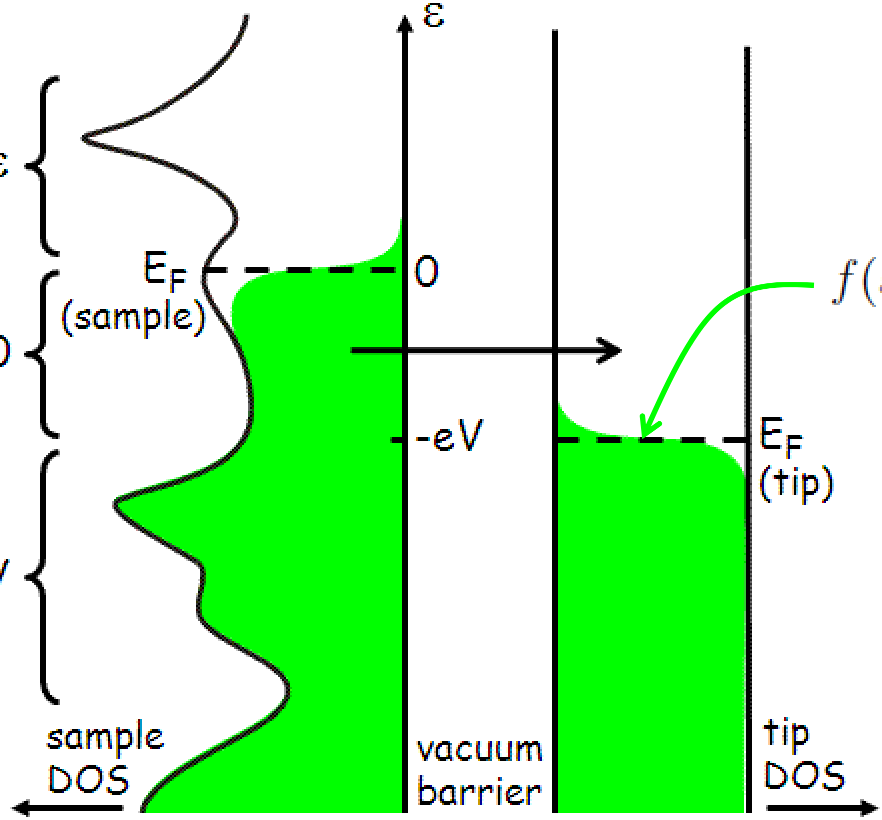

$$f(\varepsilon) = \frac{1}{1 + e^{\varepsilon / k_B T}}$$

$$I_{\text{sample}\rightarrow\text{tip}} = -2e \cdot \frac{2\pi}{\hbar}|M|^2 \underbrace{(\rho_s(\varepsilon) \cdot f(\varepsilon))}_{\substack{\#\text{ filled sample states} \\ \text{for tunneling from}}} \underbrace{(\rho_t(\varepsilon + eV) \cdot [1 - f(\varepsilon + eV)])}_{\substack{\#\text{ empty tip states} \\ \text{for tunneling to}}}$$

$$I = -\frac{4\pi e}{\hbar} \int_{-\varepsilon_F(\text{tip})}^{\infty} |M|^2 \rho_s(\varepsilon)\rho_t(\varepsilon + eV) \{ f(\varepsilon) [1 - f(\varepsilon + eV)] - [1 - f(\varepsilon)] f(\varepsilon + eV) \} d\varepsilon$$

Scanning Tunneling Microscopy

Apply negative voltage to the sample:

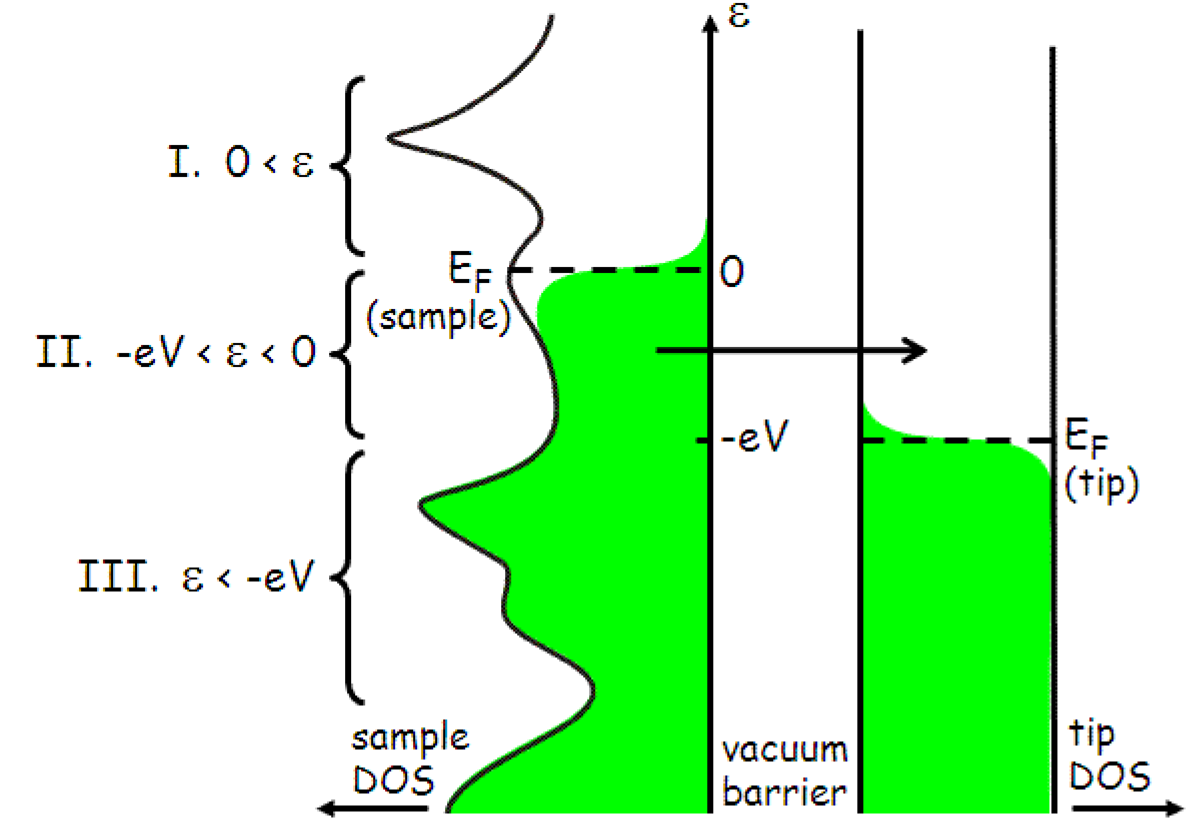

Assume T ~ 0

$$I \approx -\frac{4\pi e}{\hbar}\int_{-eV}^{0}|M|^2\rho_s(\varepsilon)\rho_t(\varepsilon+eV)d\varepsilon$$

Assume tip DOS is flat

$$I \approx \frac{4\pi e}{\hbar}\rho_t(0)\int_{-eV}^{0}|M|^2\rho_s(\varepsilon)d\varepsilon$$

But what is $|M|^2$?

Scanning Tunneling Microscopy

Apply negative voltage to the sample:

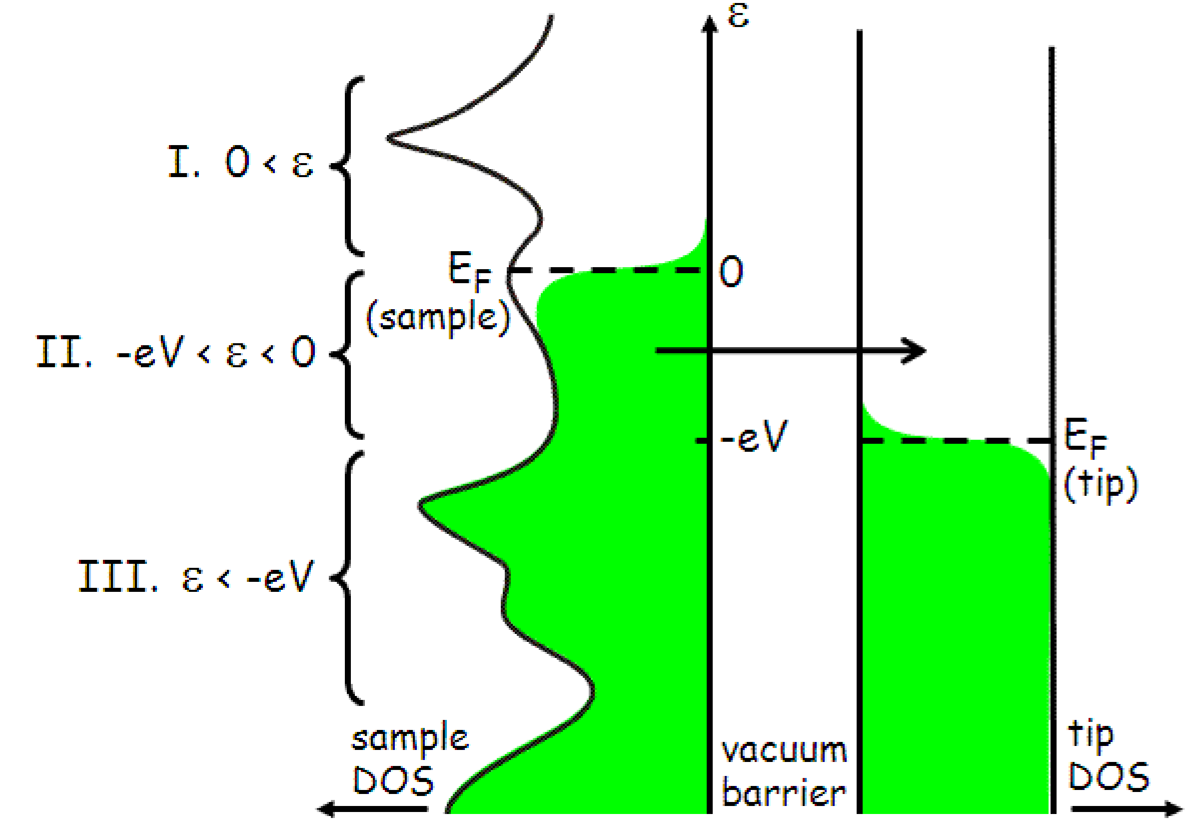

WKB says that the tunneling probability through a barrier will be $|M|^2 = e^{-2\gamma}$ where:

$$\gamma = \int_0^s \sqrt{\frac{2m\varphi}{\hbar^2}}dx = \frac{s}{\hbar}\sqrt{2m\varphi} \longrightarrow I \approx \frac{4\pi e}{\hbar} e^{-\frac{1}{s}\sqrt{\frac{8m\varphi}{\hbar^2}}} \rho_t(0) \int_{-eV}^{0} \rho_s(\varepsilon) d\varepsilon$$

s = tip-sample distance
φ = tip-sample work function

Details: Tersoff & Hamman, PRL 50, 1988 (1983) & PRB 31, 805 (1985)

STM: setup condition

$$I_{set} = e^{-z(\vec{r})/z_0} \int_0^{eV_{set}} N(\vec{r},\varepsilon)\,d\varepsilon$$

This eqn fixes $z(\vec{r})$

$$I(\vec{r},V) = \underbrace{e^{-z_{set}(\vec{r})/z_0}}_{\dfrac{I_{set}}{\int_0^{eV_{set}} N(\vec{r},\varepsilon)\,d\varepsilon}} \int_0^{eV} N(\vec{r},\varepsilon)\,d\varepsilon$$

$$\frac{dI}{dV}(\vec{r},\varepsilon) = \frac{e I_{set}}{\int_0^{eV_{set}} N(\vec{r},\varepsilon)\,d\varepsilon} \underbrace{N(\vec{r},\varepsilon)}$$

← this is the raw DOS that we want

→ Define:

$$Z(\vec{r},\varepsilon) = \frac{N(\vec{r},+\varepsilon)}{N(\vec{r},-\varepsilon)}$$

Z-maps

Theory:

$$Z(V) \equiv \frac{\overline{N}(E=+eV)}{\overline{N}(E=-eV)} \approx \frac{2n}{1+n}$$

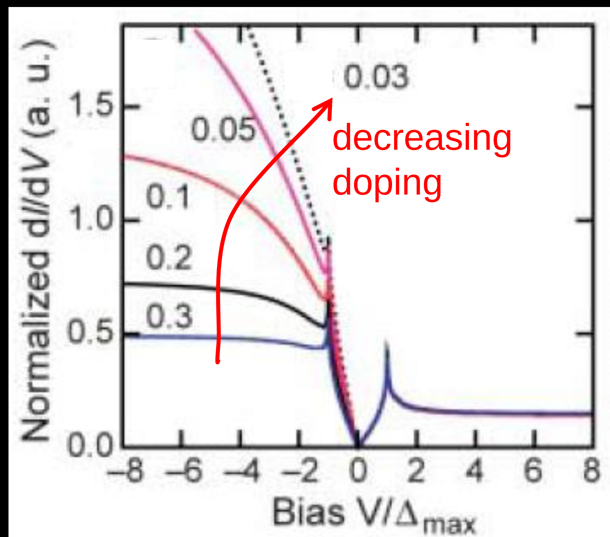

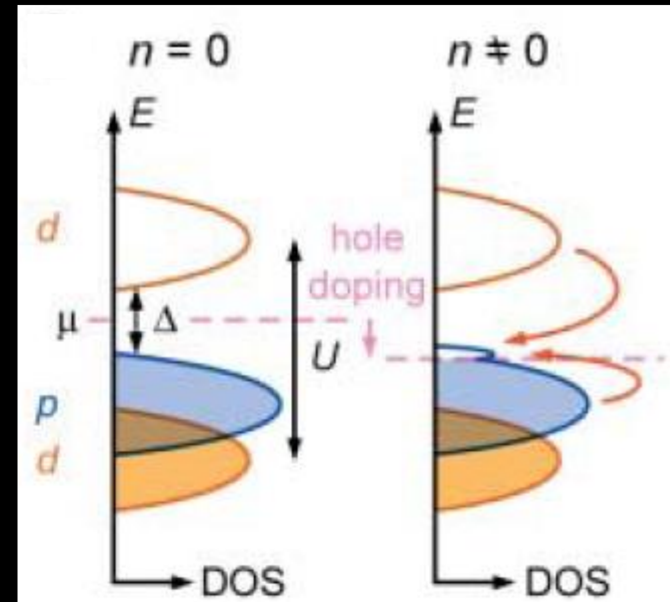

P. W. Anderson, N. P. Ong, *J. Phys. Chem. Solids* **67**, 1 (2006).

Experiment:

$$Z(\vec{r},V) \equiv \frac{\frac{\mathrm{d}I}{\mathrm{d}V}(\vec{r},z,+V)}{\frac{\mathrm{d}I}{\mathrm{d}V}(\vec{r},z,-V)}$$

R-maps

Theory:

$$R(\vec{r}) \equiv \frac{\int_0^{\Omega_c} N(\vec{r},E)\ \mathrm{d}E}{\int_{-\infty}^{0} N(\vec{r},E)\mathrm{d}E} = \frac{2n(\vec{r})}{1-n(\vec{r})} + O\left(\frac{nt}{U}\right)$$

($\Omega_c \sim 1$ eV)

10%

Randeria, *PRL* **95**, 137001 (2005).

Experiment:

$$R(\vec{r}, V) \equiv \frac{I(\vec{r}, z, +V)}{I(\vec{r}, z, -V)}$$

(V = 150 mV)

Z vs. R maps

	Z	R
Theory:	$\frac{\overline{N}(E=+eV)}{\overline{N}(E=-eV)} \approx \frac{2n}{1+n}$ Anderson, *JPCM* (2006)	$\frac{\int_0^{\Omega_c} N(\vec{r},E)\ \mathrm{d}E}{\int_{-\infty}^{0} N(\vec{r},E)\mathrm{d}E} = \frac{2n(\vec{r})}{1-n(\vec{r})}$ Randeria, *PRL* (2005)
Experiment:	$Z(\vec{r},V) \equiv \frac{\frac{\mathrm{d}I}{\mathrm{d}V}(\vec{r},z,+V)}{\frac{\mathrm{d}I}{\mathrm{d}V}(\vec{r},z,-V)}$	$\frac{I(\vec{r},z,+V)}{I(\vec{r},z,-V)}$
Advantages:	<u>Divides out the setup condition artifact!</u>	
	Maintain energy resolution	Integrate over all energies, integrates a small signal, catches a signal at unknown energy.
Disadvantages:	<u>Assumes particle-hole symmetry of the signal of interest!</u>	
		Lose energy resolution. What cutoff to use? Theory: Ω_c ~ 1 eV; Expt: V = 150 mV
In practice:	QPI	static checkerboards

Types of STM Measurements

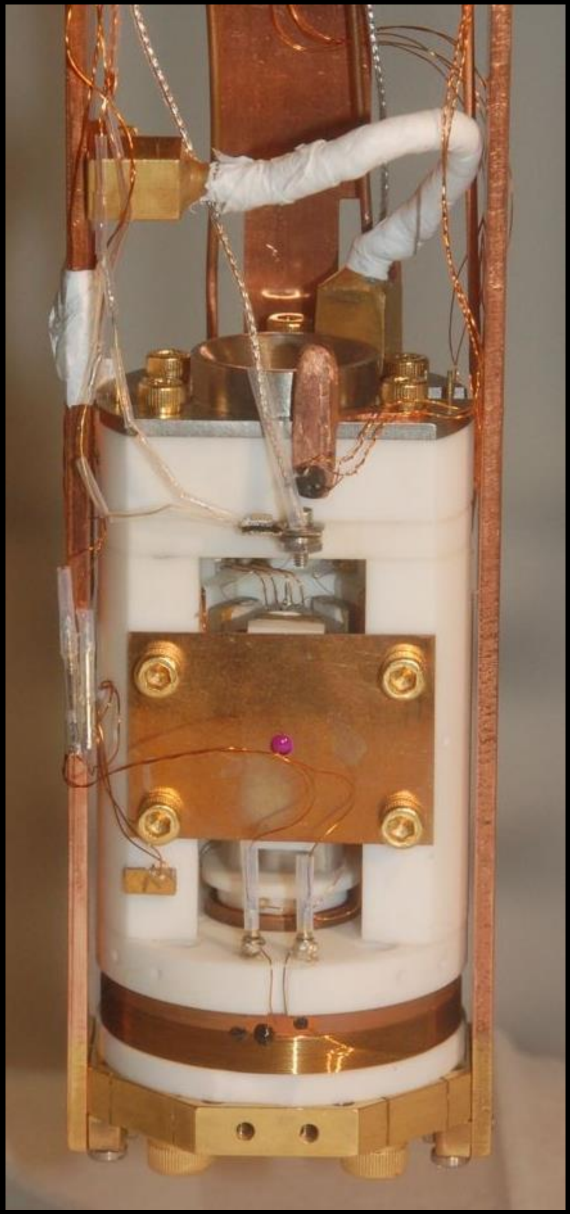

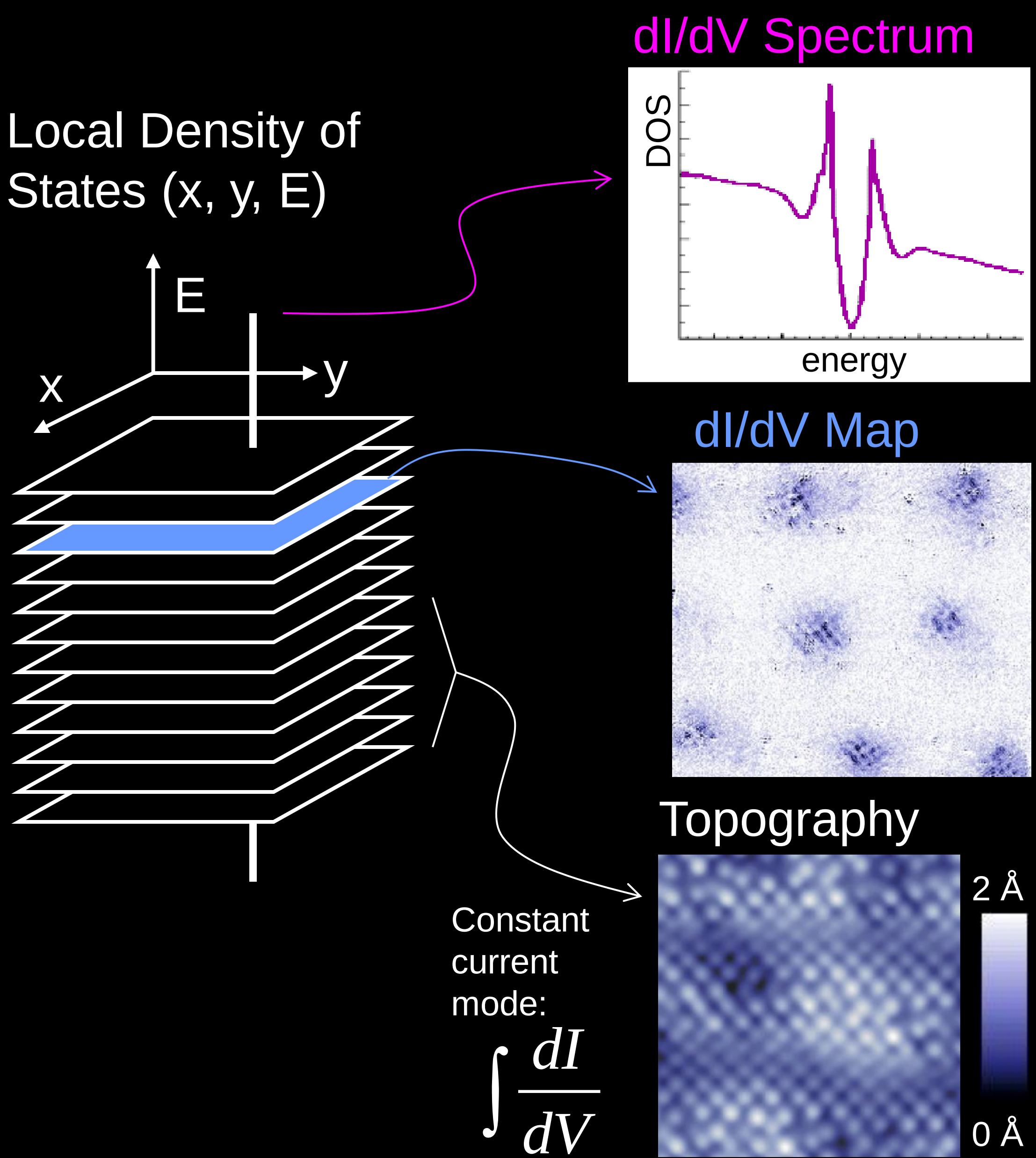

STM: pros & cons

Advantages

- Filled and empty states
- sub-meV energy resolution
- B-field dependence
- Atomic spatial resolution
- k-information w/ nanoscale resolution (via QPI)

Challenges

- Surface sensitivity
- polarity, termination, reconstruction
- vibration sensitivity

Superconductivity Tunneling Milestones

1960: gap measurement (Pb)

1965: boson energies & coupling (Pb)

1985: charge density wave ($TaSe_2$)

1989: vortex lattice ($NbSe_2$)

1997: single atom impurities (Nb)

2002: quasiparticle interference
→ band structure & gap symmetry (BSCCO)

2009: phase-sensitive gap measurement (Na-CCOC)

2010: intra-unit-cell structure (BSCCO)

Superconductivity Tunneling Milestones

1960: gap measurement (Pb)

1965: boson energies & coupling (Pb)

1985: charge density wave ($TaSe_2$)

1989: vortex lattice ($NbSe_2$)

1997: single atom impurities (Nb)

2002: quasiparticle interference

→ band structure & gap symmetry (BSCCO)

2009: phase-sensitive gap measurement (Na-CCOC)

2010: intra-unit-cell structure (BSCCO)

1960: Tunneling measurements of Δ

VOLUME 5, NUMBER 4 PHYSICAL REVIEW LETTERS AUGUST 15, 1960

ENERGY GAP IN SUPERCONDUCTORS MEASURED BY ELECTRON TUNNELING

Ivar Giaever
General Electric Research Laboratory, Schenectady, New York
(Received July 5, 1960)

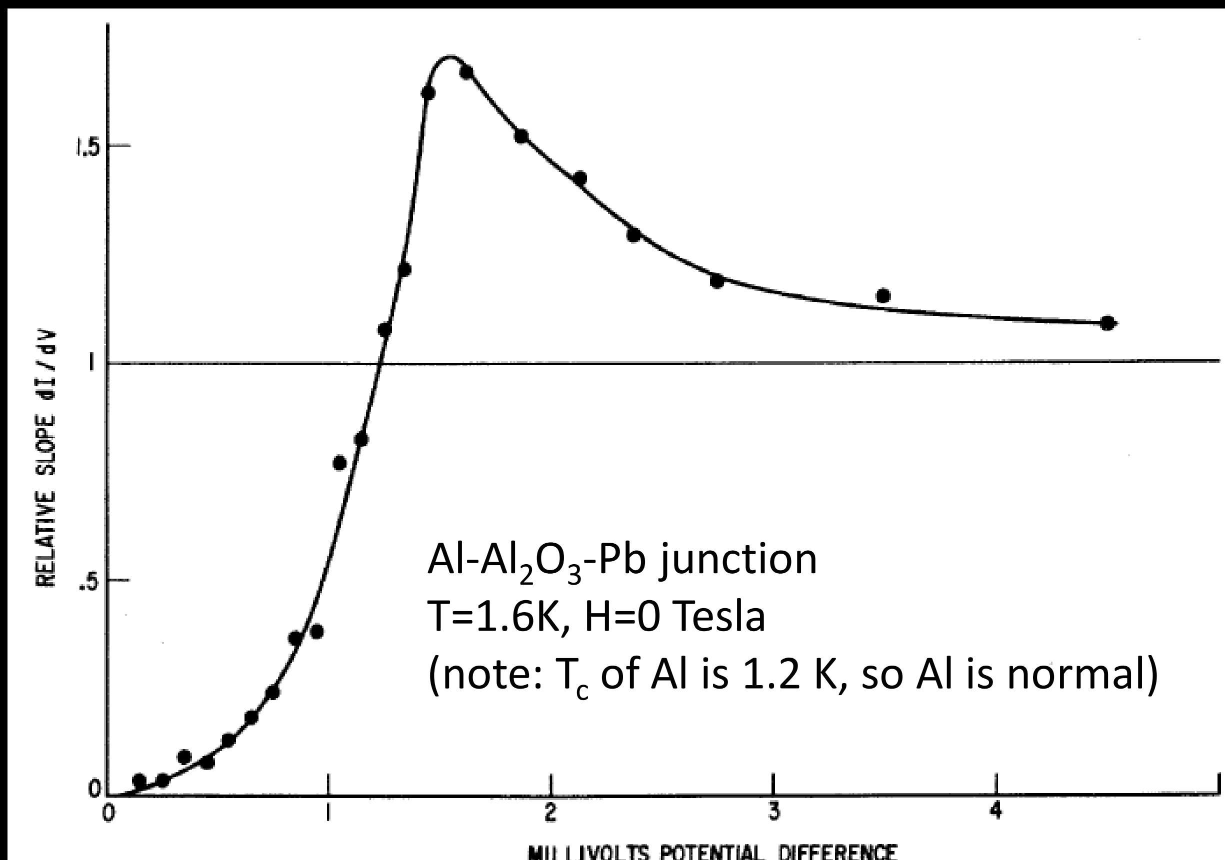

Giaever, PRL 5, 174 (1960)

Structure of $Bi_2Sr_2CaCu_2O_{8+\delta}$

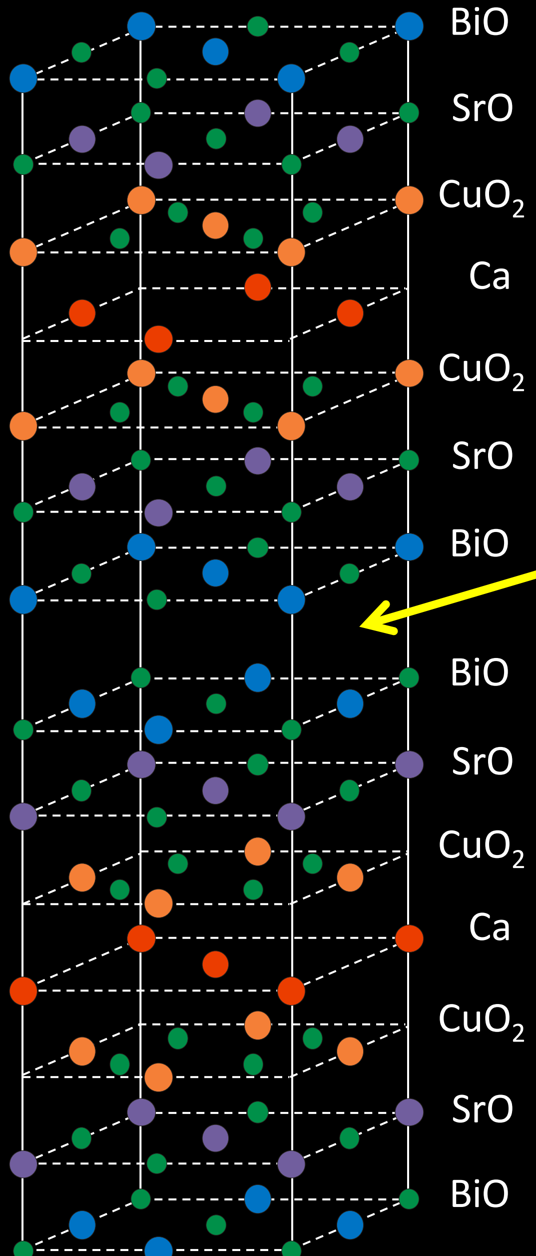

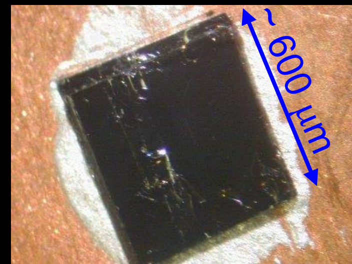

Cleave Here
Reveals
BiO Surface

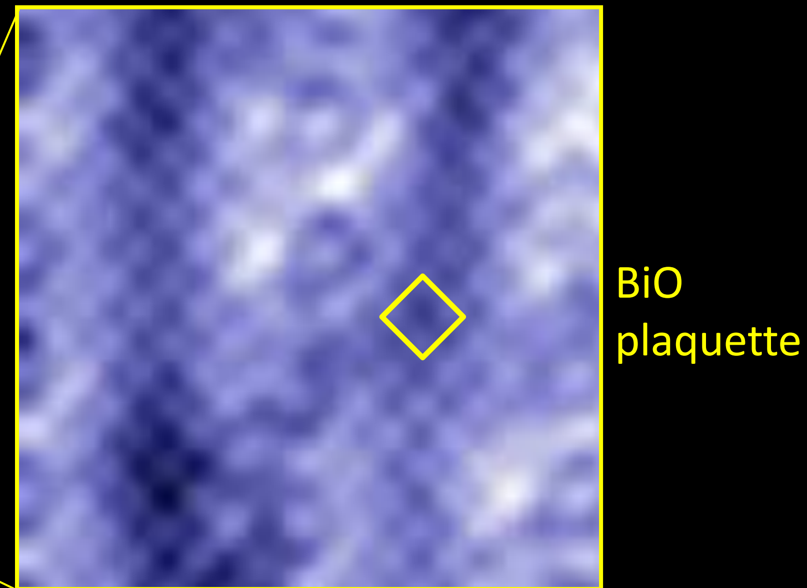

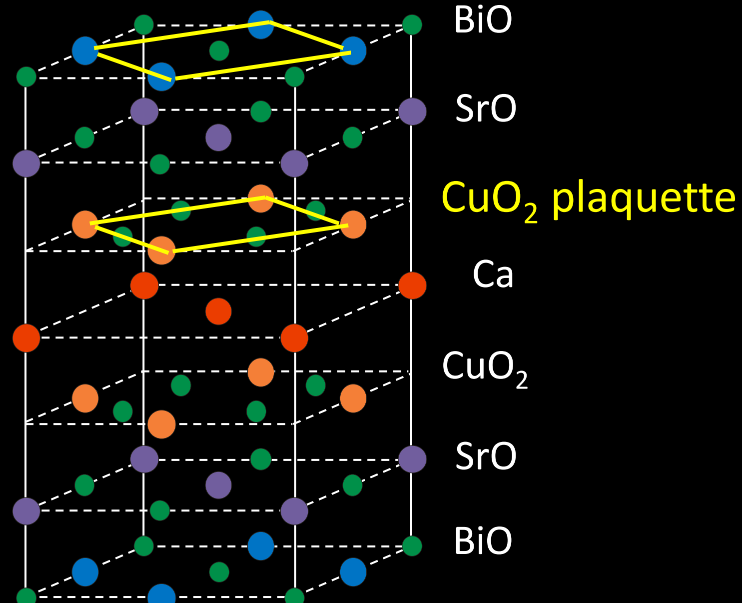

Δ inhomogeneity in BSCCO

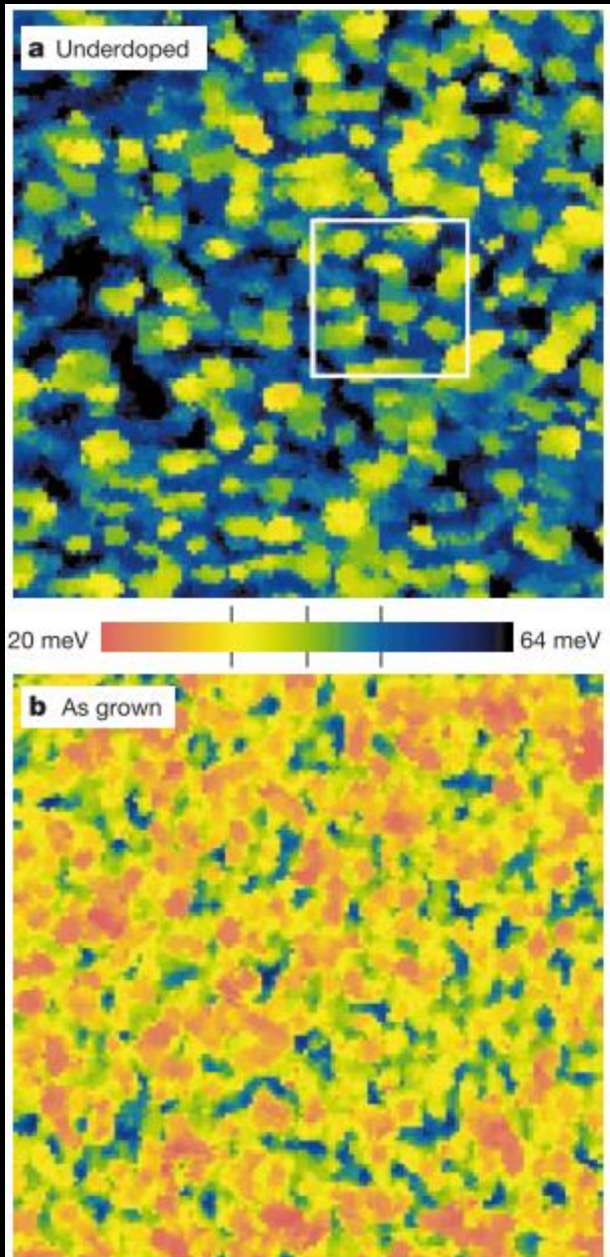

← Δ

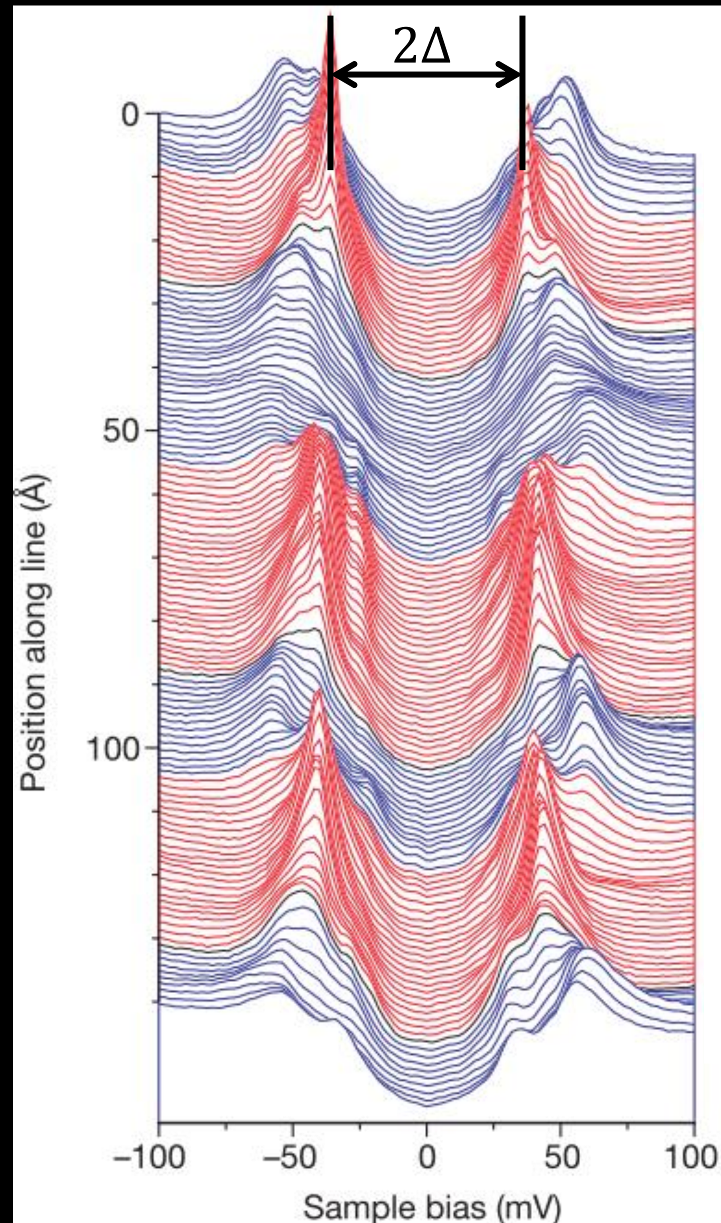

Lang, Nature 415, 412 (2002)

Suggests the existence of a local “hidden” variable we could use to control Δ? (and raise Tc?)

Δ inhomogeneity in BSCCO

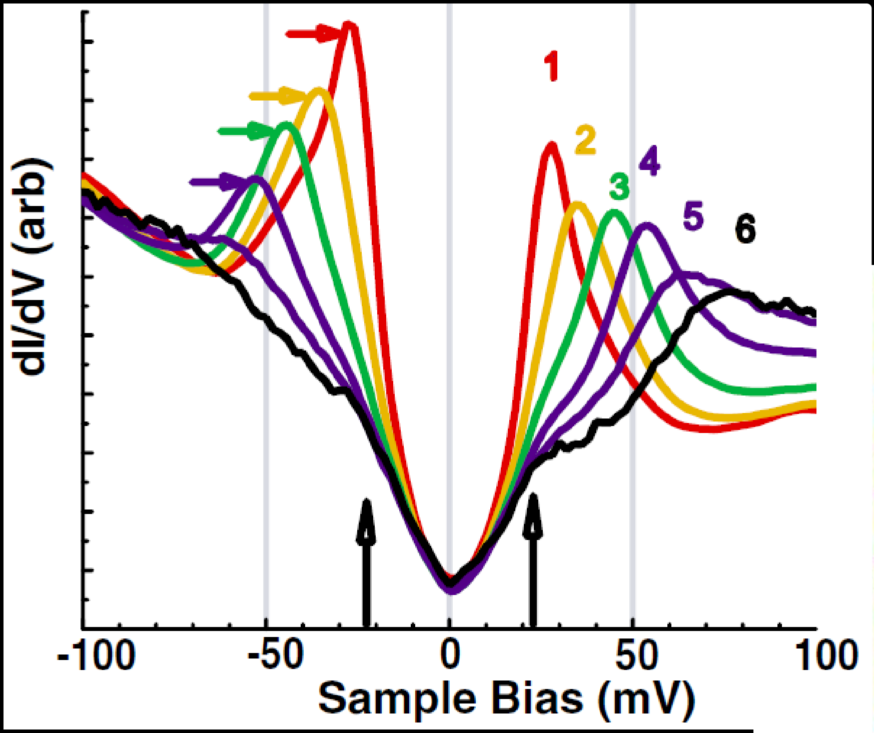

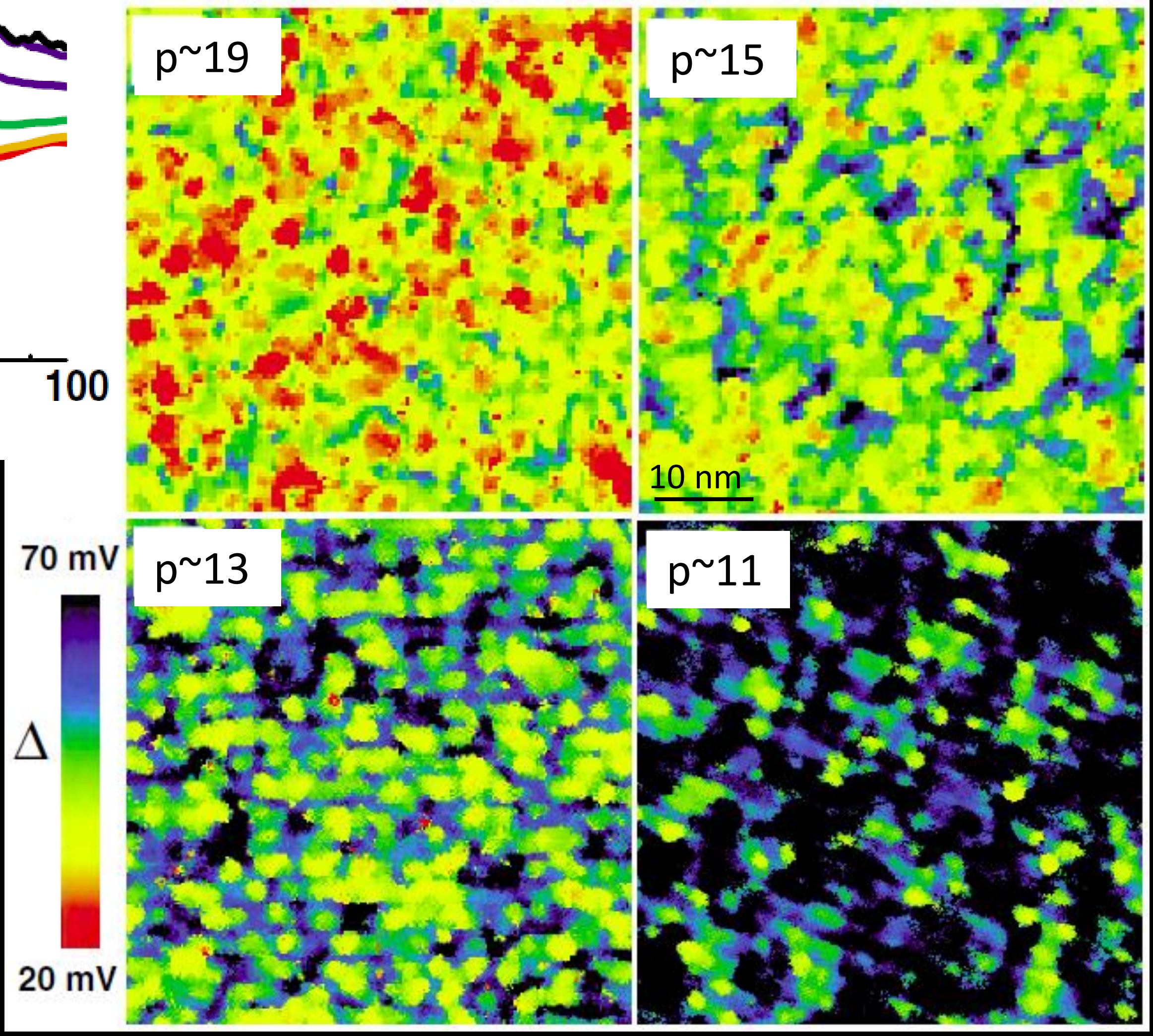

McElroy, PRL 94, 197005 (2005)

Inhomogeneity of T(Δ closure) in BSCCO

Tc=65K (overdoped)

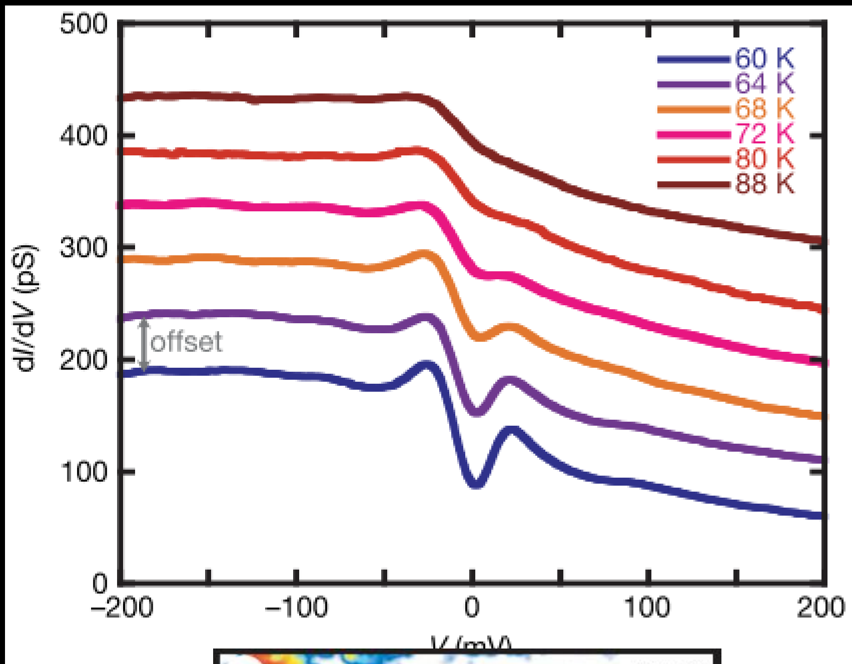

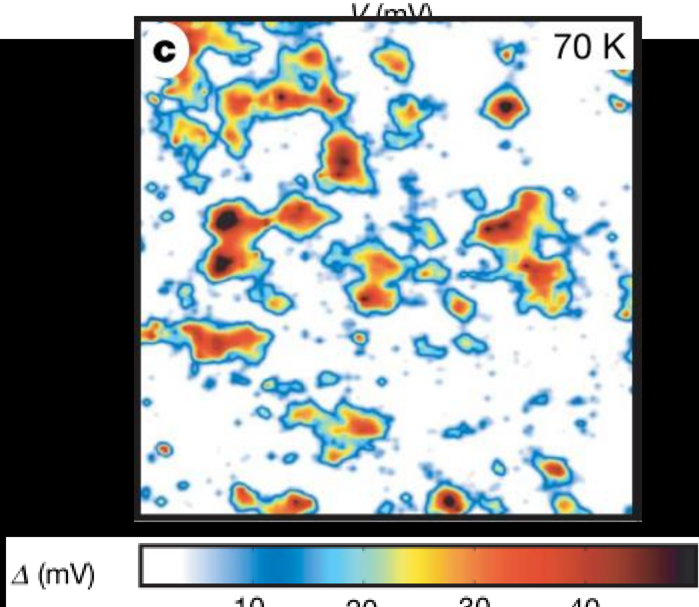

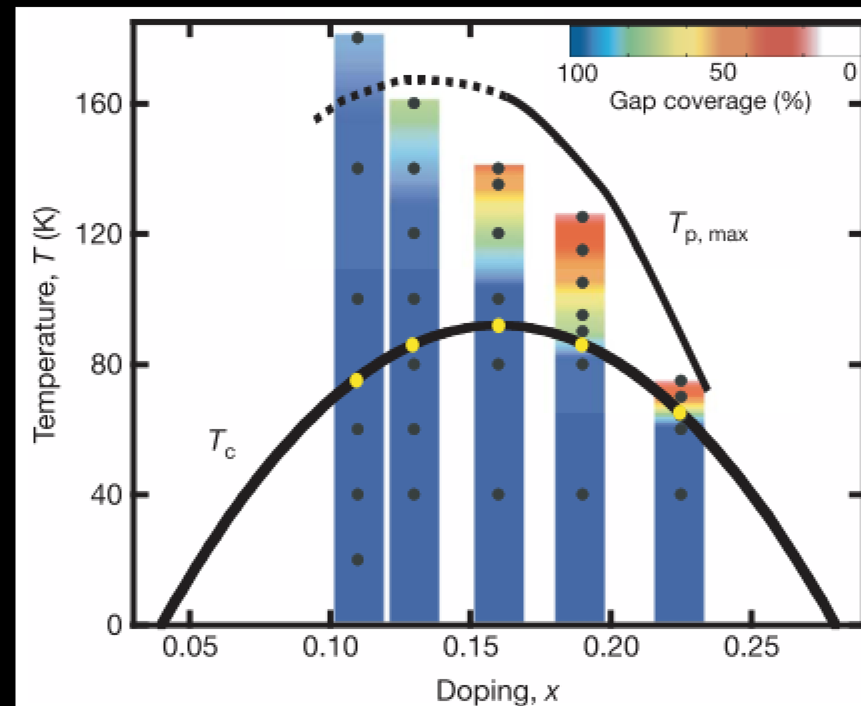

Gomes, Nature 447, 569 (2007)

Are oxygen dopants causing inhomogeneity?

Conclusions about interstitial oxygen:

(1) Observed at -0.96 V in dI/dV

(2) “Strong correlations” exist between these oxygen dopants and “the gap”

(3) These oxygen dopants are primarily positioned in the minima of the “QPI”

dI/dV at -1V

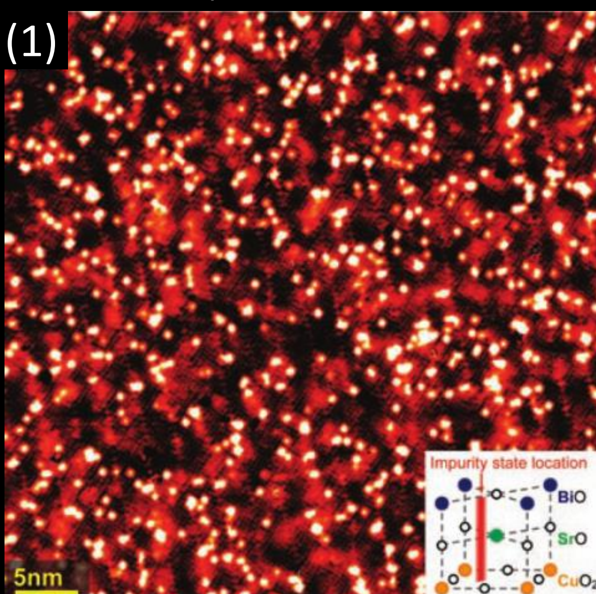

0.4 nS 0.7 nS

gapmap

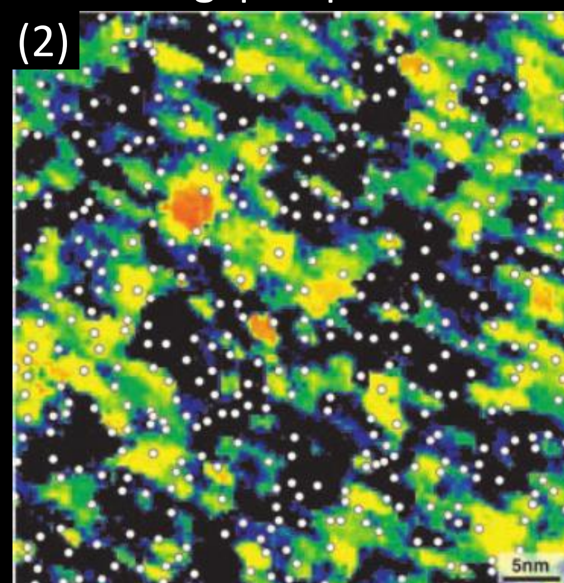

20 meV 70 meV

dI/dV at -24 mV

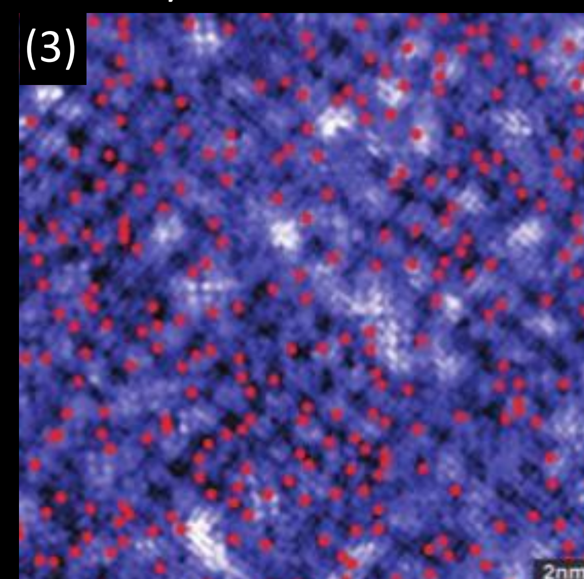

McElroy, Science 309, 1048 (2005)

Puzzle: local trend opposes global trend

$\bar{\Delta}$ = 65 meV; N=455 | $\bar{\Delta}$ = 55 meV; N=580 | $\bar{\Delta}$ = 45 meV; N=883

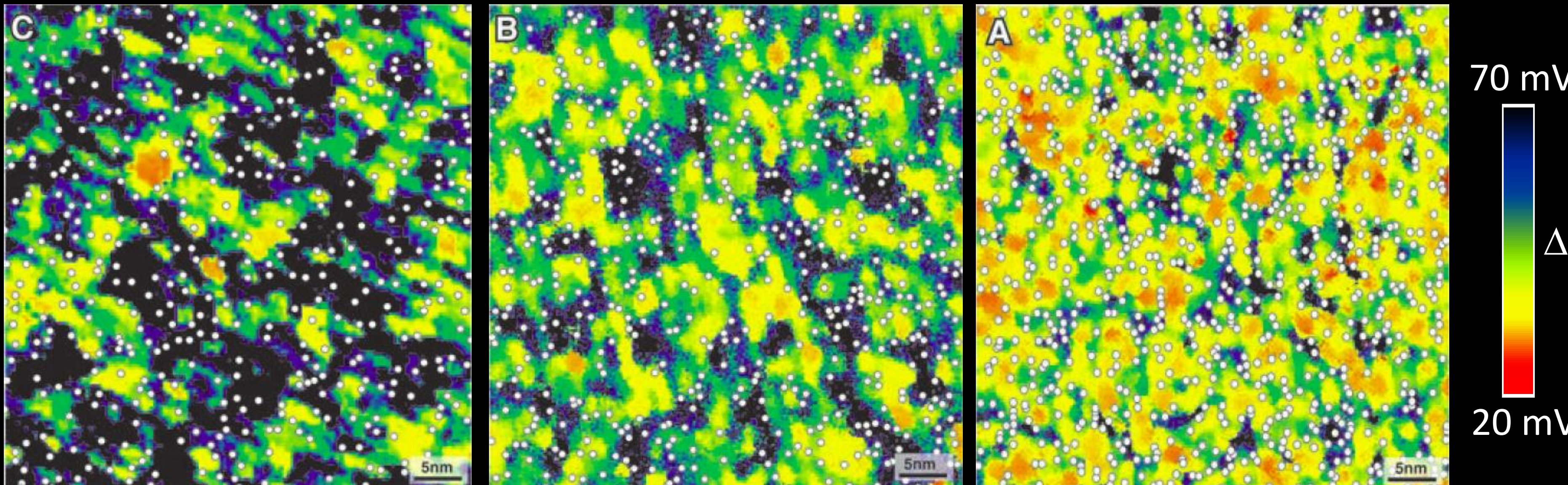

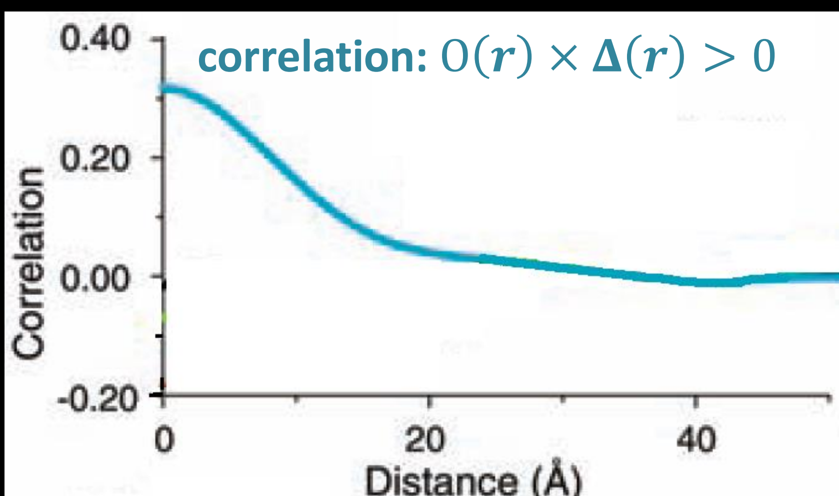

McElroy, Science 309, 1048 (2005)

→ Assumption: oxygen dopants ***cause*** local regions of large Δ

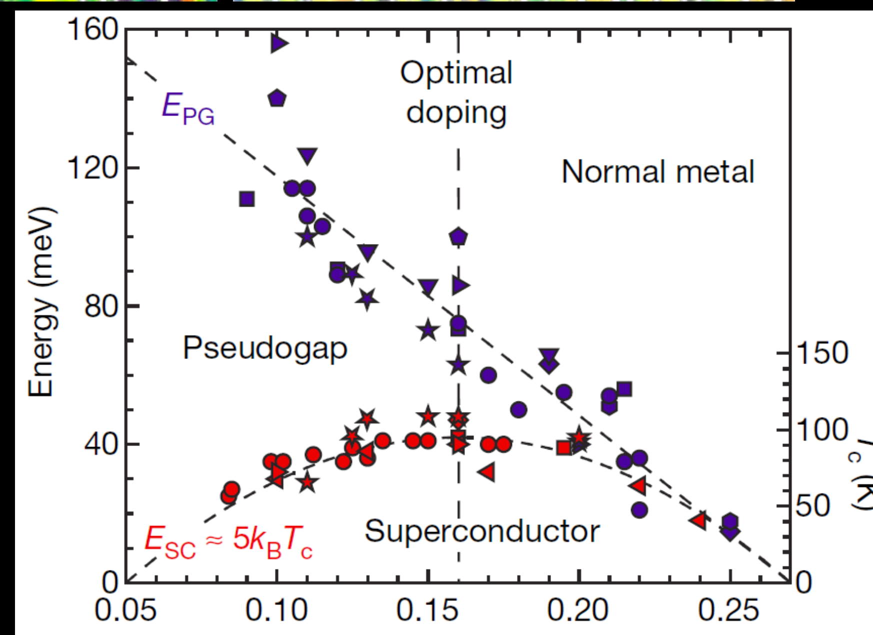

Hufner, ROPP

Zhou prediction: type-A oxygen

B-site disorder:
(e.g. Pb^{2+} on Bi^{3+} site
or Y^{3+} on Ca^{2+} site)
does not couple to CuO_2

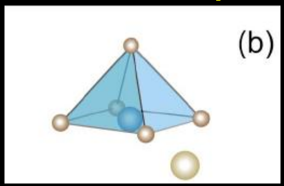

Eisaki, PRB 69, 064512 (2004)

interstitial O in BiO plane
weakly couples to CuO_2
provides charge carriers
but little local effect
→ “type-B oxygen”

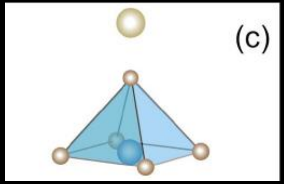

seen at -0.96V
McElroy, Science 309, 1048 (2005)

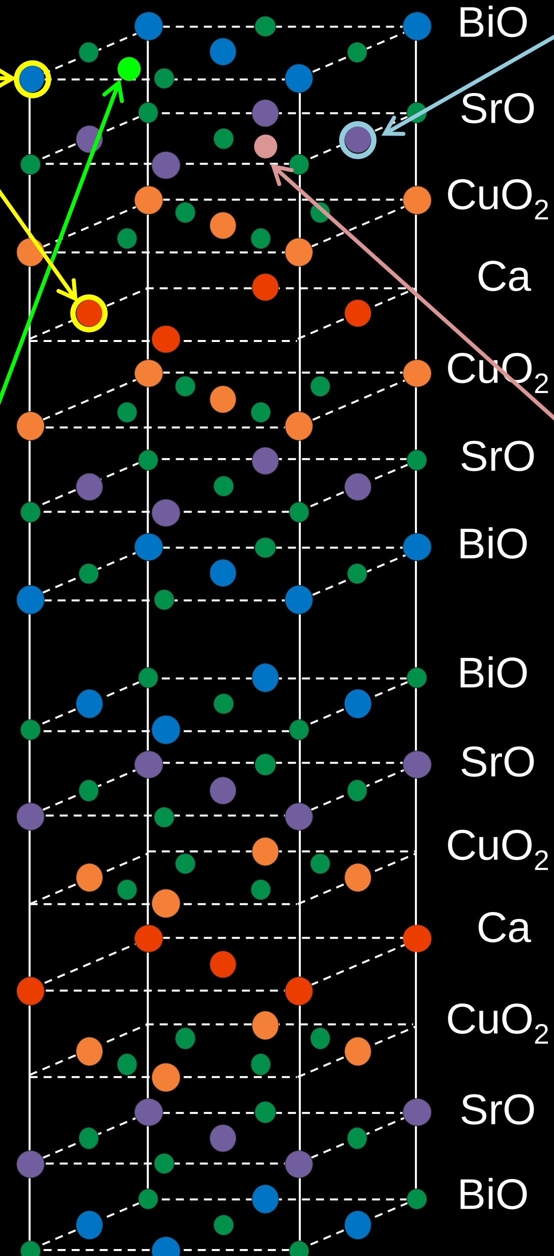

A-site disorder:
(Bi^{3+} on Sr^{2+} site)
strongly couples to apical O

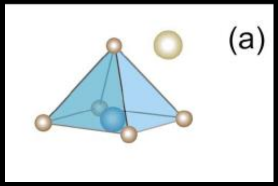

claim: seen at +1.8V
Kinoda, PRB 67, 224509 (2003)

interstitial O in SrO plane
strongly couples to CuO_2
provides charge carriers
and disorder
→ “type-A oxygen”

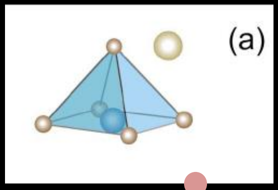

Zhou, PRL 98, 076401 (2007)

expected << -1V

Mapping additional dopants (T_c=55K)

-1.5V, type-A Oxygen | -1V, type-B Oxygen | +1V, unknown ???

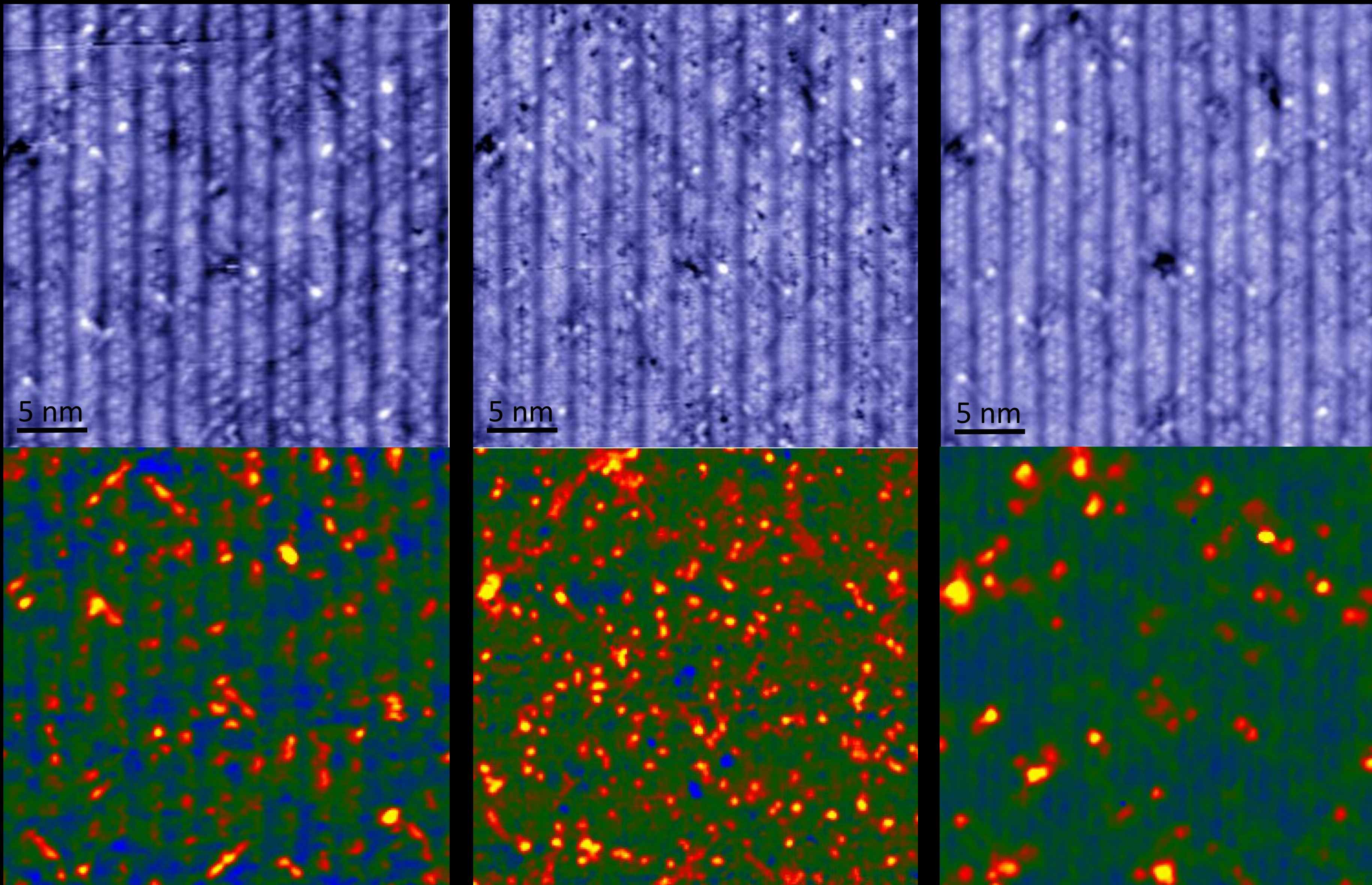

Zelkjovic + JEH, Science (2012)

Spectral signatures (T_c=82K)

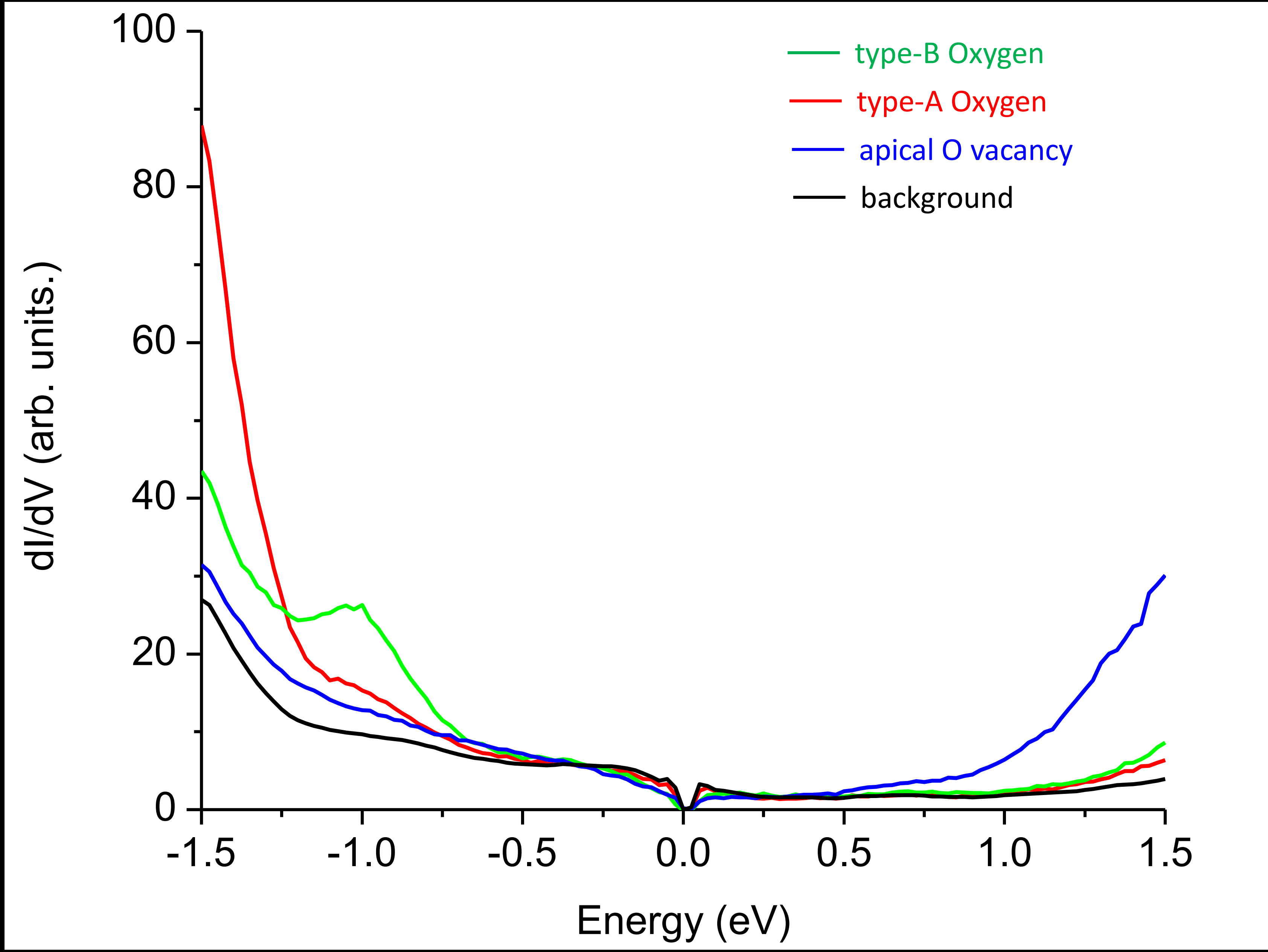

Zelkjovic + JEH, Science (2012)

Tc = 55K

● O, type-B

expect $O_B(r) \times \Delta(r) > 0$
(correlation)

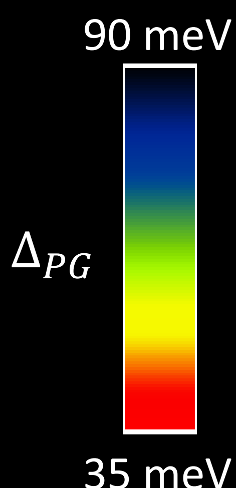

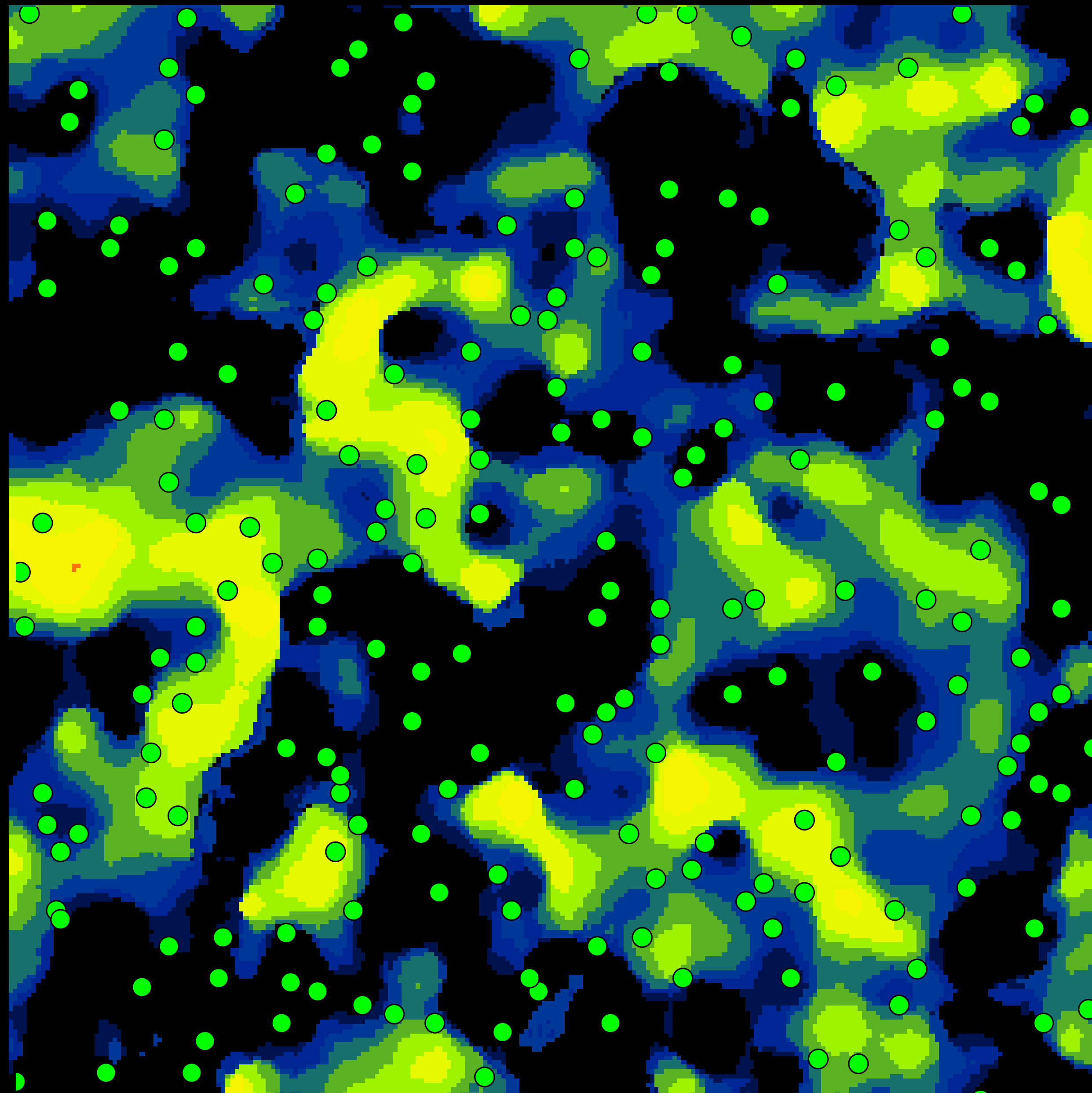

29 x 29 nm^2

Tc = 55K

- O, type-A

expect $O_A(r) \times \Delta(r) < 0$
(causality)

→ NOT OBSERVED

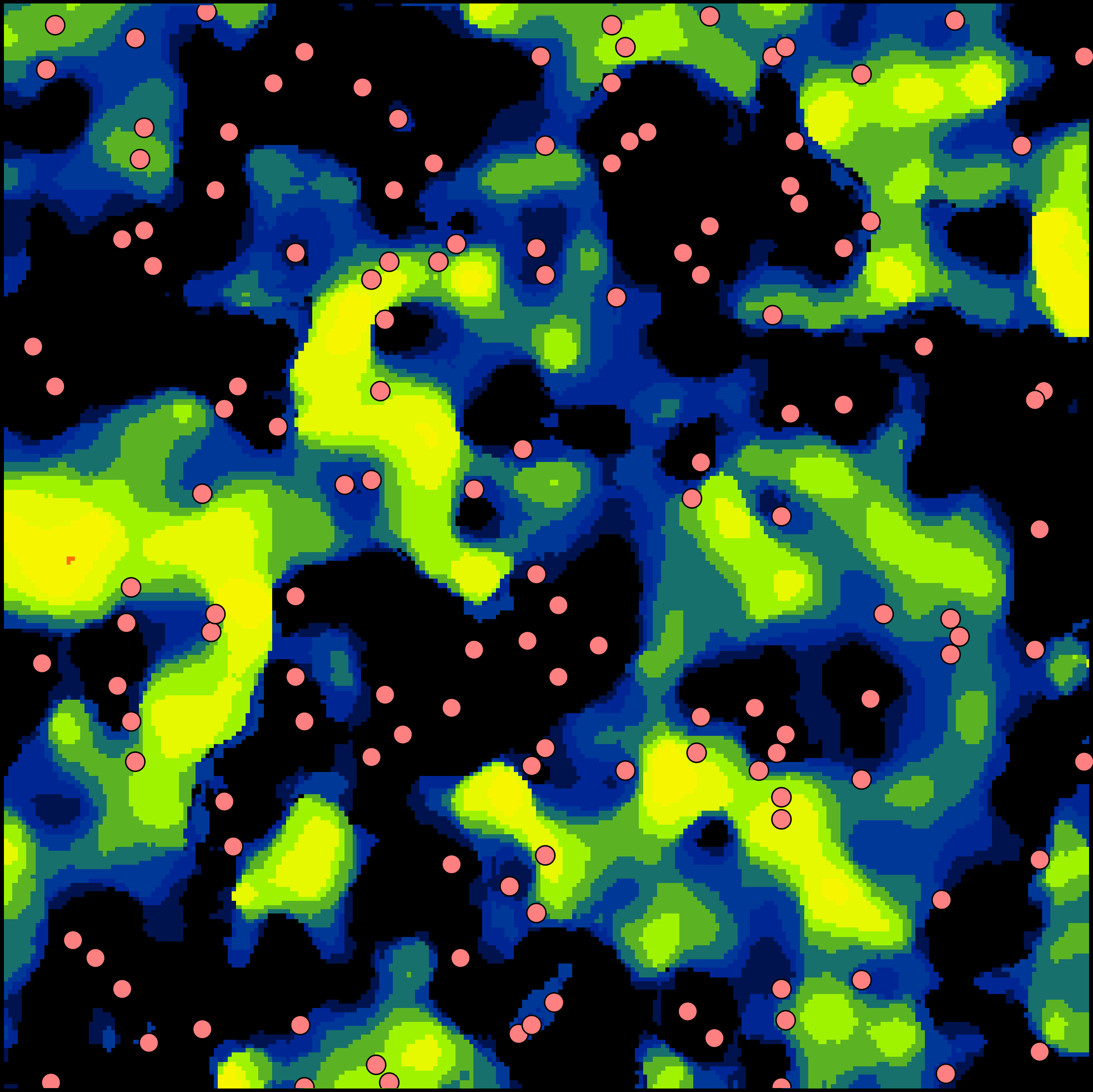

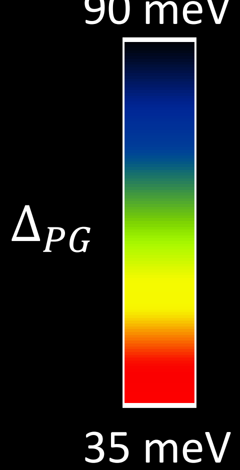

29 x 29 nm^2

Tc = 55K

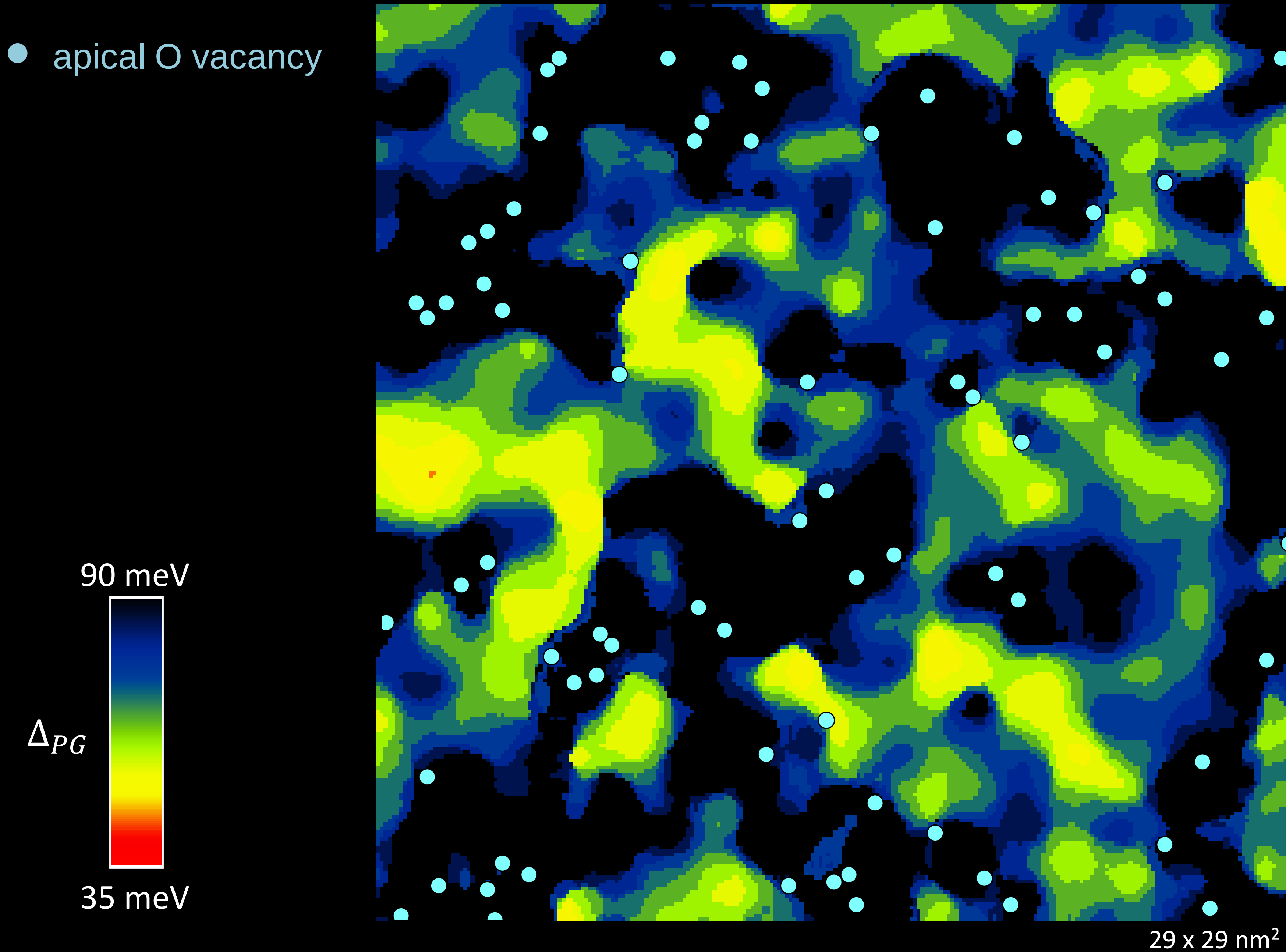

Resolved! local vs. global dependence

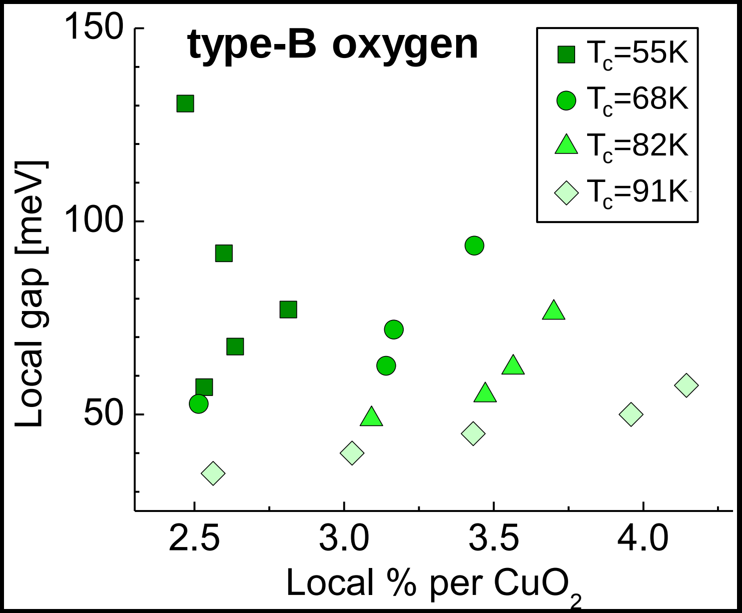

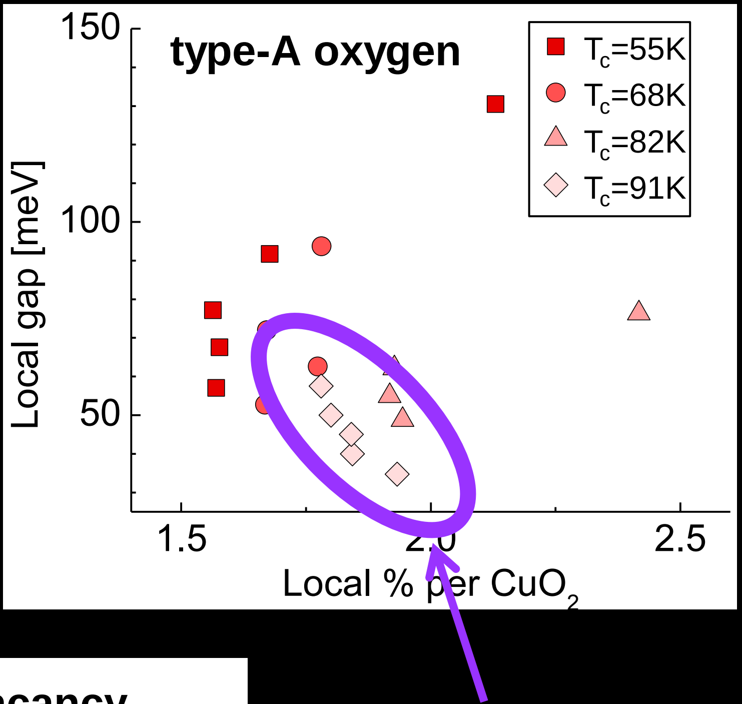

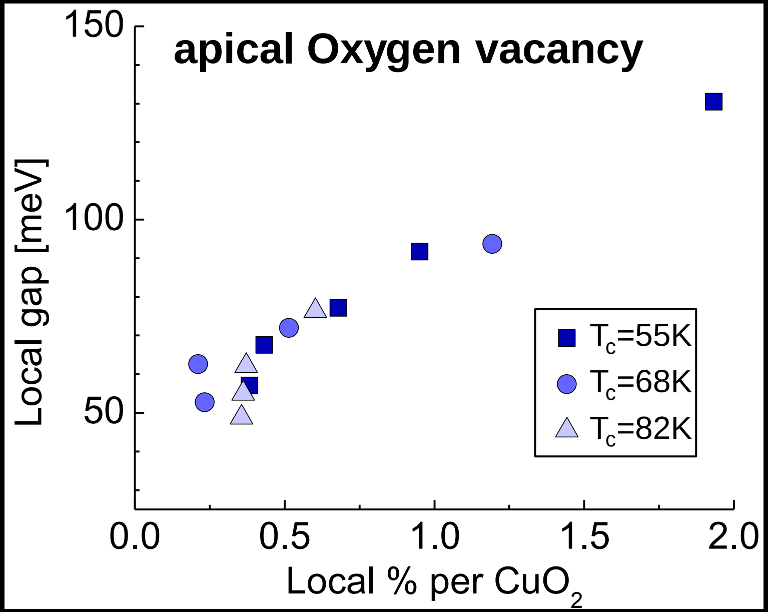

Optimal doping:
no apical O vacancies

→ local charge controlled by type-A interstitial O

Zelkjovic + JEH, Science (2012)

Part I: Conclusions

- Doubled the energy range for local spectroscopy on BSCCO
- Found all oxygen dopants: type-A & B oxygen, apical O vacancies

- apical O vacancies
  - strongly enhance the gap energy
  -

* type-A oxygens
  - attracted to apical O vacancies in UD
  - control local charge in OPT

- type-B oxygens
  - weakly correlate, secondary effect

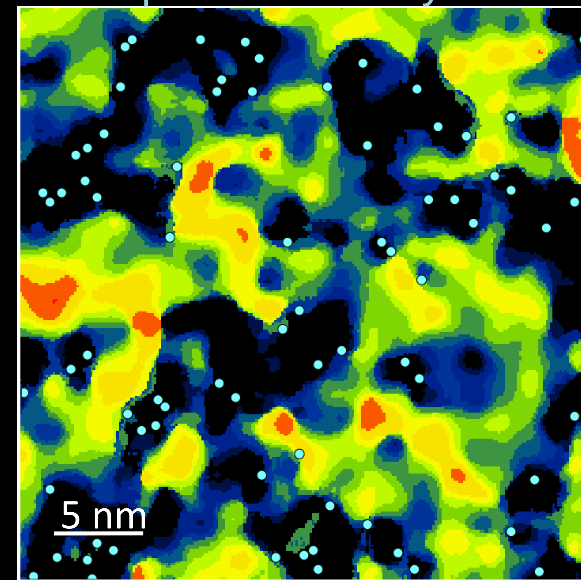

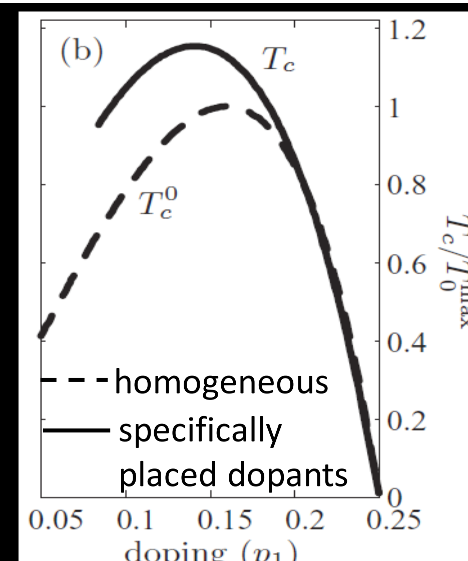

Next steps:

- control dopants to raise T_c ??
- fit to find effective charge & radius of dopants
- understand how dopants affect CDW

Theory: *Goren, Altman, PRB 84, 094508 (2011)*

Superconductivity Tunneling Milestones

1960: gap measurement (Pb)

1965: boson energies & coupling (Pb)

1985: charge density wave ($TaSe_2$)

1989: vortex lattice ($NbSe_2$)

1997: single atom impurities (Nb)

2002: quasiparticle interference
→ band structure & gap symmetry (BSCCO)

2009: phase-sensitive gap measurement (Na-CCOC)

2010: intra-unit-cell structure (BSCCO)

ARPES: first evidence of gap anisotropy

VOLUME 70, NUMBER 10 PHYSICAL REVIEW LETTERS 8 MARCH 1993

Anomalously Large Gap Anisotropy in the *a*-*b* Plane of $Bi_2Sr_2CaCu_2O_{8+\delta}$

Z.-X. Shen,[(1),(2)] D. S. Dessau,[(1),(2)] B. O. Wells,[(1),(2),(a)] D. M. King,[(2)] W. E. Spicer,[(2)] A. J. Arko,[(3)] D. Marshall,[(2)] L. W. Lombardo,[(1)] A. Kapitulnik,[(1)] P. Dickinson,[(1)] S. Doniach,[(1)] J. DiCarlo,[(1),(2)] A. G. Loeser,[(1),(2)] and C. H. Park[(1),(2)]

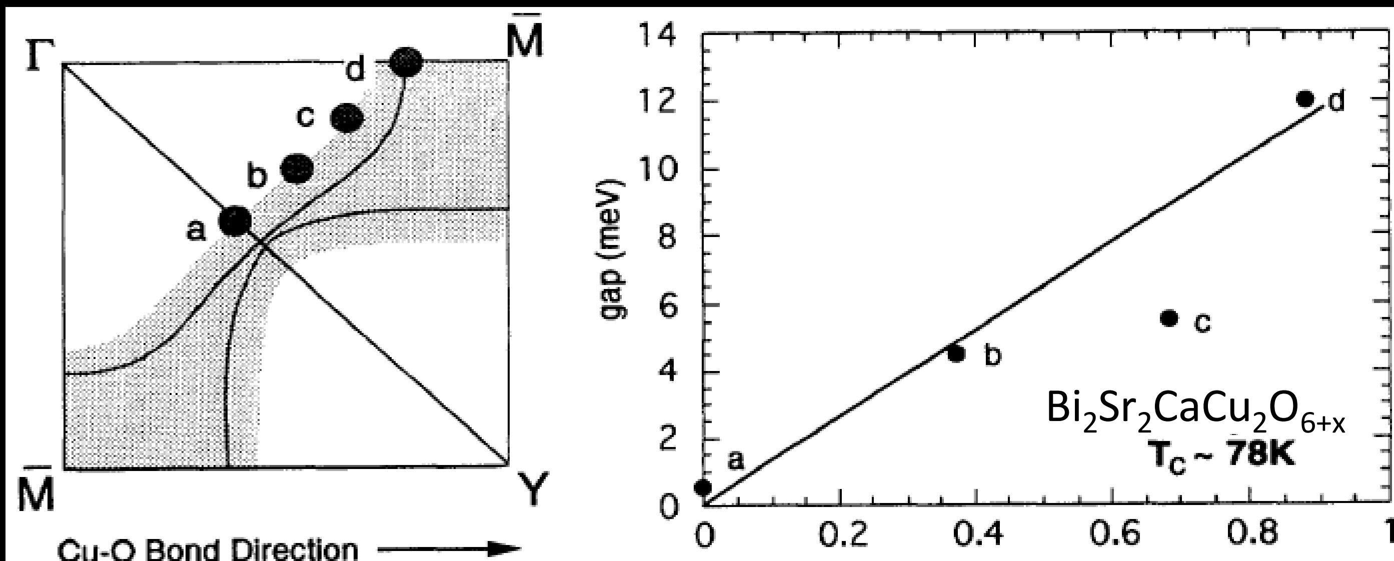

PRL 54, 9678 (1993)

Questions

1. What is the pairing symmetry of a superconductor?

Conventional: s-wave

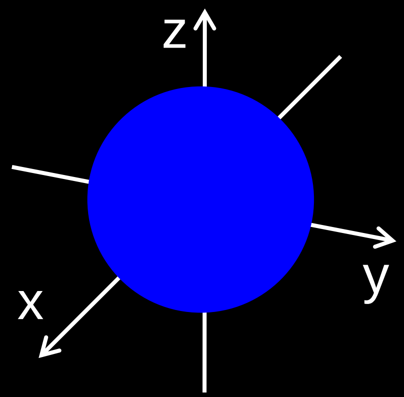

Cuprate: $d_{x^2-y^2}$ wave

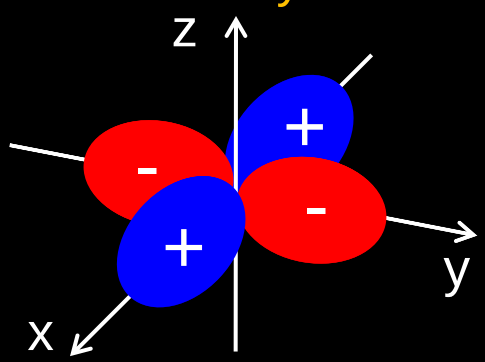

Iron: s? d? p?

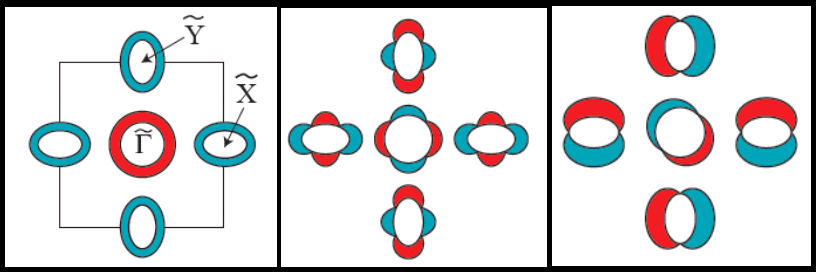

Hicks, JPSJ 78, 013708 (2009)

2. Where on the Fermi surface does the pairing occur?

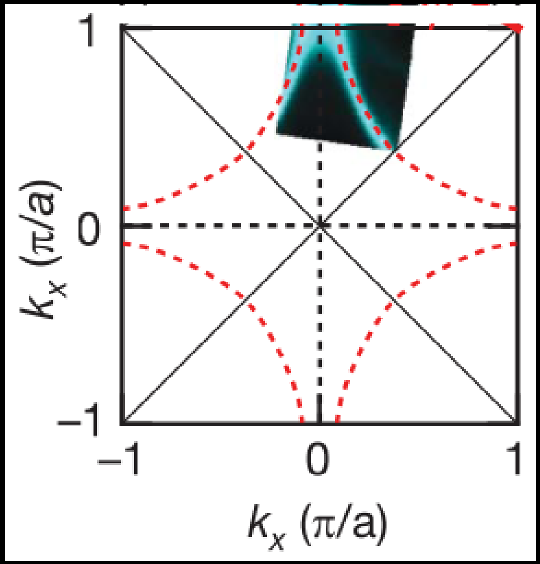

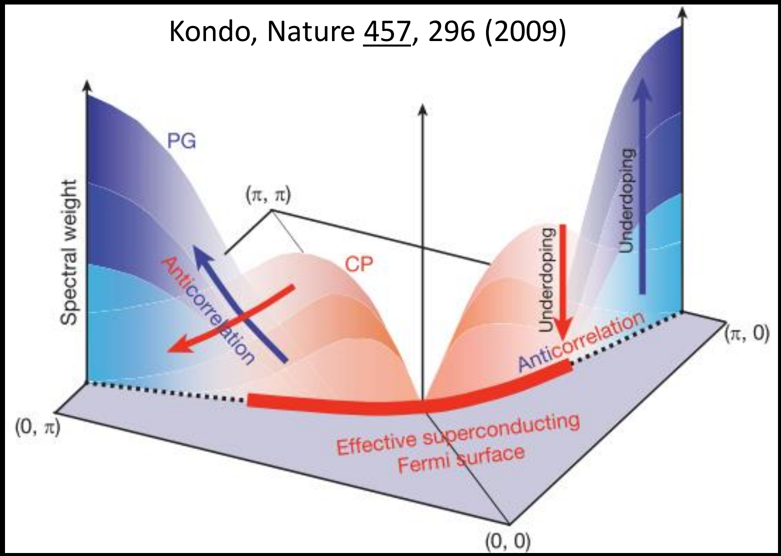

How can disorder help us?

H_2O

ME (experimentalist)

perturbation

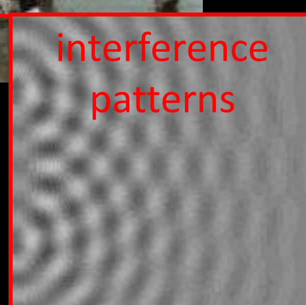

$Bi_2Sr_2CaCu_2O_{8+d}$

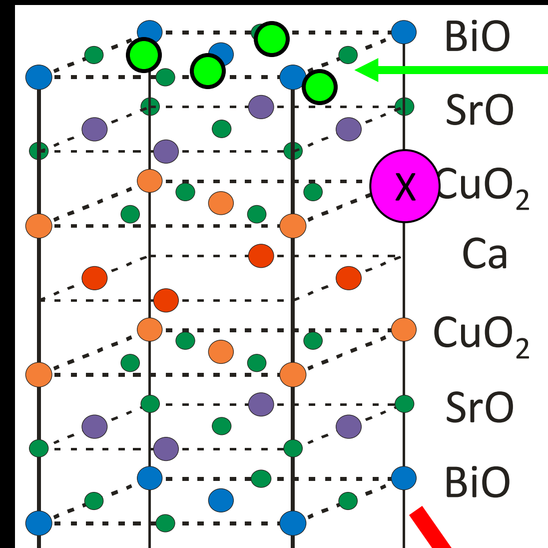

oxygen

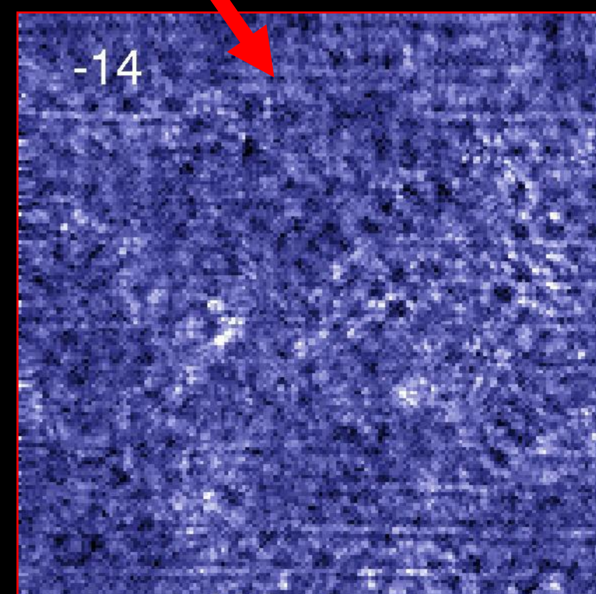

First QPI: metals, real space

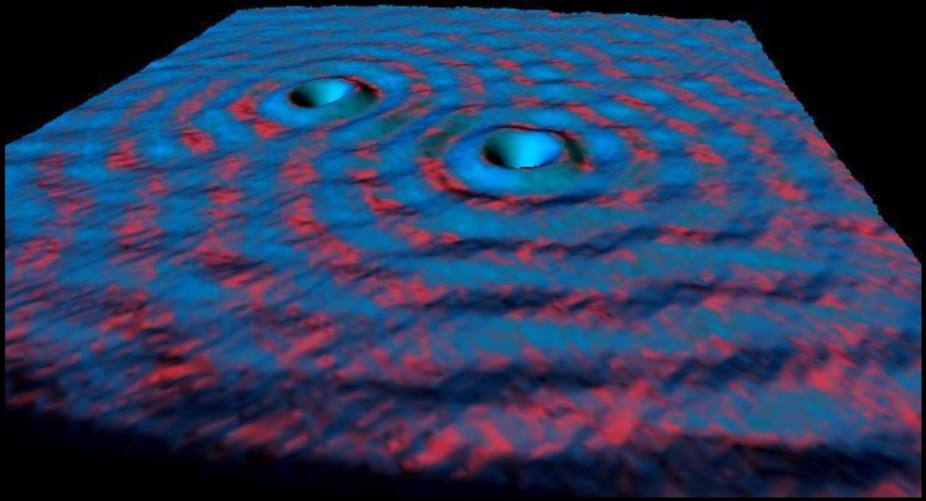

Crommie, Lutz & Eigler, Nature 363, 524 (1993)

Au:

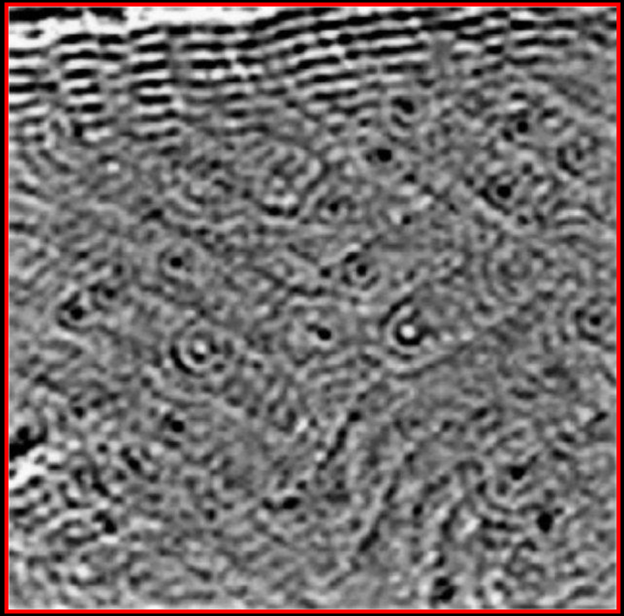

Cu:

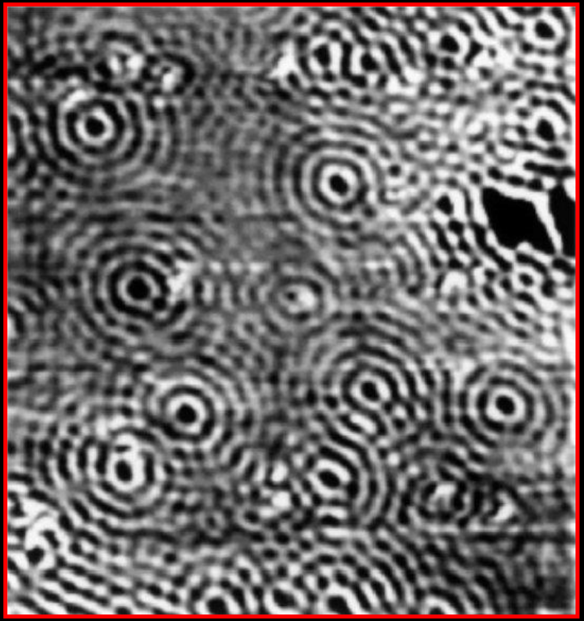

Peterson, Hofmann, Plummer & Besenbacher, J. Electron Spectroscopy 109, 97 (2000)

2-dim band structure: topographic map for e⁻

Power spectrum of scattering:

$$P(\varepsilon,\vec{q}) \propto |V(\vec{q})|^2\, n_i(\varepsilon_i,\vec{k}_i)\, n_f(\varepsilon_f,\vec{k}_f)$$

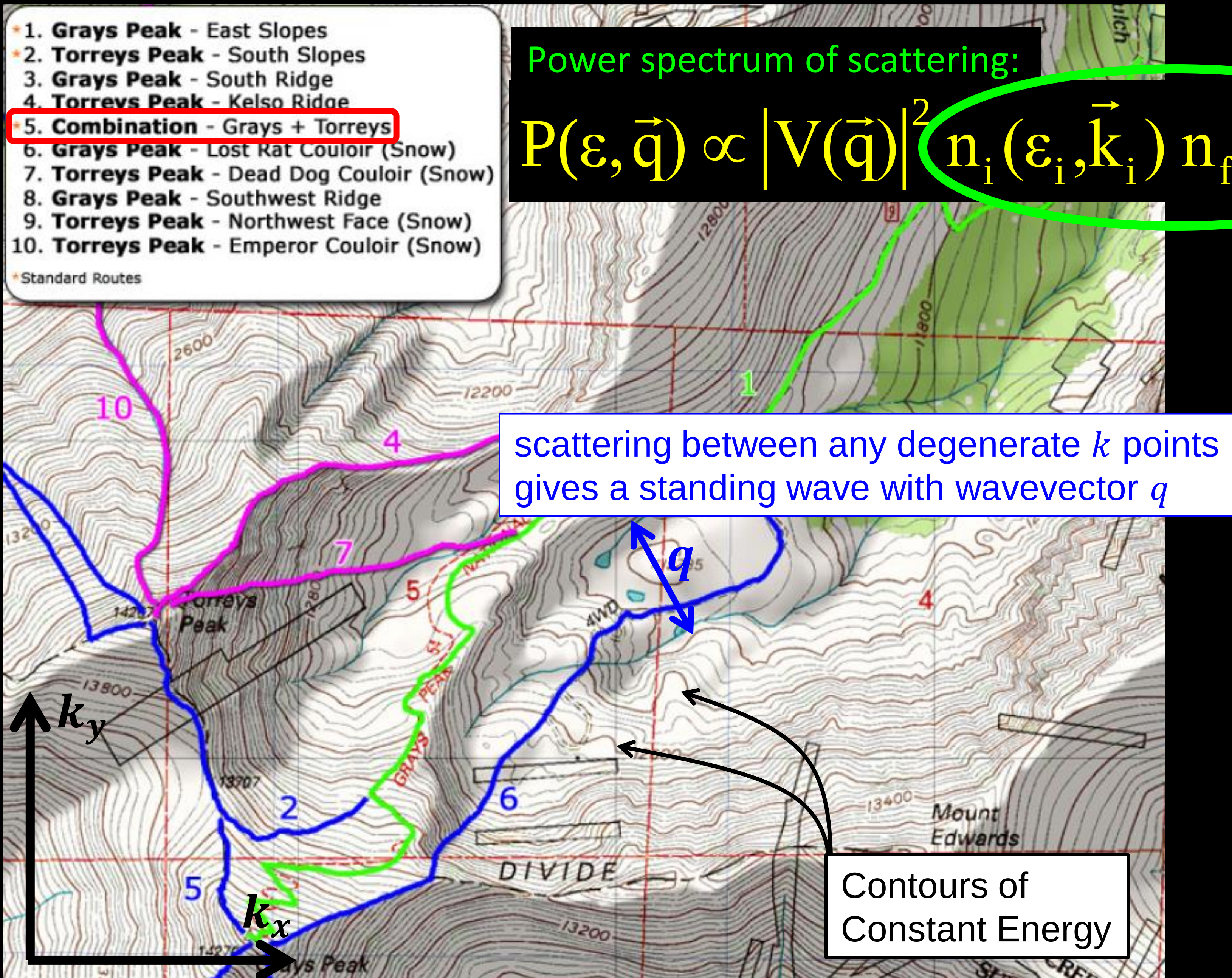

The real theory…

Density of states:

$$n(\mathbf{q},\omega)=n_0(\mathbf{q},\omega)-\frac{1}{2\pi i}[A_{11}(\mathbf{q},\omega)+A_{22}(\mathbf{q},-\omega)-A_{11}^*(-\mathbf{q},\omega)-A_{22}^*(-\mathbf{q},-\omega)]$$

$$A(\mathbf{q},\omega)=\int\frac{d^2k}{(2\pi)^2}G_0(\mathbf{k}+\mathbf{q},\omega)T(\mathbf{k}+\mathbf{q},\mathbf{k};\omega)G_0(\mathbf{k},\omega)$$

scattering

Greens functions

→ There will be cross terms.

Wang & Lee, PRB 67, 020511 (2003)

But empirically, simple real model is a good approximation to the data:

$$P(\varepsilon,\vec{q})\propto|V(\vec{q})|^2\,n_i(\varepsilon_i,\vec{k}_i)\,n_f(\varepsilon_f,\vec{k}_f)$$

McElroy, PRL 96, 067005 (2006)

ARPES: Normal State Fermi Surface & Band Structure

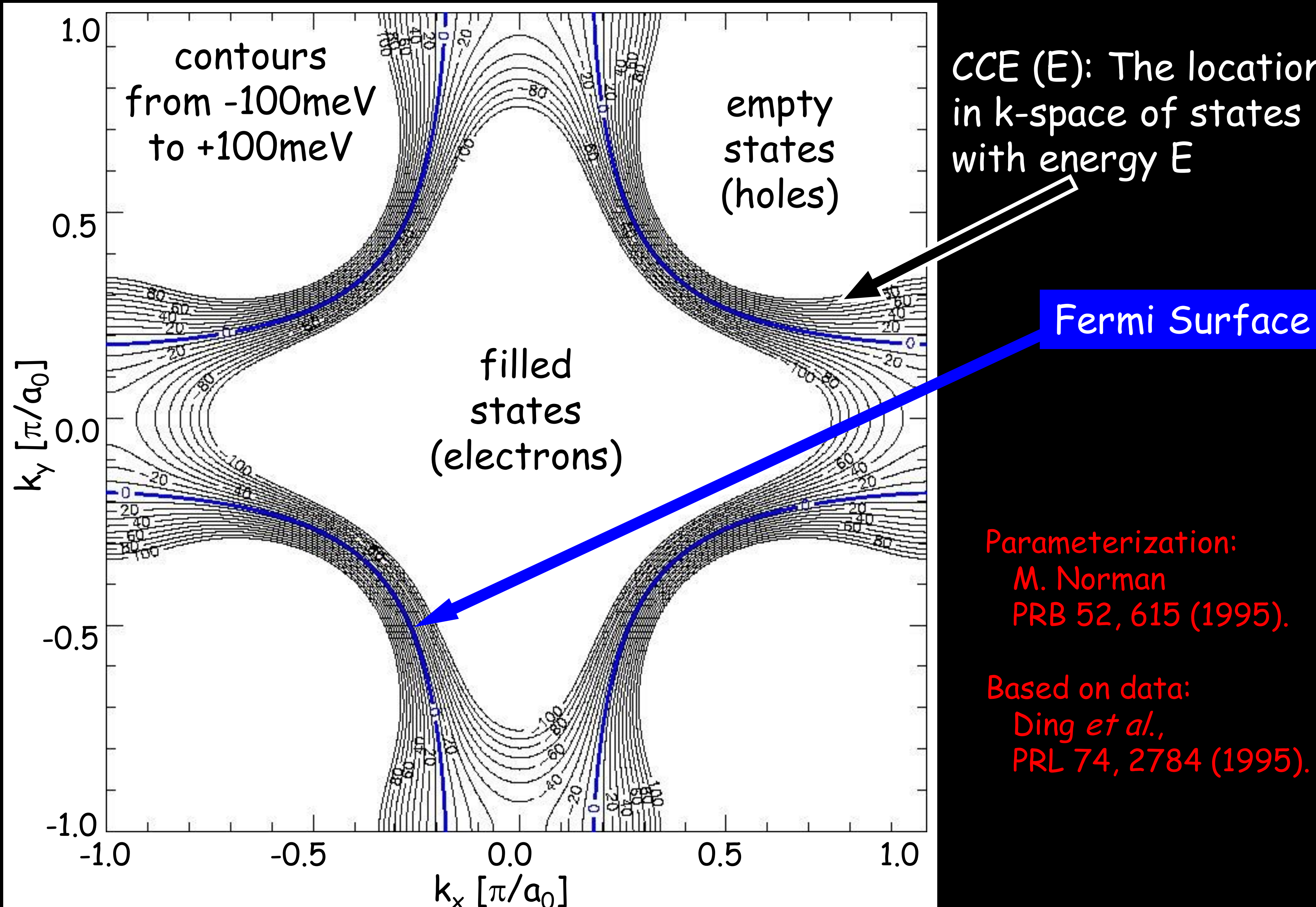

Parameterization:
M. Norman
PRB 52, 615 (1995).

Based on data:
Ding *et al.*,
PRL 74, 2784 (1995).

ARPES: Superconducting anisotropic gap $\Delta(\vec{k})$

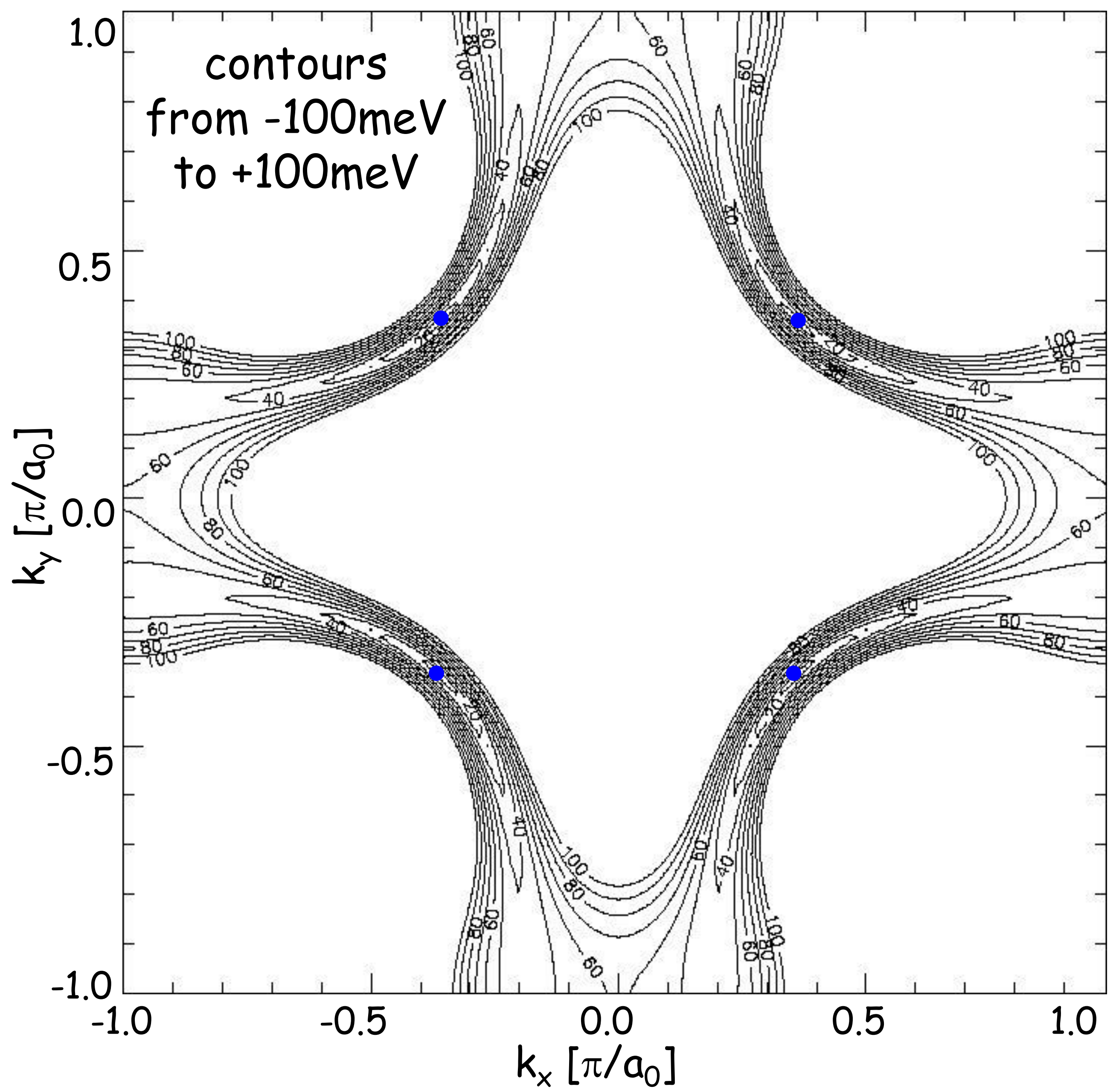

Ding *et al.*, PRLB 54, 9678 (1996)

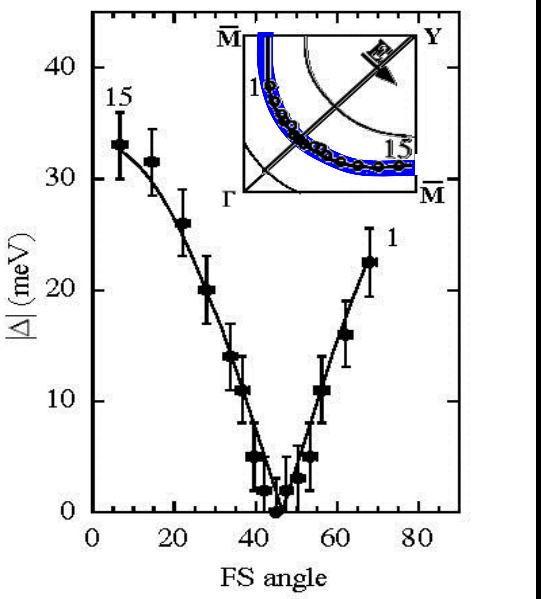

Shen *et al*, PRL **70** 1553 (1993)
Ding *et al*, PRB **54** 9678 (1996)
Mesot *et al*, PRL **83** 840 (1999)

0 meV CCE: the Fermi points

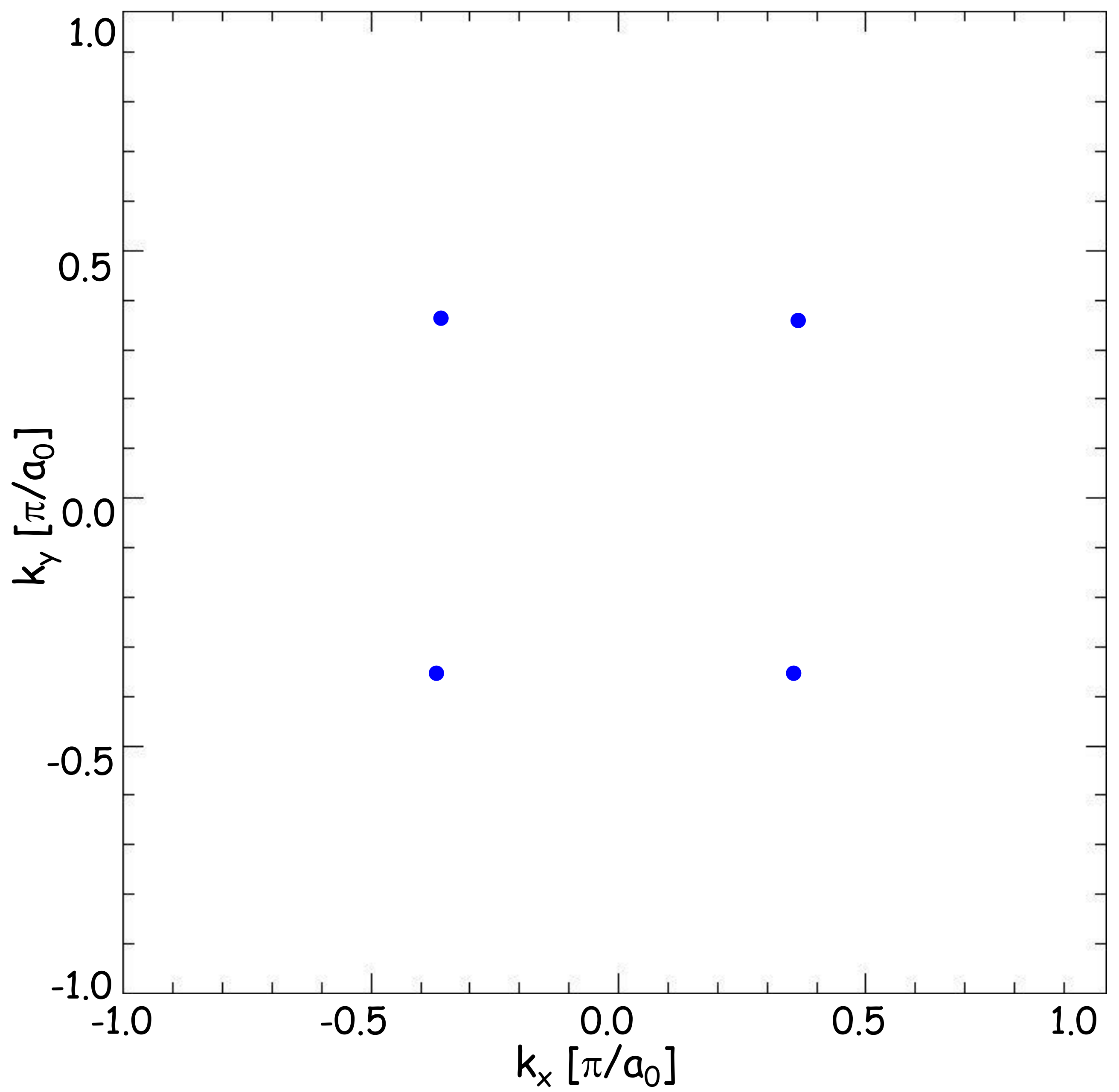

10 meV CCE

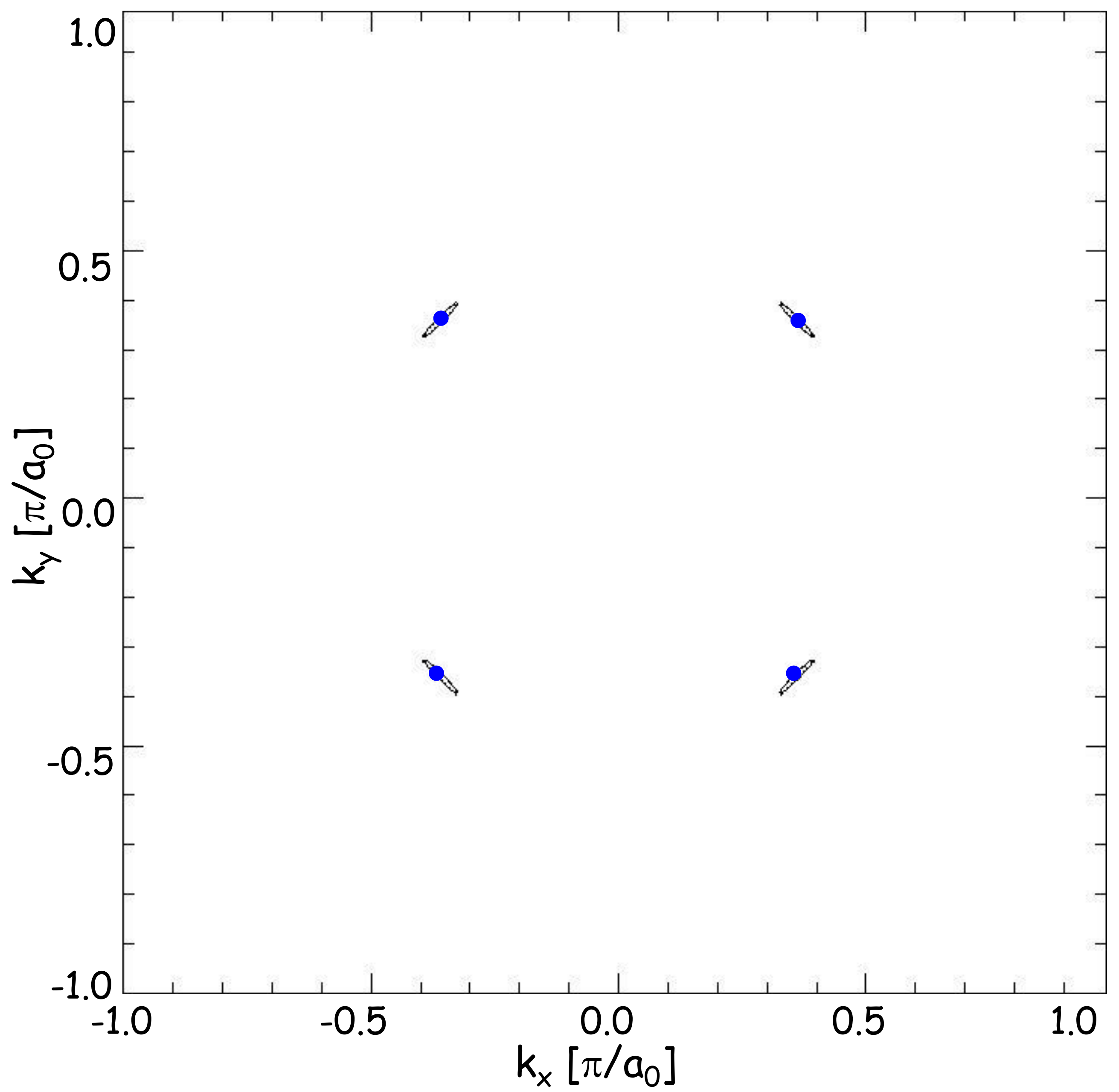

20 meV CCE

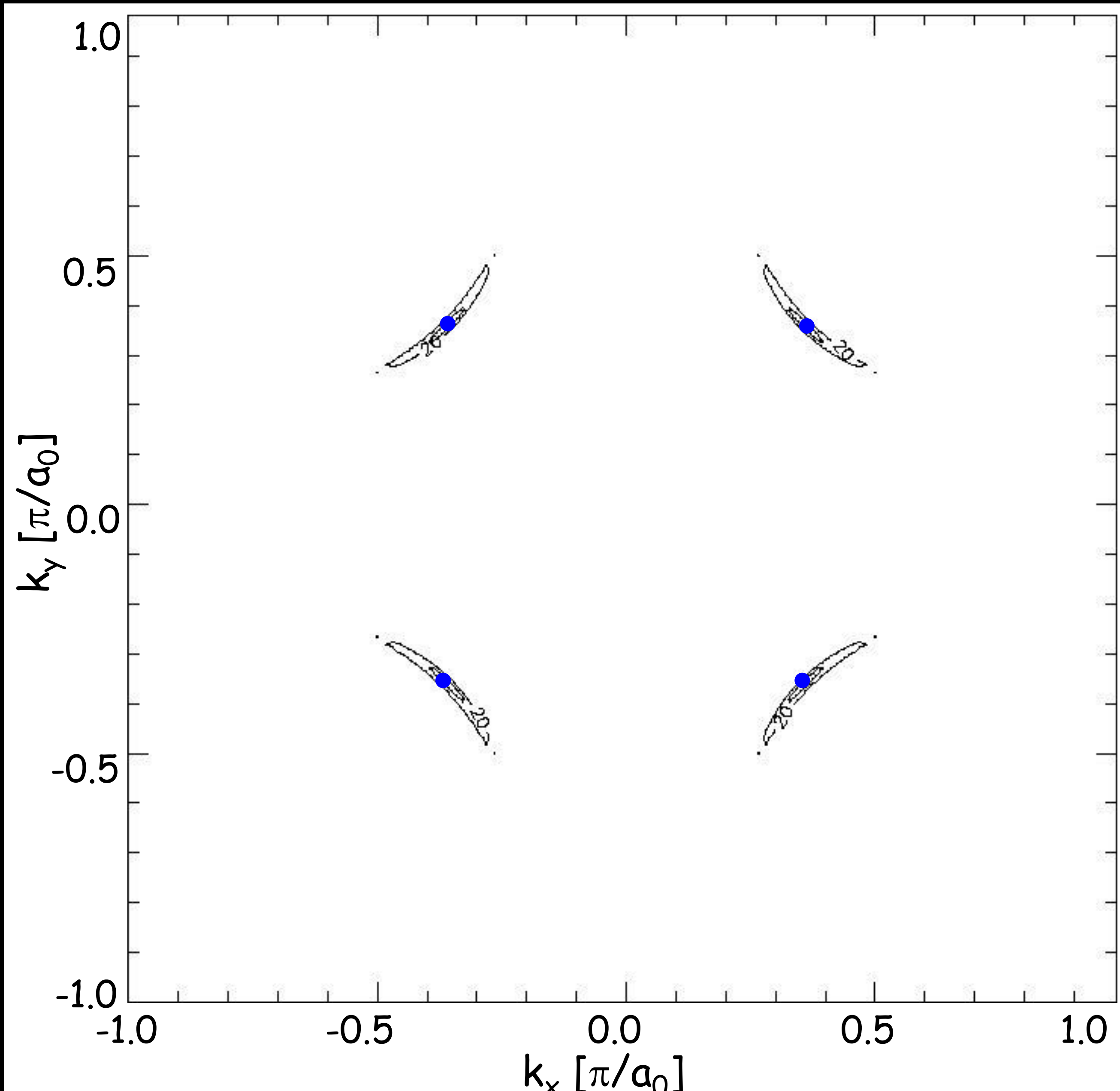

30 meV CCE

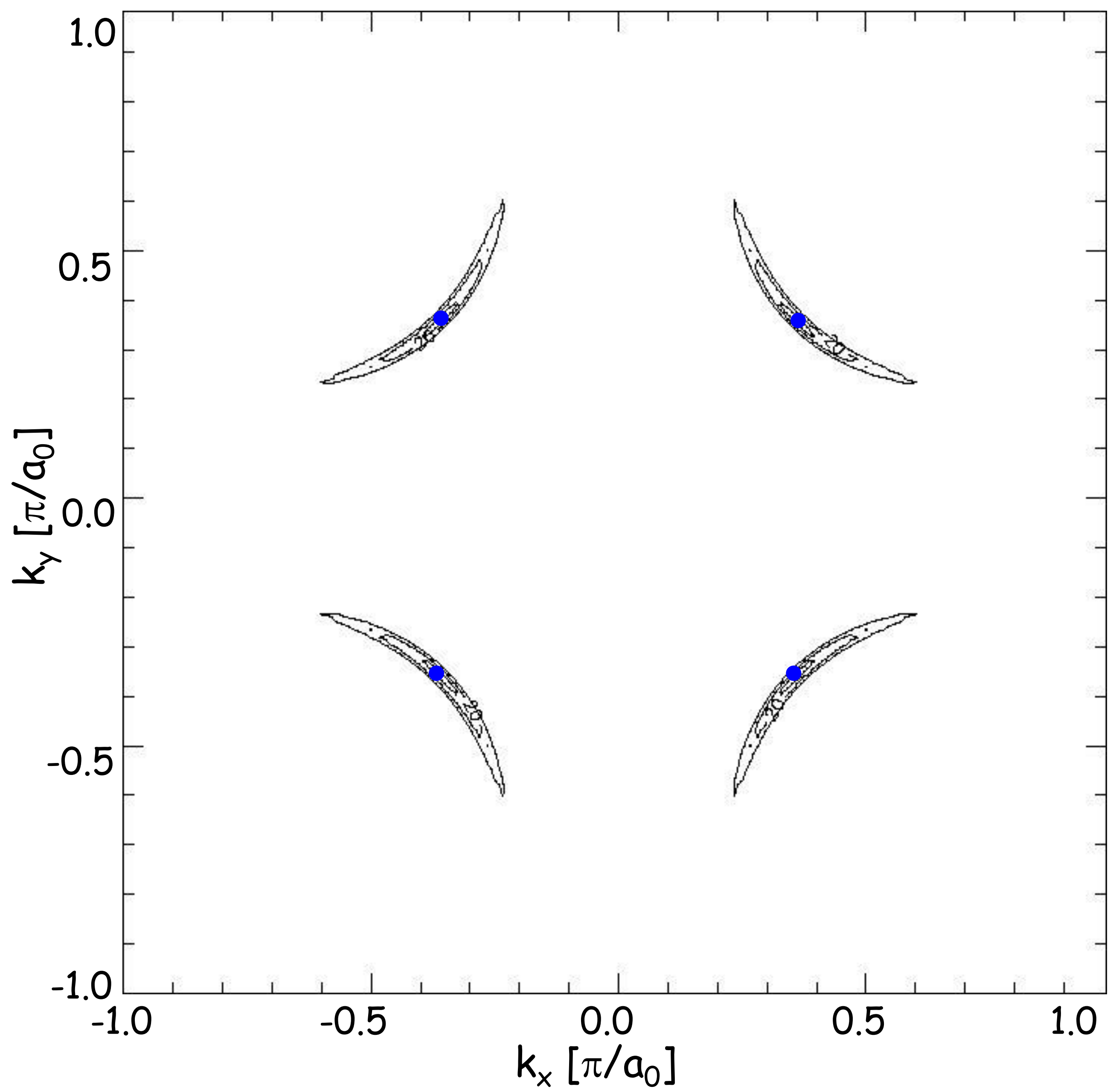

40 meV CCE

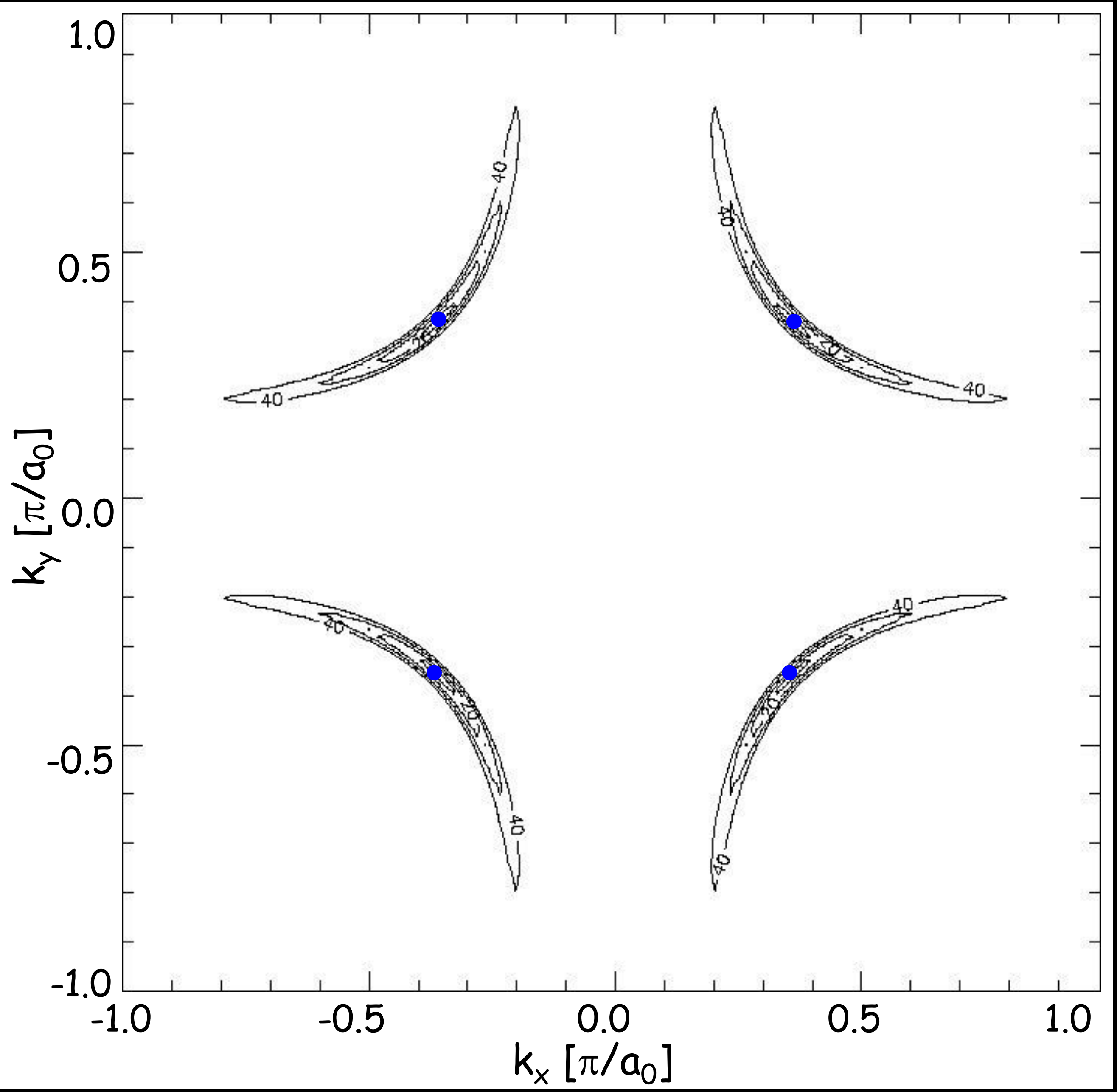

1.0
0.5
0.0
-0.5
-1.0
-1.0
-0.5
0.0
0.5
1.0
k_y [π/a_0]
k_x [π/a_0]
40
40
40
40
40
40
40
40
20
20
20
20

Octet of regions at ends of 'bananas' have largest |dk|/dE

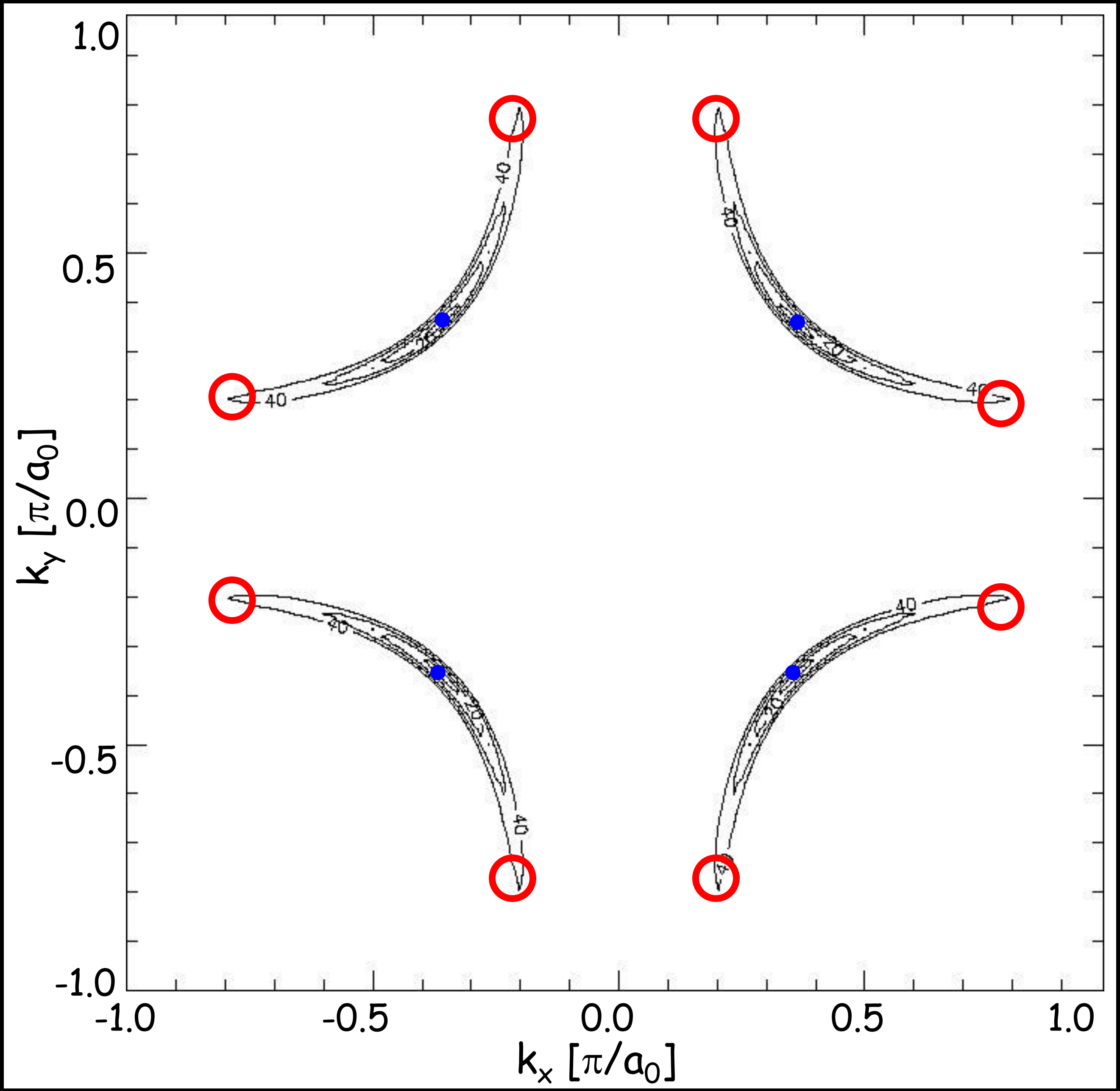

Density of States

$$n(E) = \oint_{E(k)=E} \frac{1}{\left|\nabla_k E(\vec{k})\right|} dk$$

The octet of k-space locations at the tips of the 'bananas' provide maximum contribution to $n_{i,f}(E)$ and thus dominate elastic scattering processes.

The scattering vectors of QI model

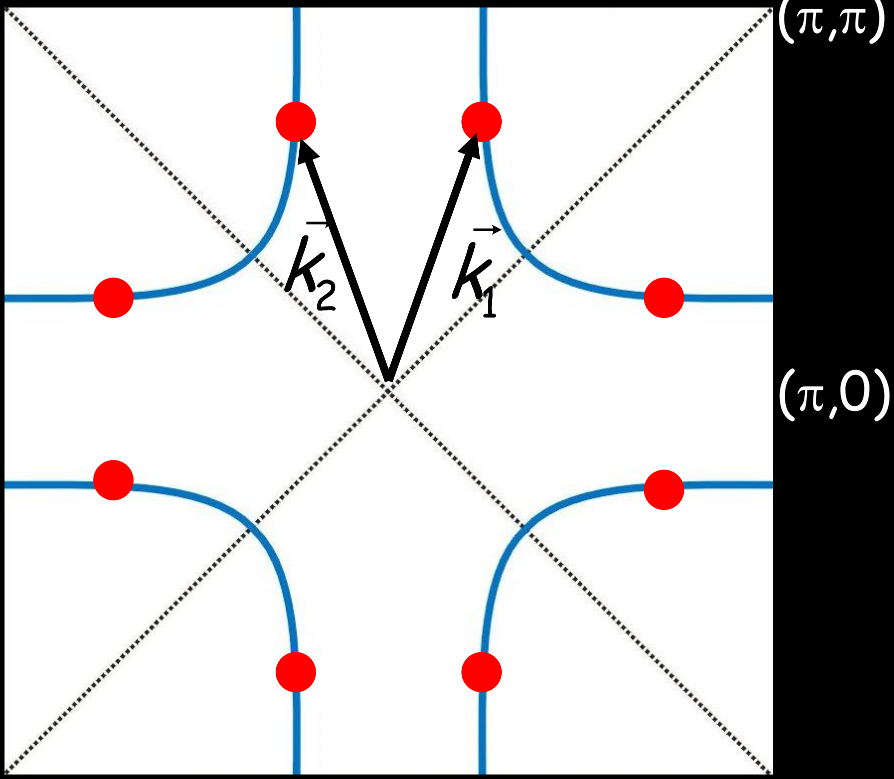

k-space:

- unperturbed eigenstates
- not directly accessible to STM
- measured by ARPES

The scattering vectors of QI model

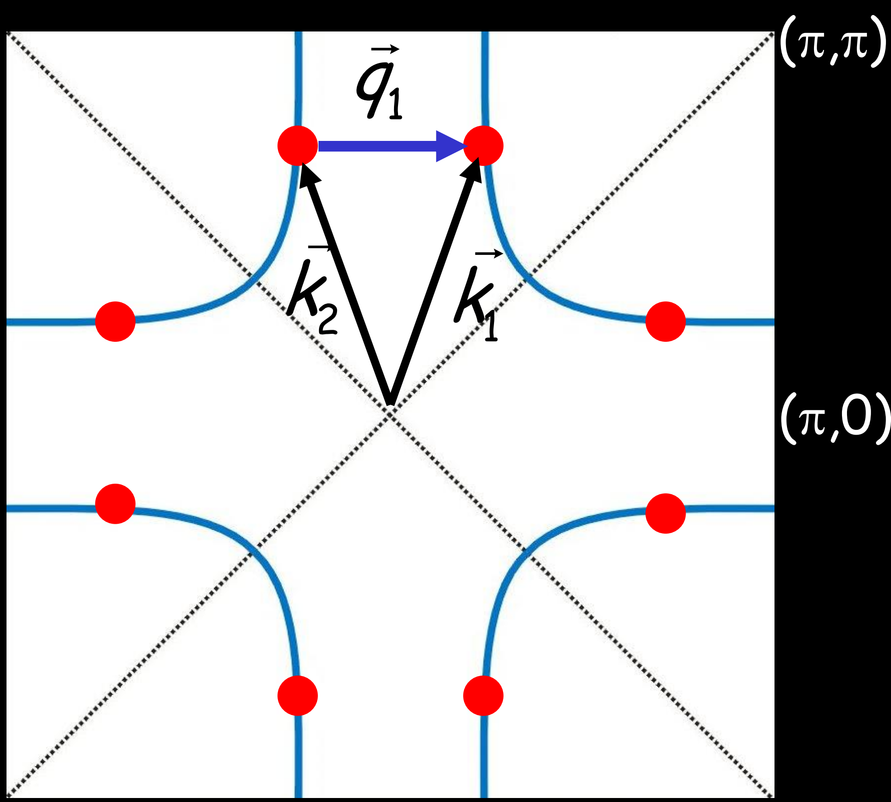

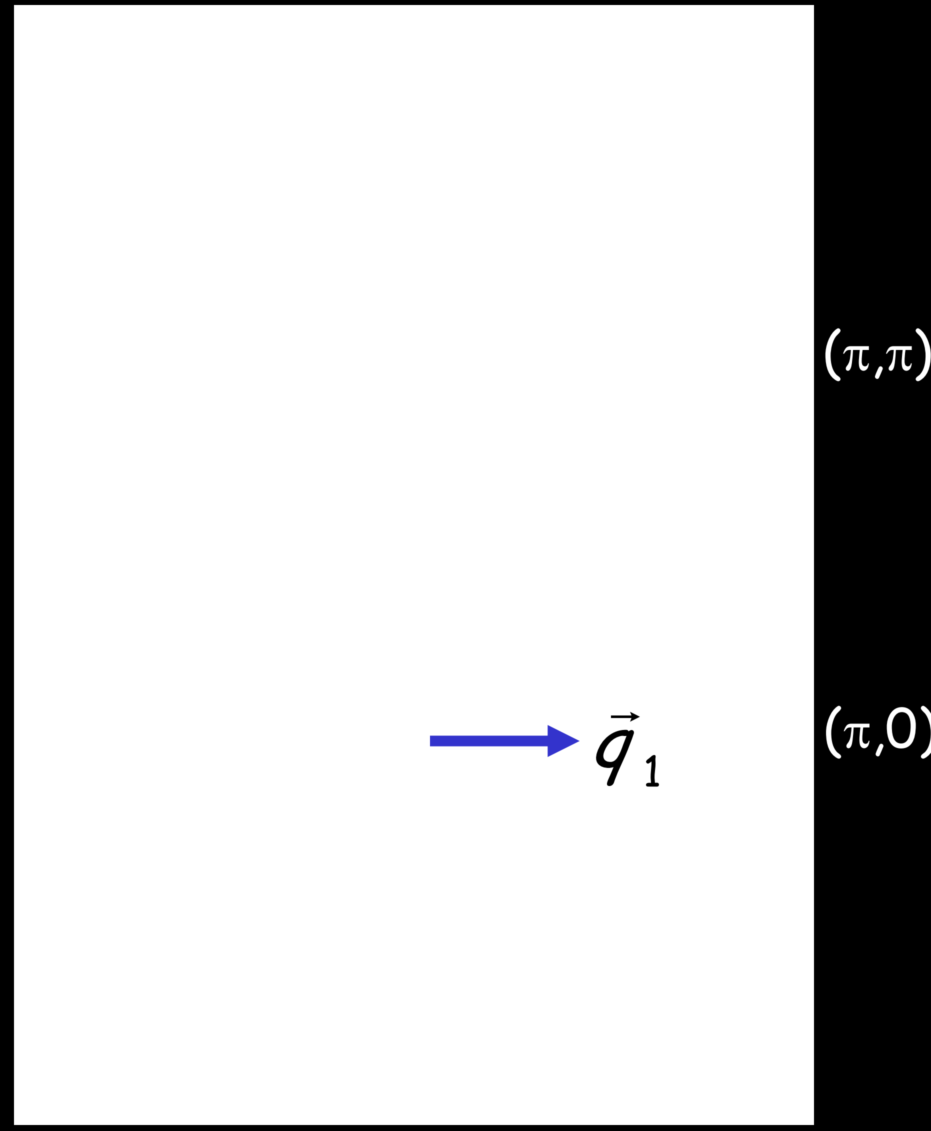

k-space:
- unperturbed eigenstates
- not directly accessible to STM
- measured by ARPES

q-space:
- Scattering → standing waves $q = 2\pi/\lambda$
- Measure *q* from FT of LDOS image

The scattering vectors of QI model

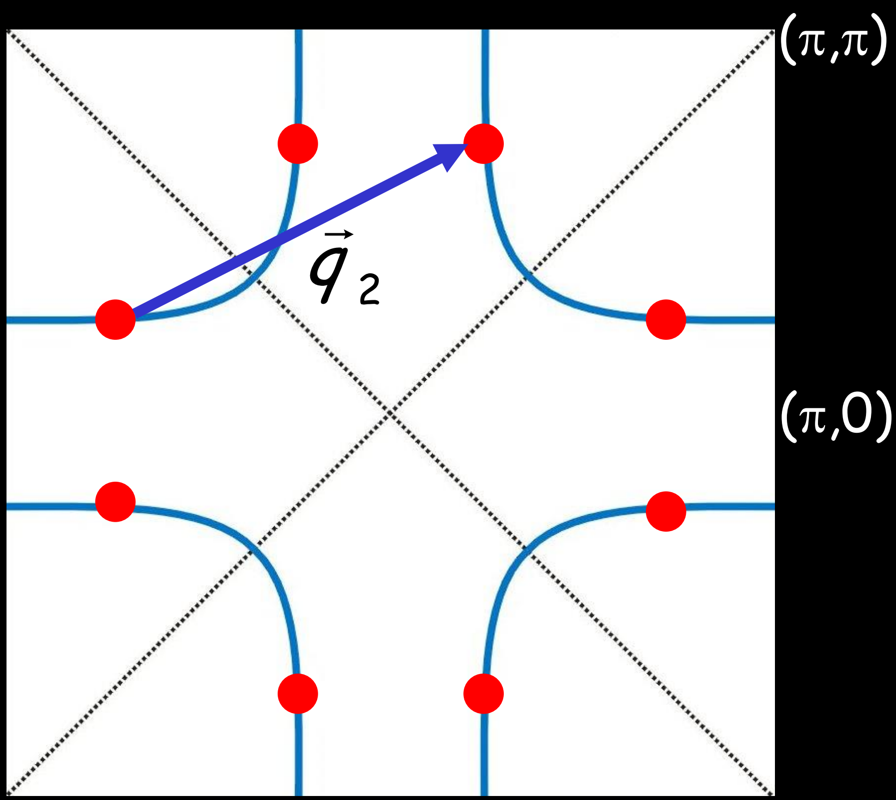

k-space:
- unperturbed eigenstates
- not directly accessible to STM
- measured by ARPES

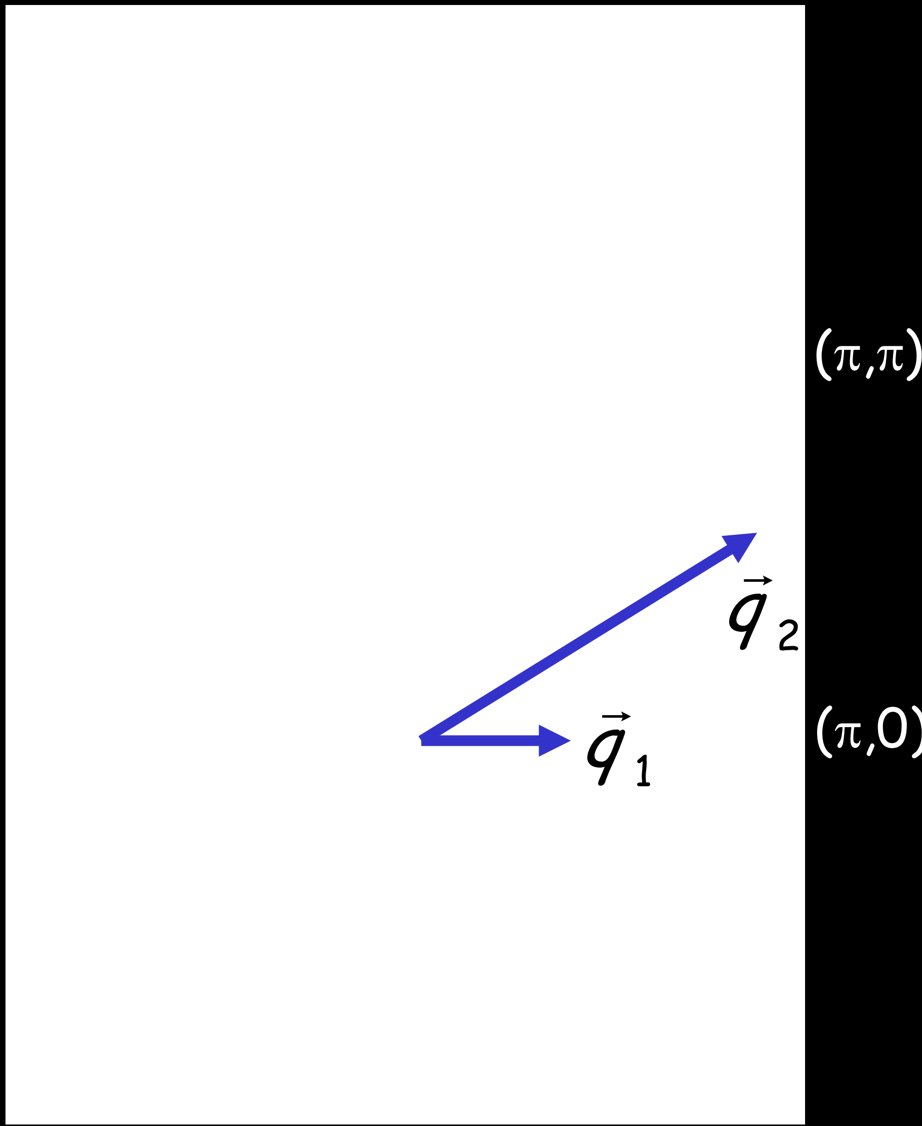

q-space:
- Scattering → standing waves $q = 2\pi/\lambda$
- Measure *q* from FT of LDOS image

The scattering vectors of QI model

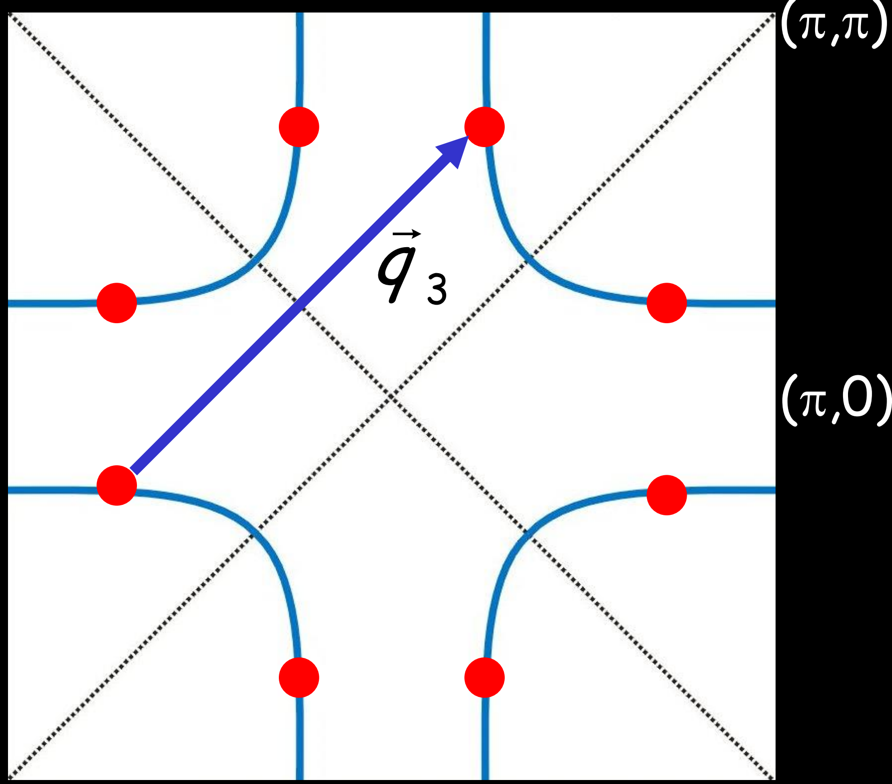

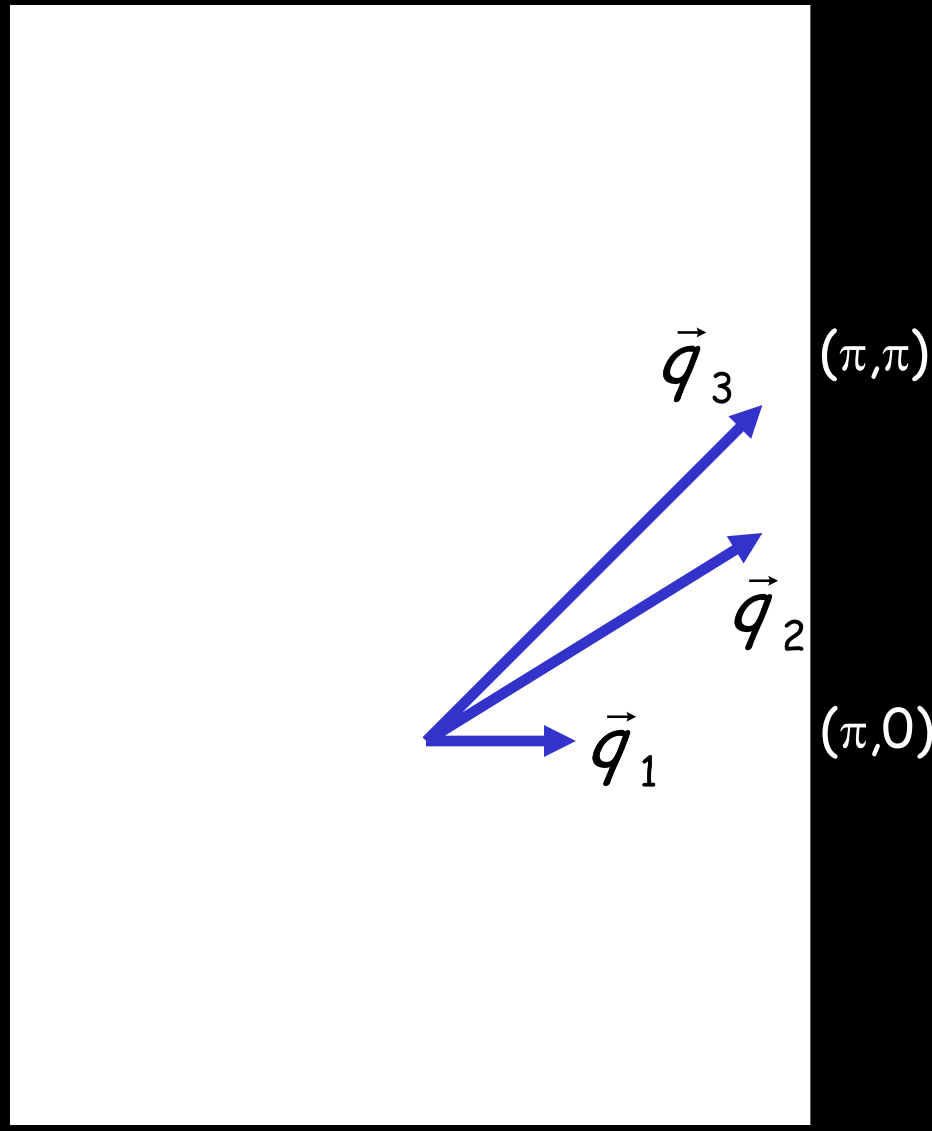

k-space:

- unperturbed eigenstates
- not directly accessible to STM
- measured by ARPES

q-space:

- Scattering → standing waves $q = 2\pi/\lambda$
- Measure *q* from FT of LDOS image

The scattering vectors of QI model

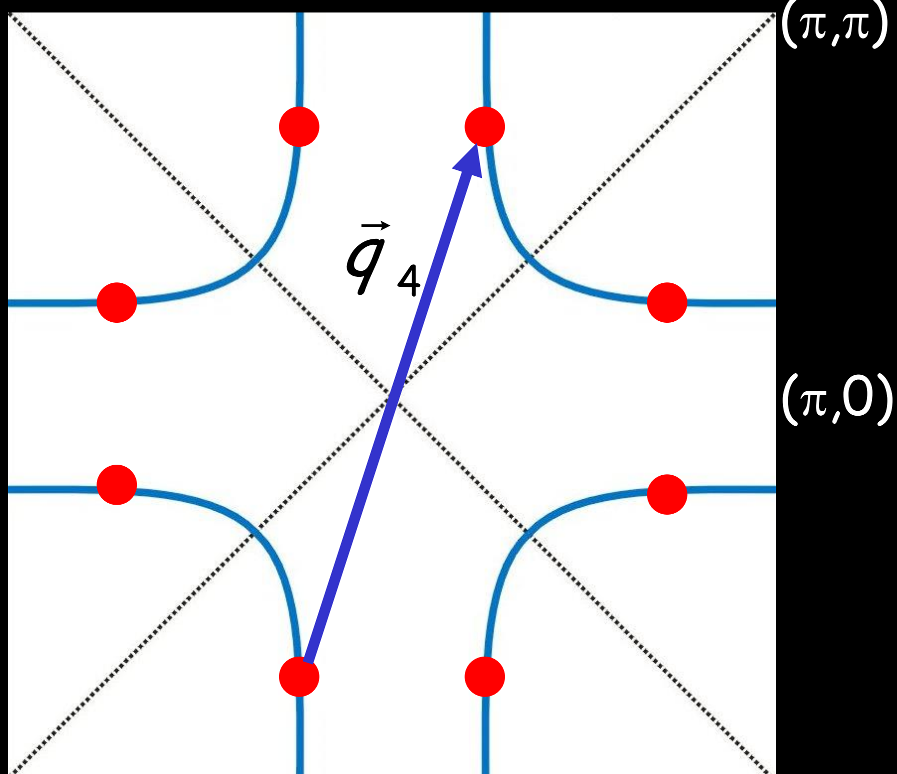

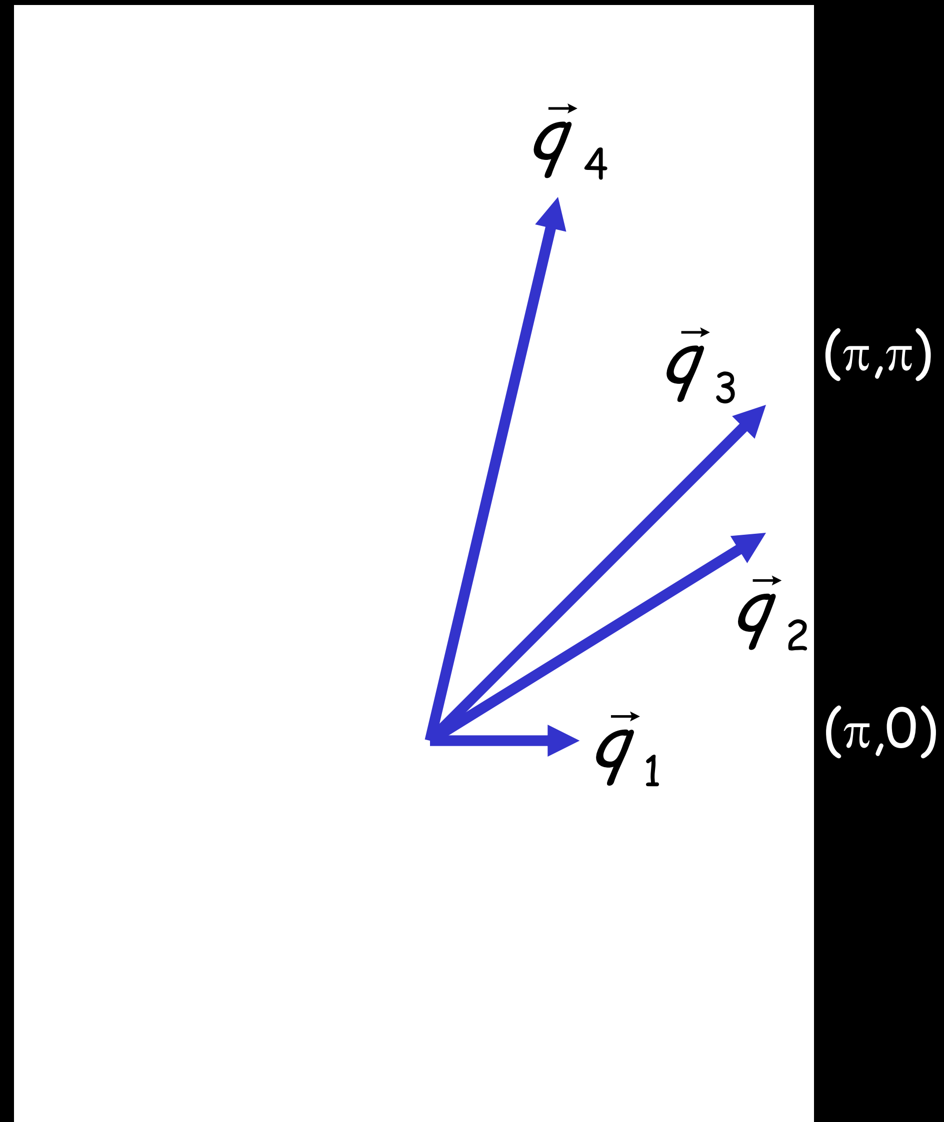

k-space:

- unperturbed eigenstates
- not directly accessible to STM
- measured by ARPES

q-space:

- Scattering → standing waves $q = 2\pi/\lambda$
- Measure *q* from FT of LDOS image

The scattering vectors of QI model

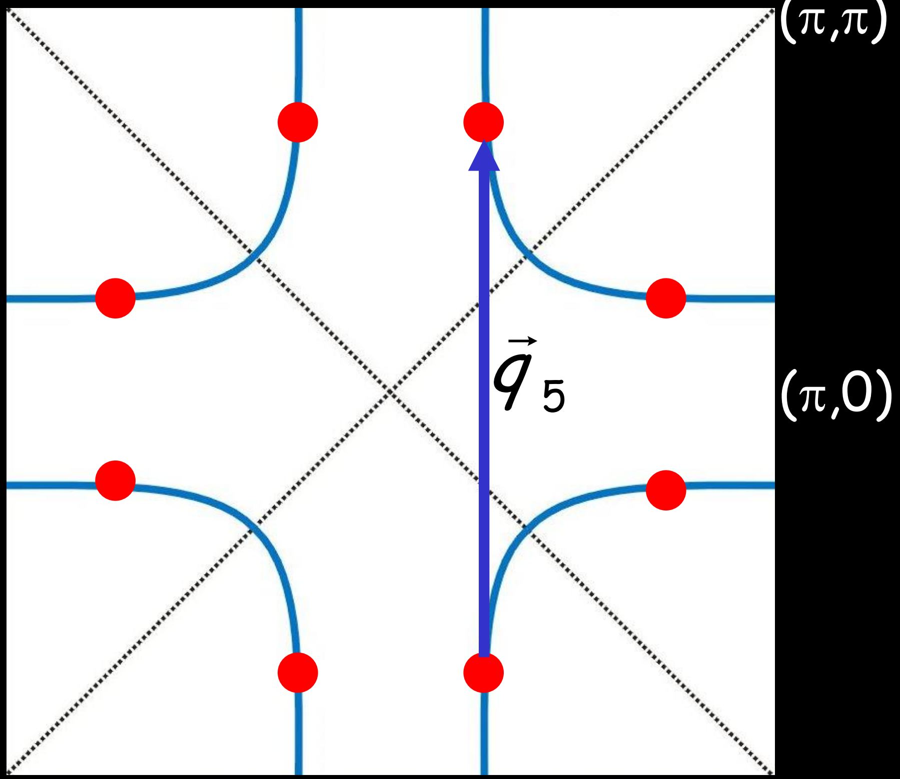

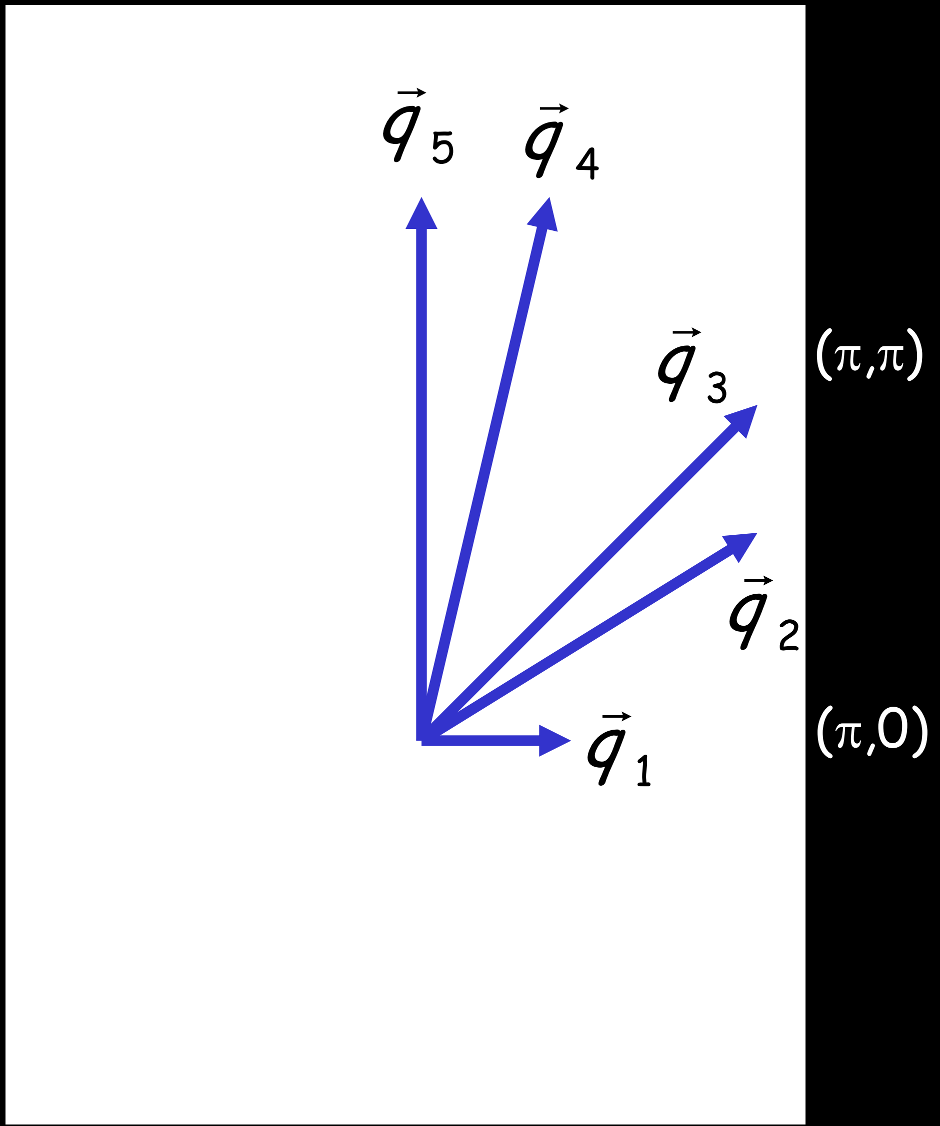

k-space:
- unperturbed eigenstates
- not directly accessible to STM
- measured by ARPES

q-space:
- Scattering → standing waves $q = 2\pi/\lambda$
- Measure *q* from FT of LDOS image

The scattering vectors of QI model

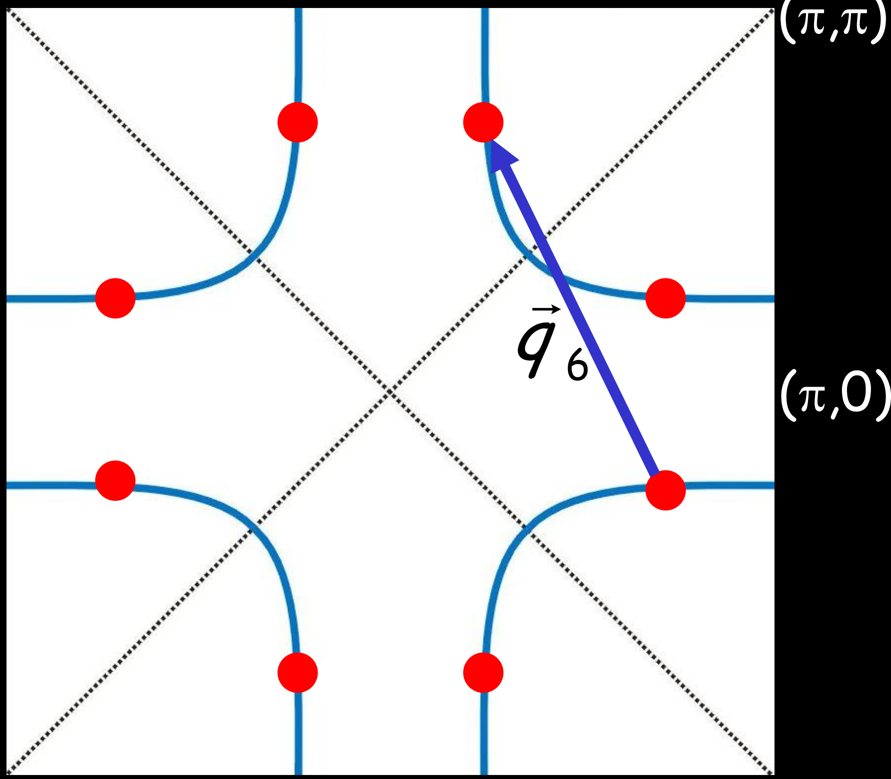

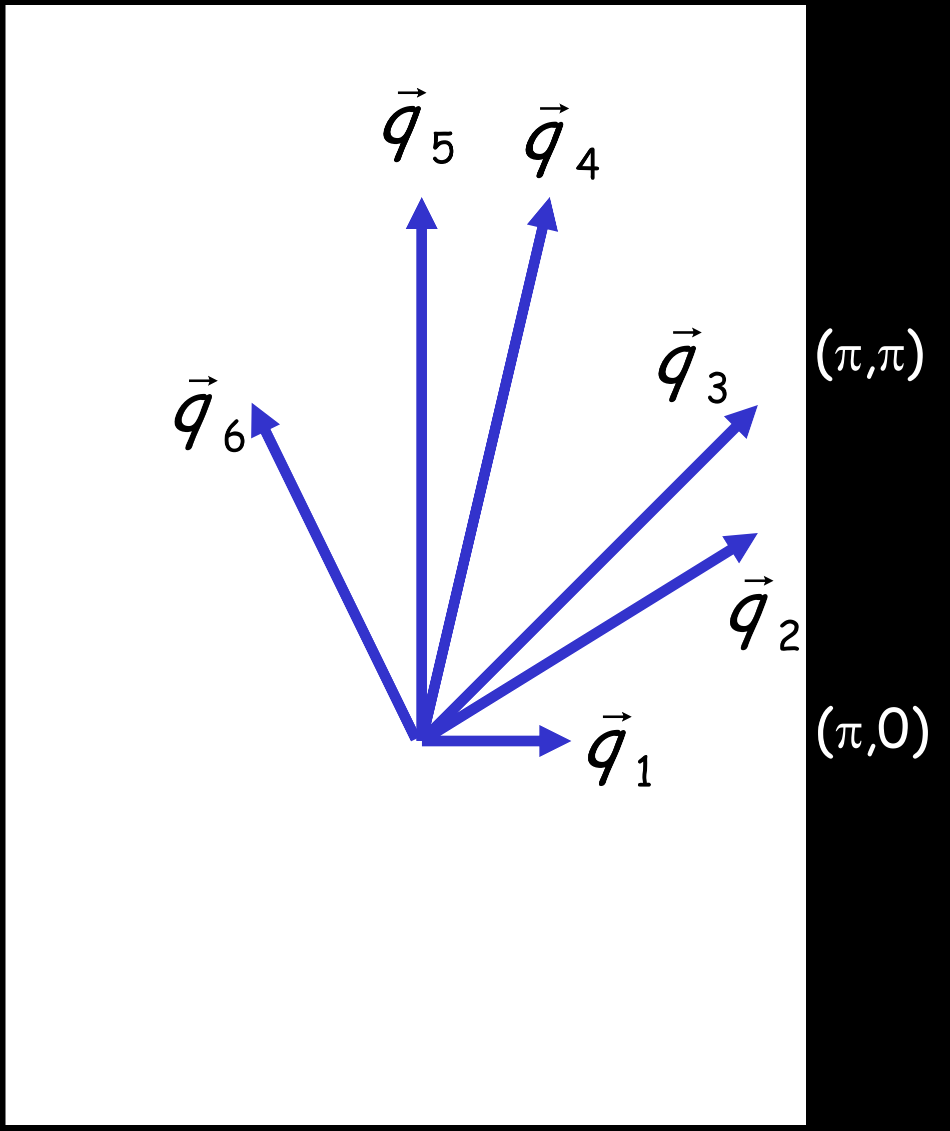

k-space:

- unperturbed eigenstates
- not directly accessible to STM
- measured by ARPES

q-space:

- Scattering → standing waves $q = 2\pi/\lambda$
- Measure *q* from FT of LDOS image

The scattering vectors of QI model

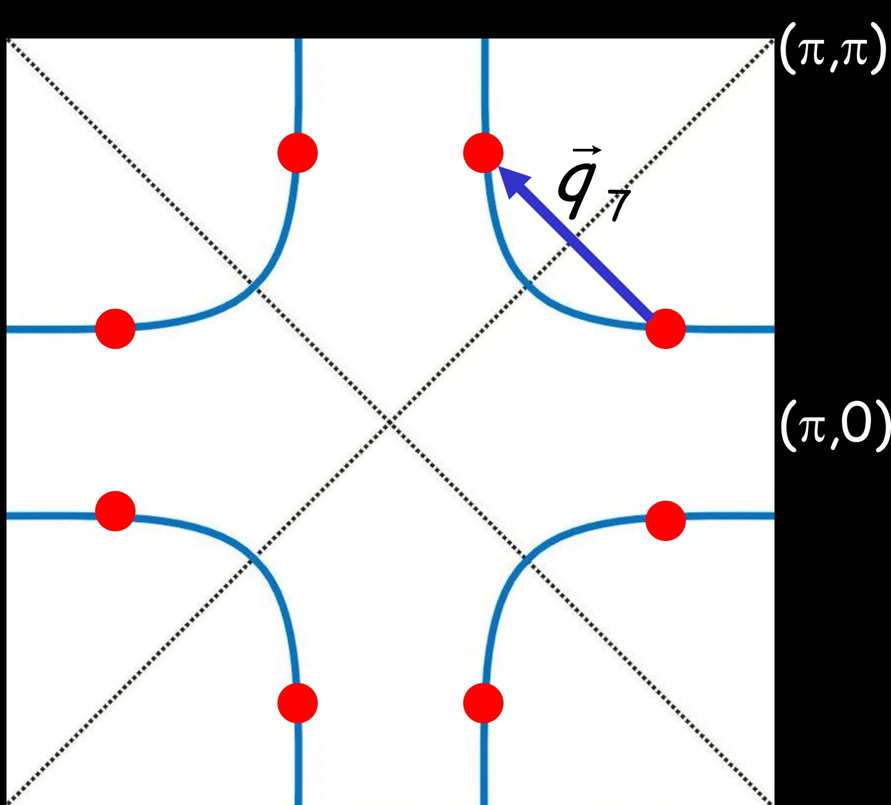

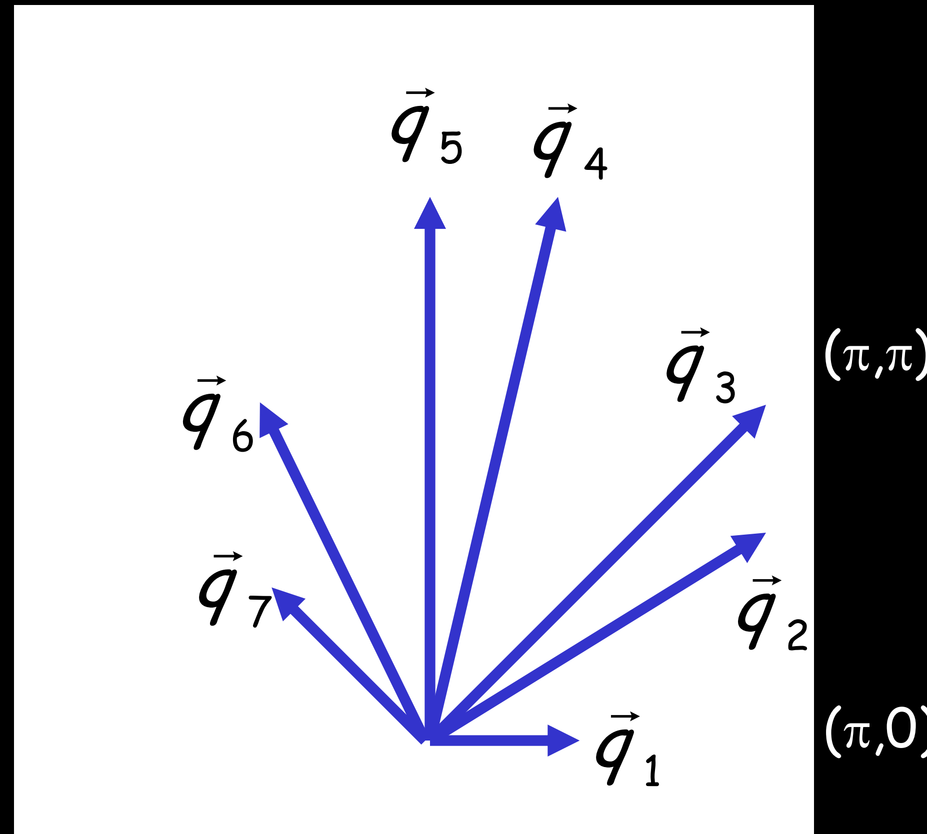

Total sets of $\boldsymbol{q}_i$ (7X8) : 56
Inequivalent sets of $\boldsymbol{q}_i$: 32
Distinguishable via FT-STS : 16

k-space:

- unperturbed eigenstates
- not directly accessible to STM
- measured by ARPES

q-space:

- Scattering → standing waves $q = 2\pi/\lambda$
- Measure *q* from FT of LDOS image

The scattering vectors of QI model

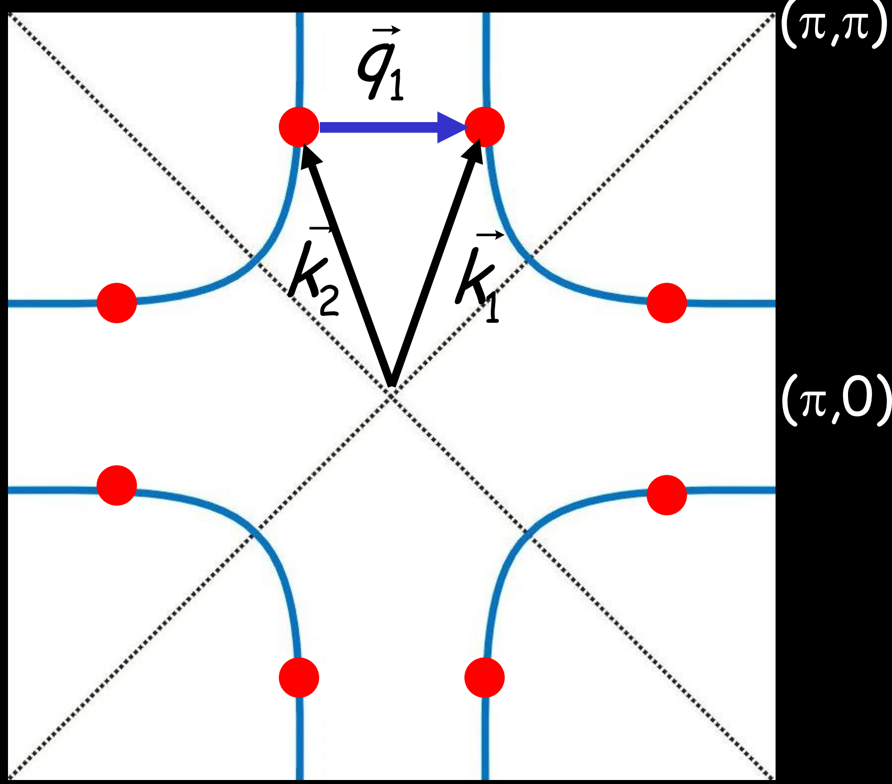

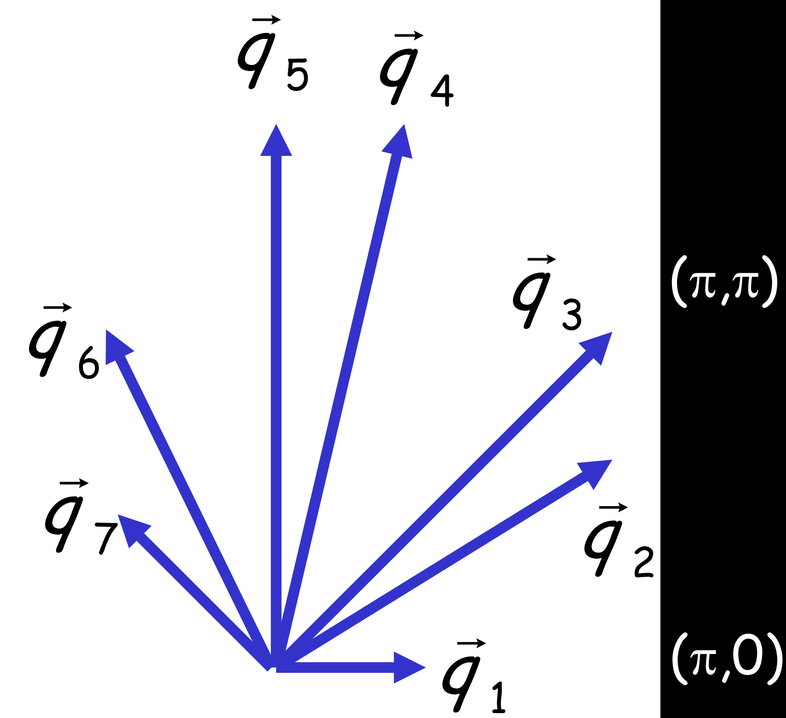

Total sets of q_i (7X8) : 56
Inequivalent sets of q_i : 32
Distinguishable via FT-STS : 16

k-space:

- unperturbed eigenstates
- not directly accessible to STM
- measured by ARPES

q-space:

- Scattering → standing waves $q = 2\pi/\lambda$
- Measure q from FT of LDOS image

Expected structure of FFT of LDOS(r,E)
(for a fixed E)

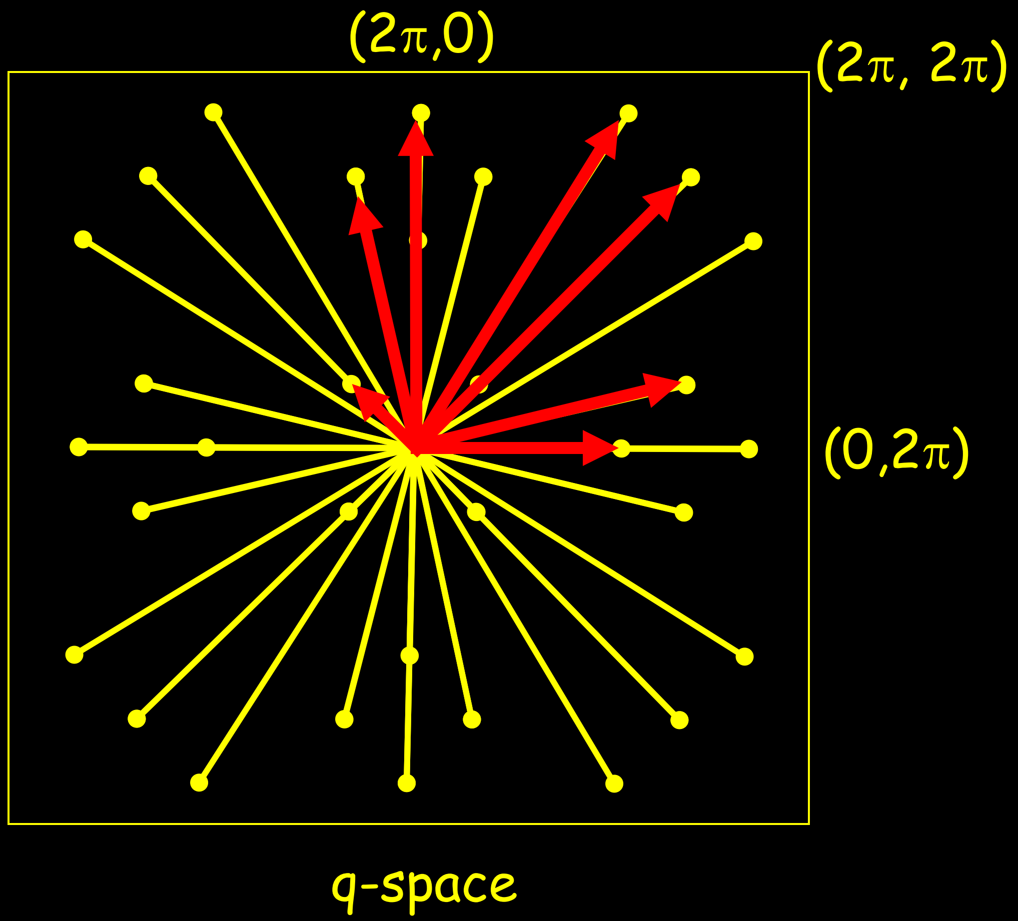

Dispersion:

how does each $\vec{q_i}$ vary with E ?

For example, look at the dispersion of:

$\vec{q_1}$ || $(\pm\pi,0)$ or $(0,\pm\pi)$

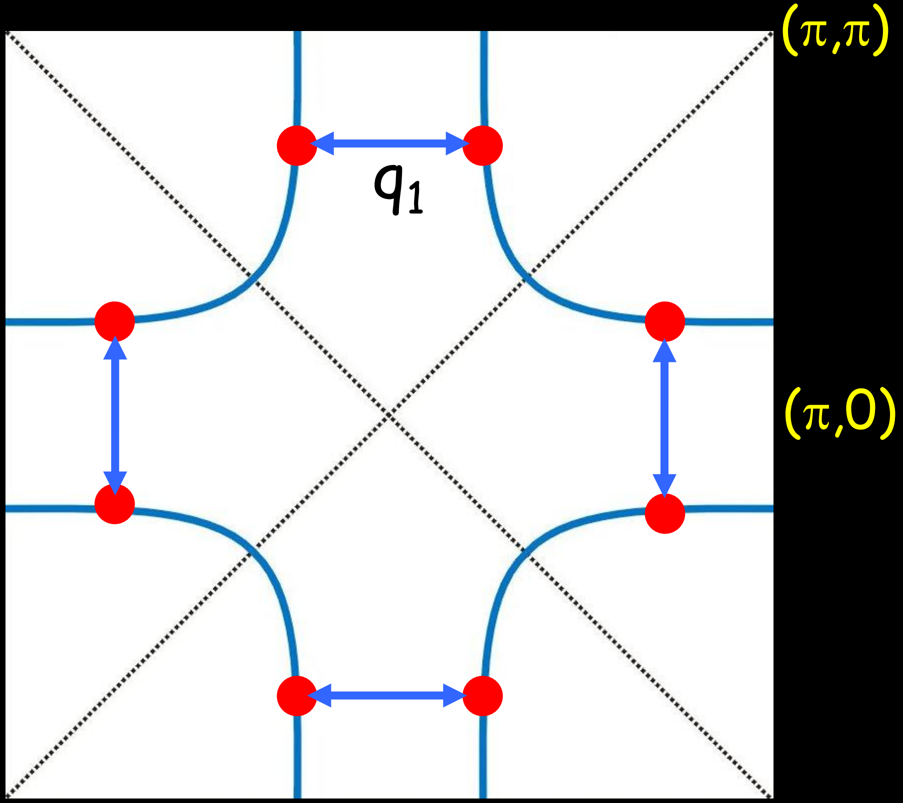

Expected energy dependence of $|\vec{q}_1|$

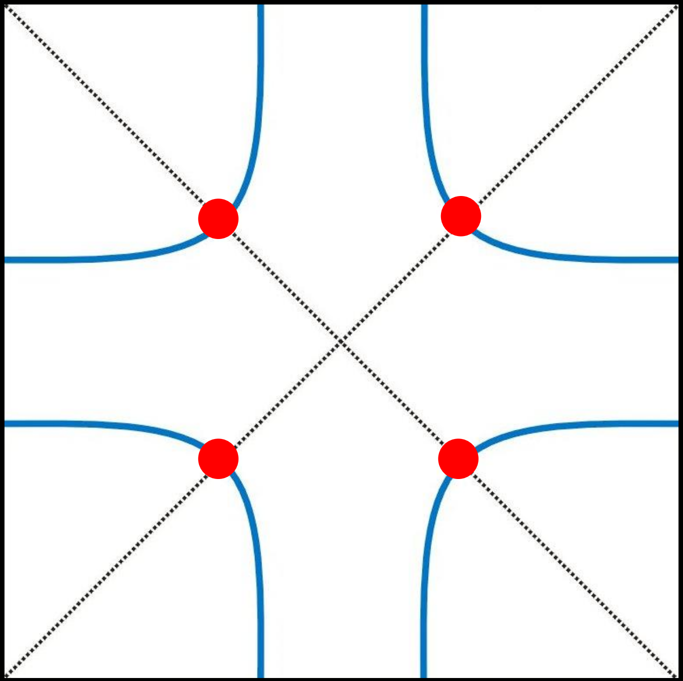

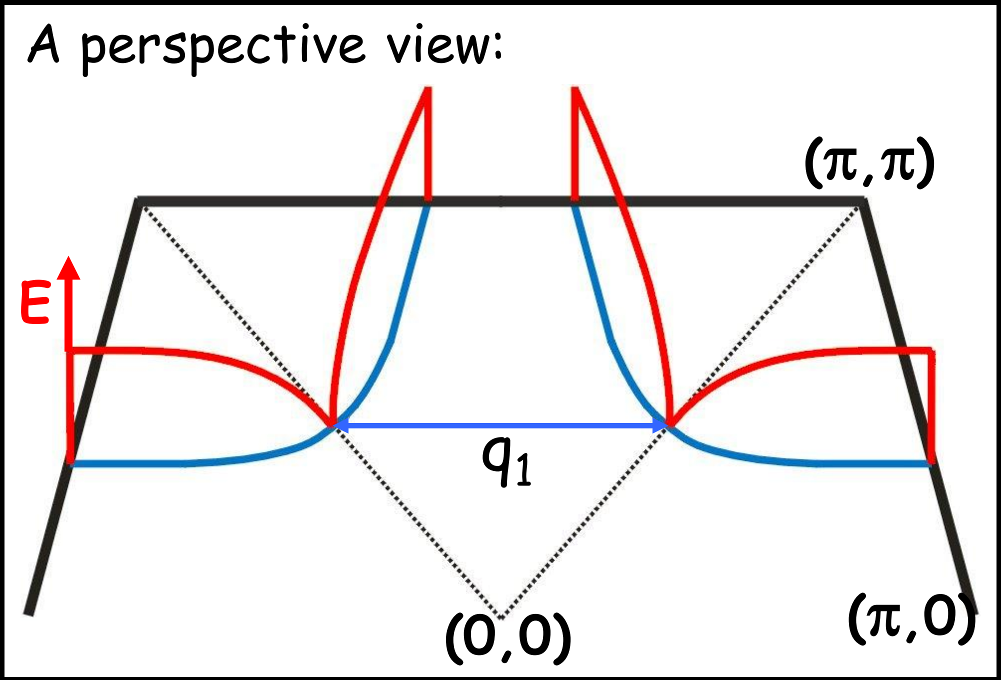

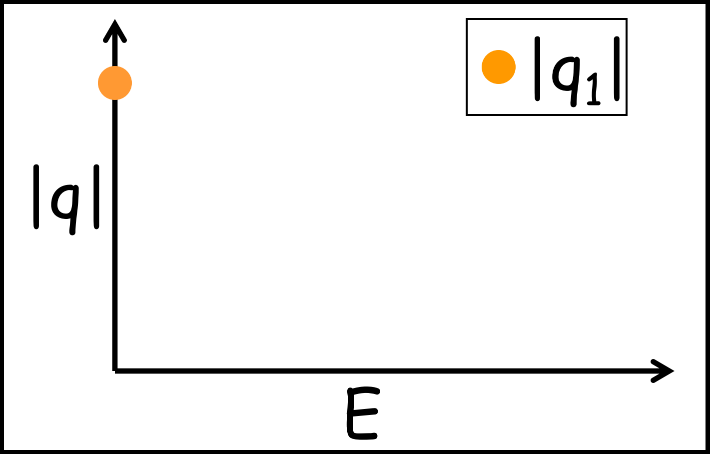

Expected energy dependence of $|\vec{q}_1|$

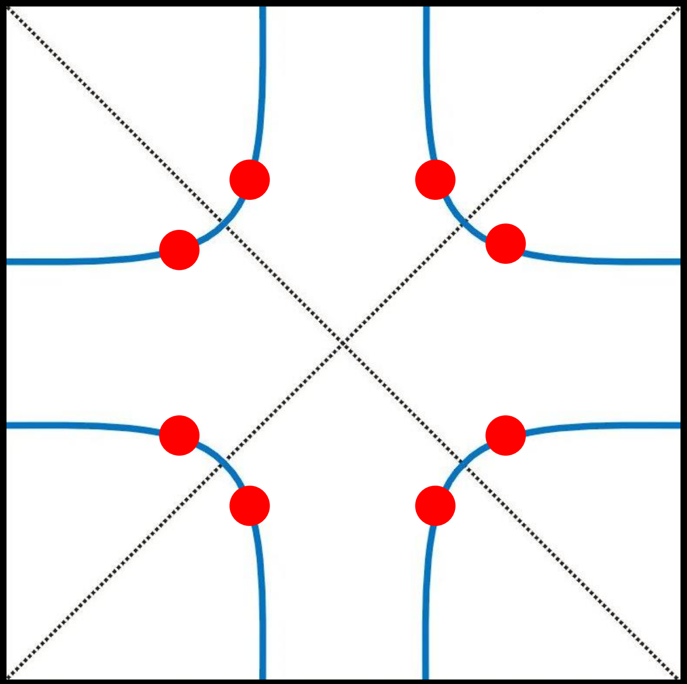

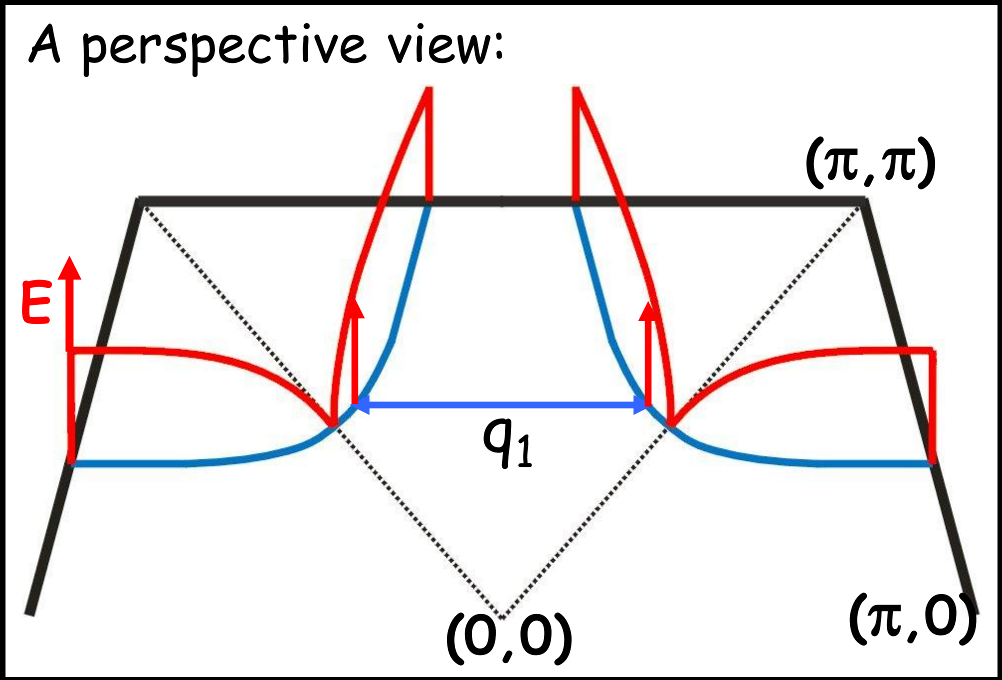

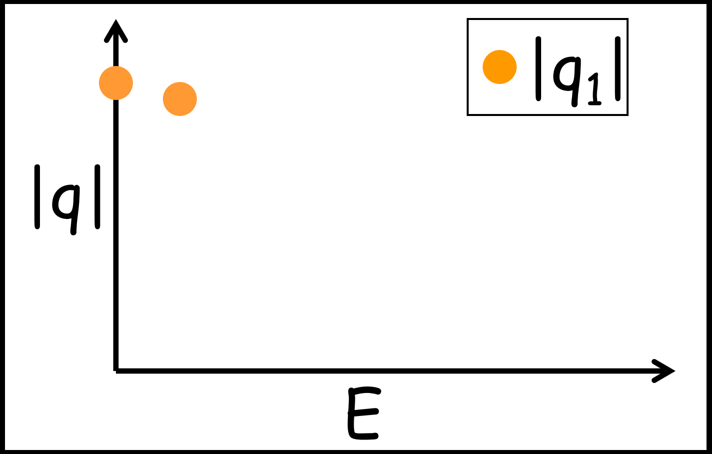

Expected energy dependence of $|\vec{q}_1|$

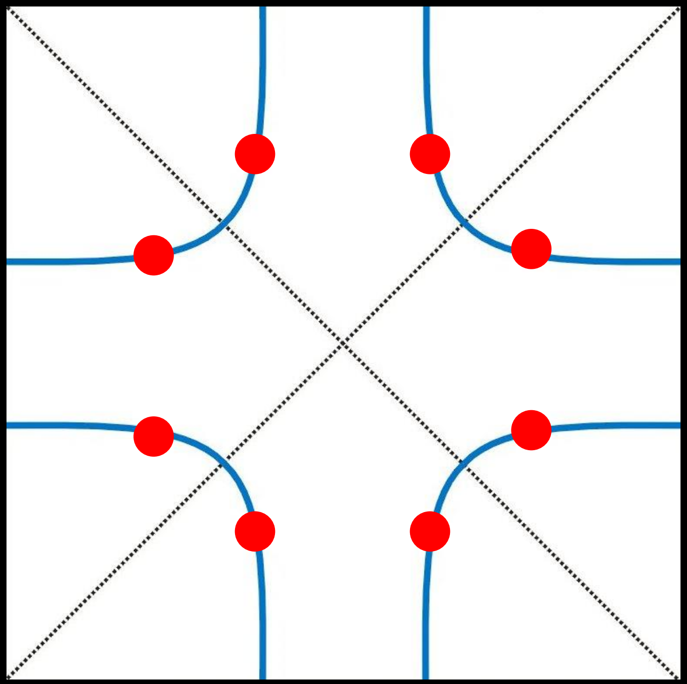

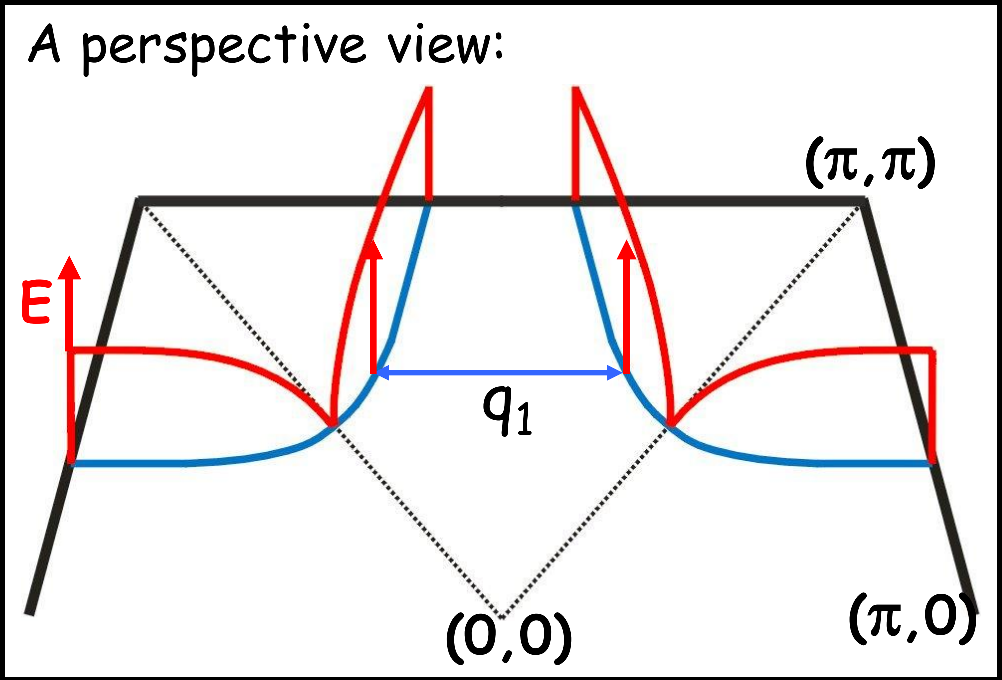

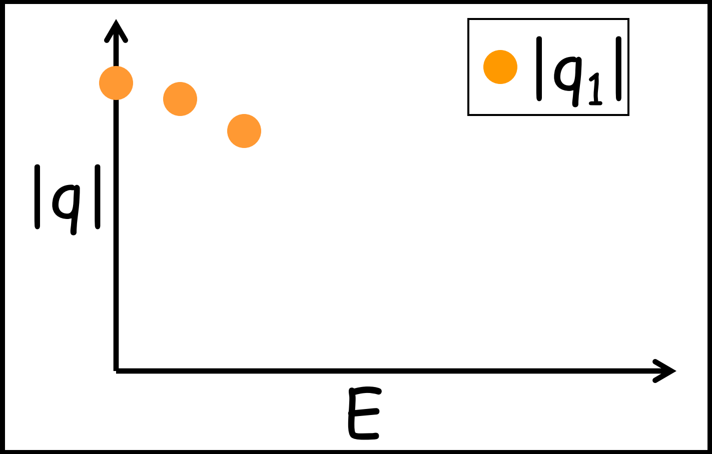

Expected energy dependence of $|\vec{q}_1|$

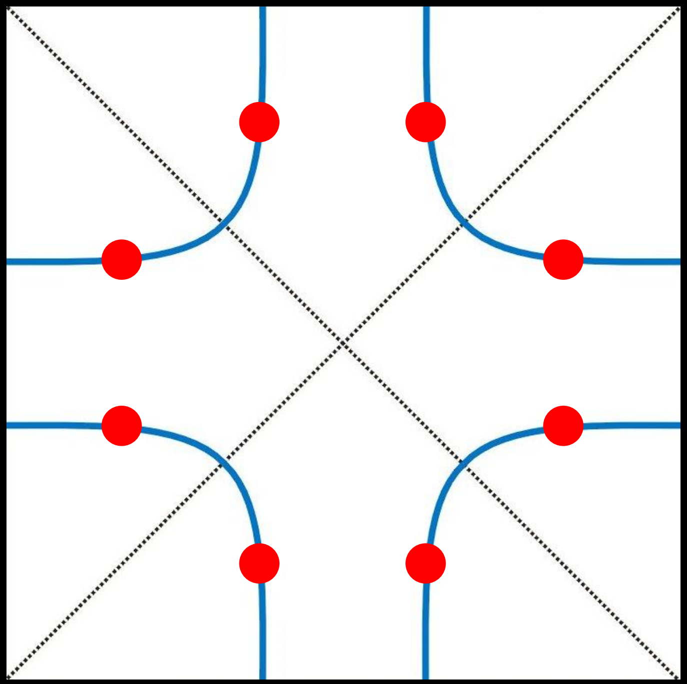

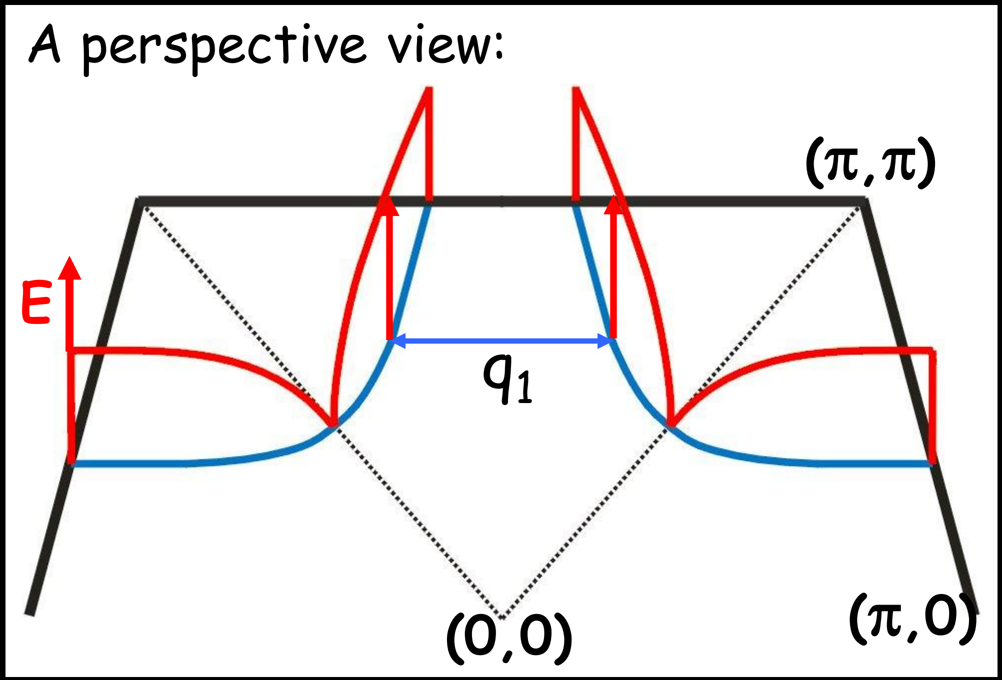

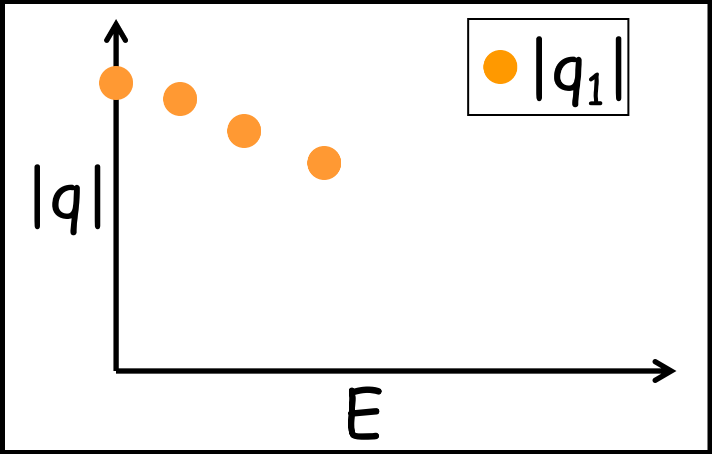

Expected energy dependence of $|\vec{q}_1|$

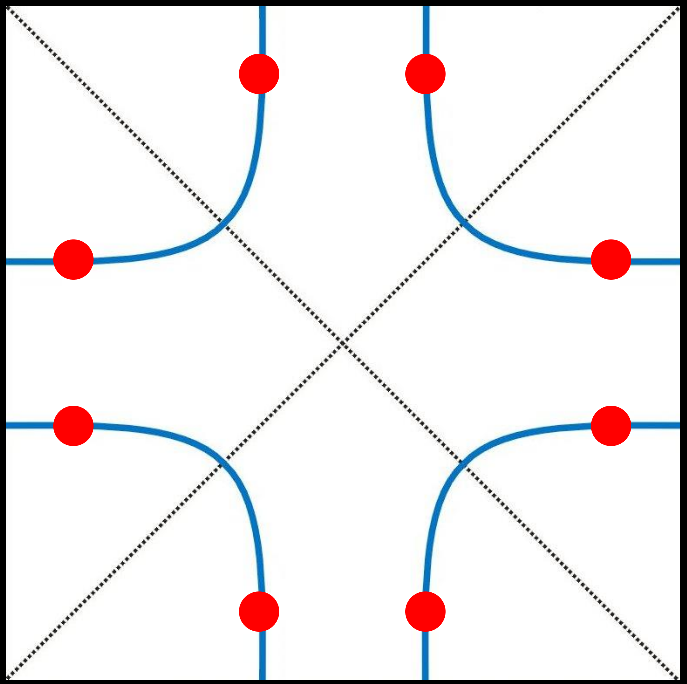

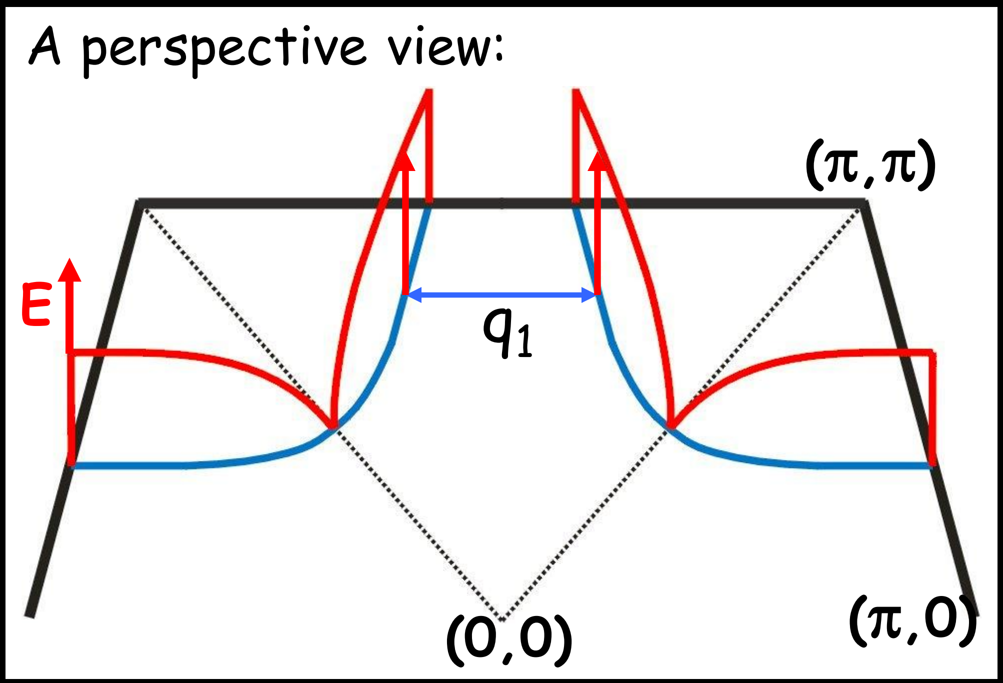

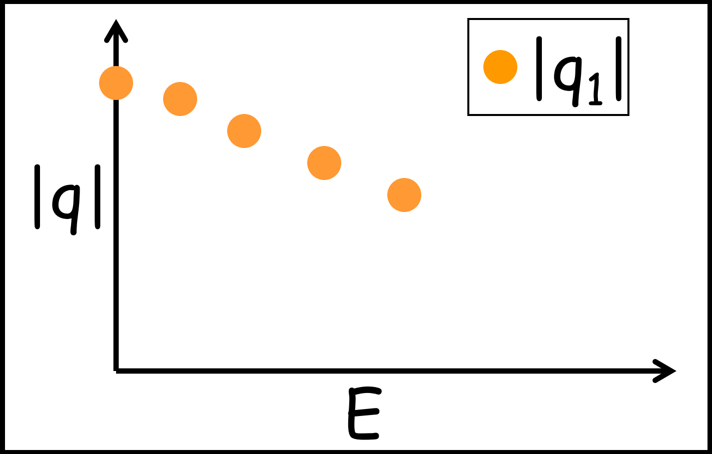

For example, look at the dispersion of:

$\vec{q_7} \parallel (\pm\pi, \pm\pi)$

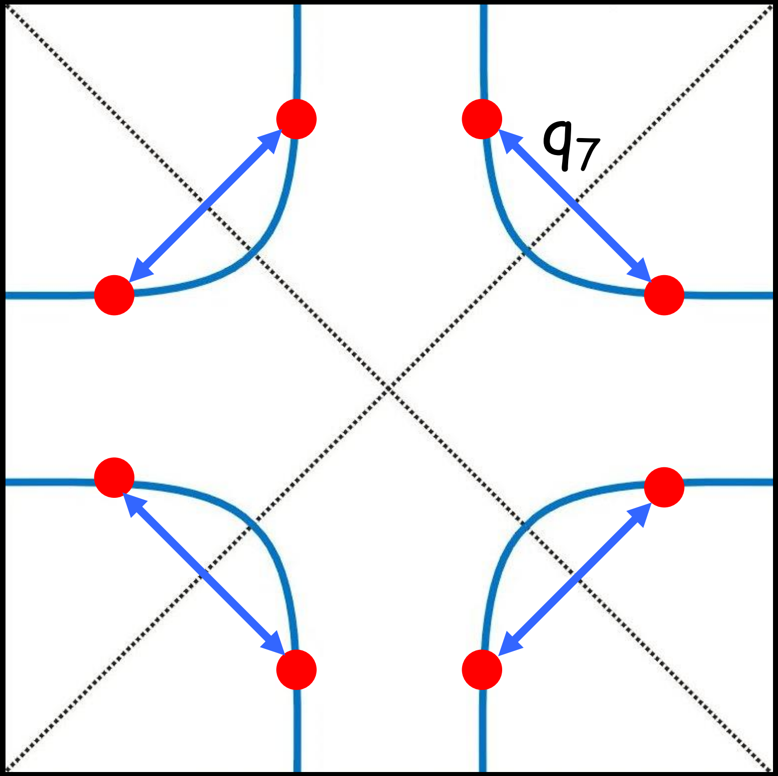

Expected energy dependence of $|\vec{q}_7|$

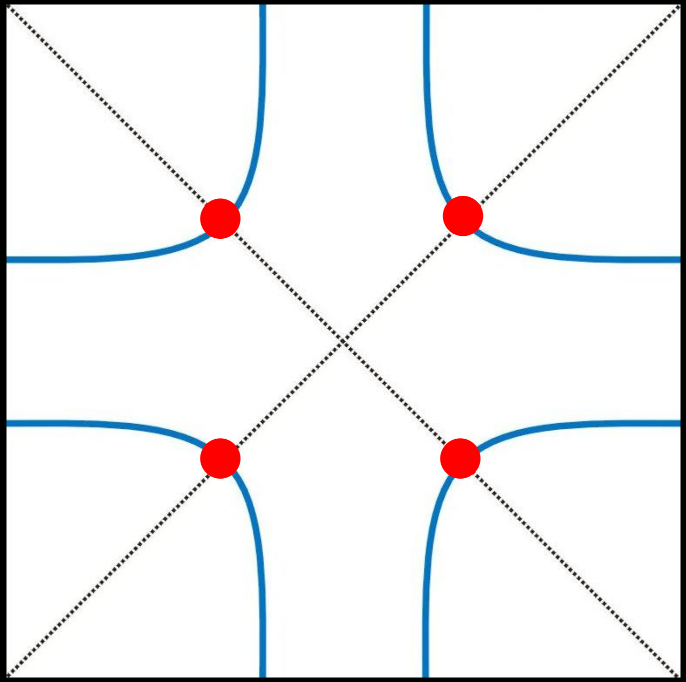

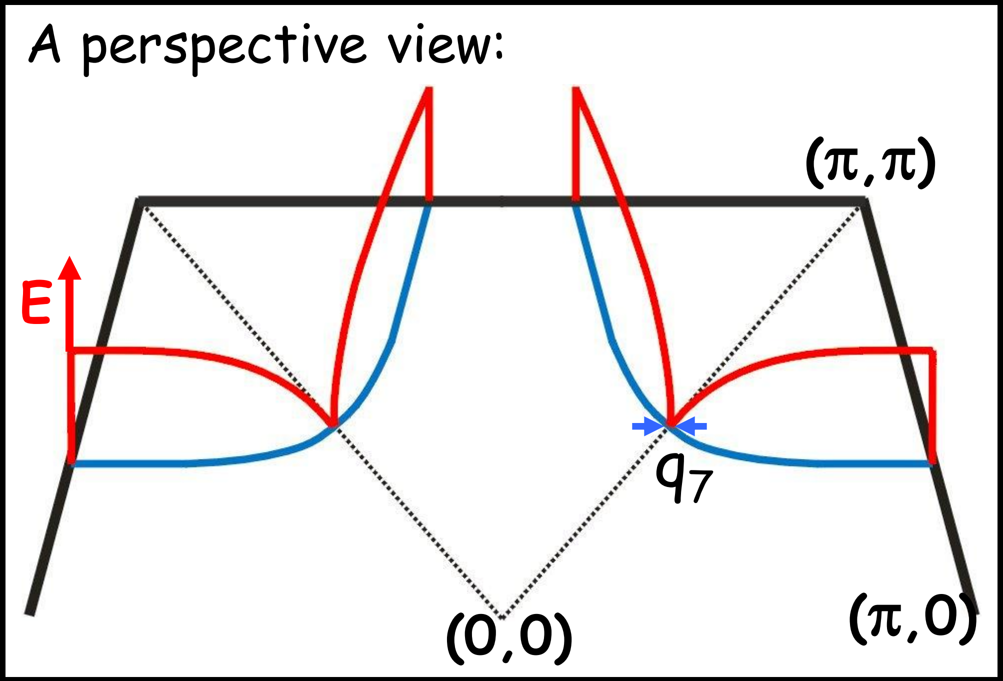

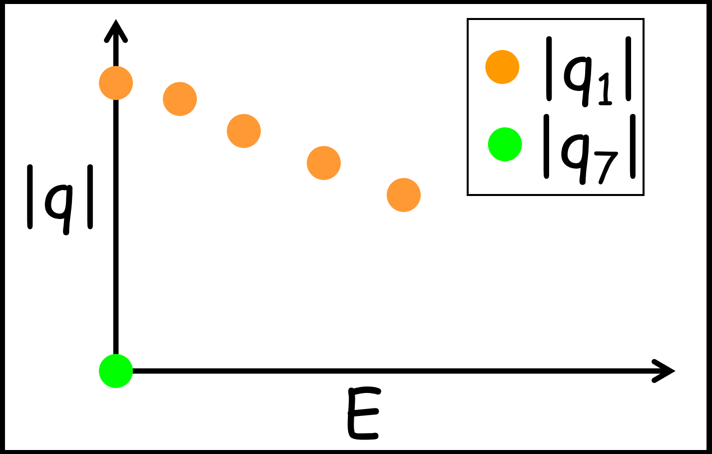

Expected energy dependence of $|\vec{q}_7|$

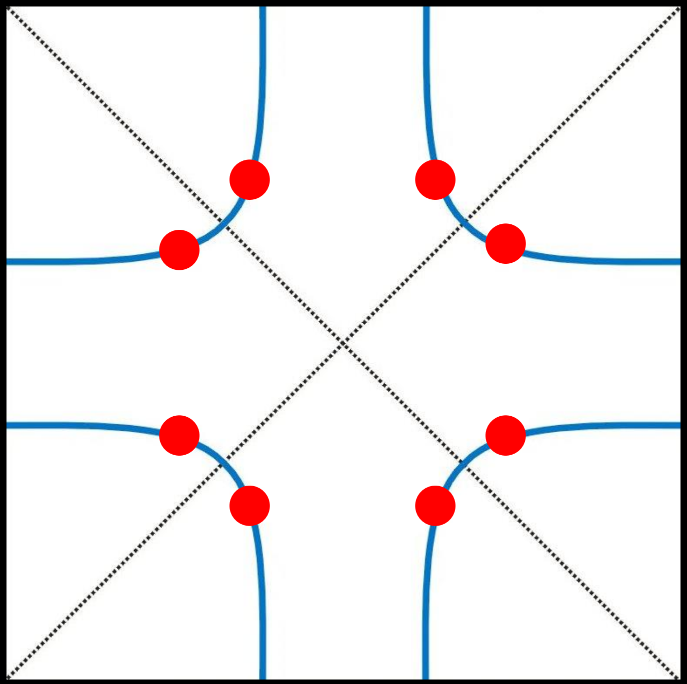

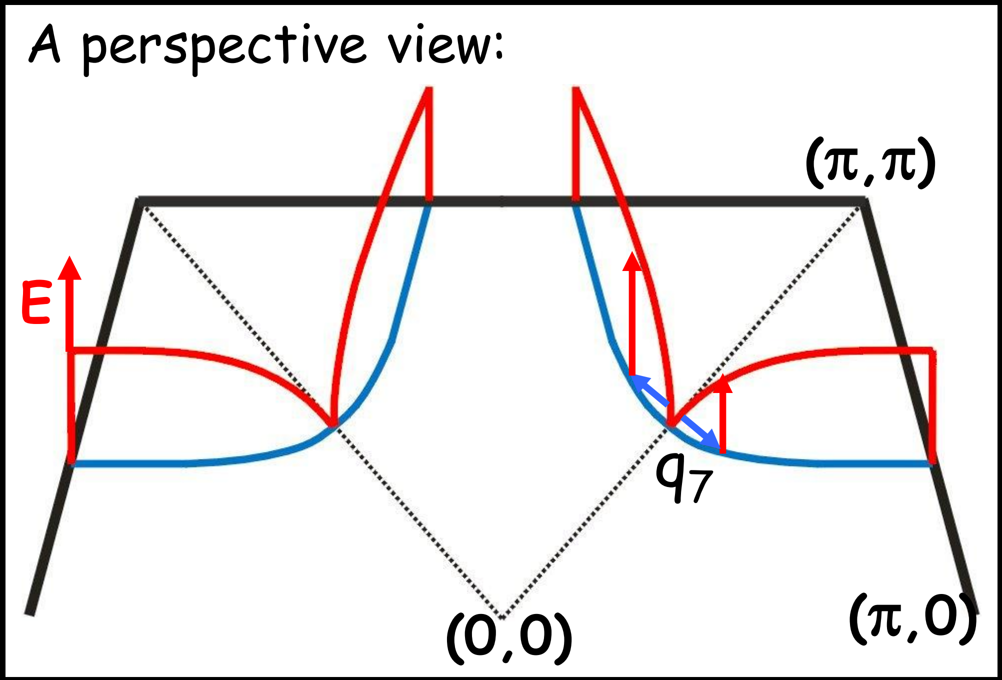

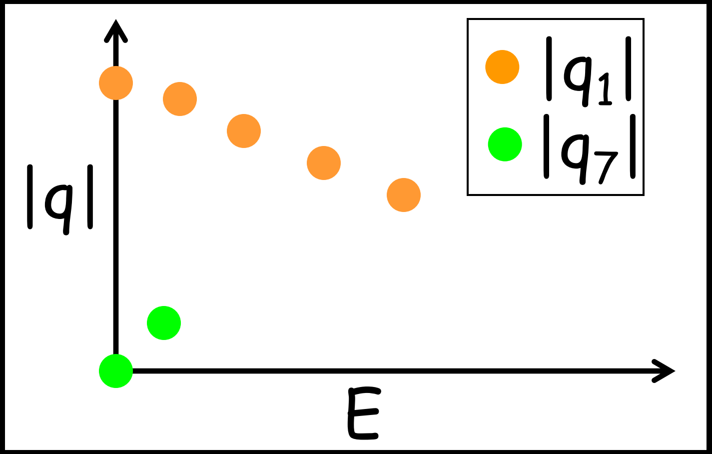

Expected energy dependence of $|\vec{q}_7|$

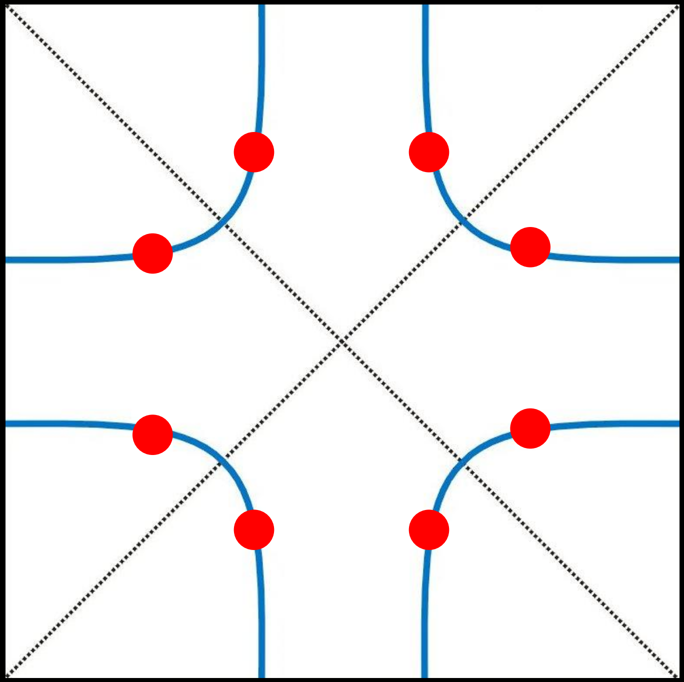

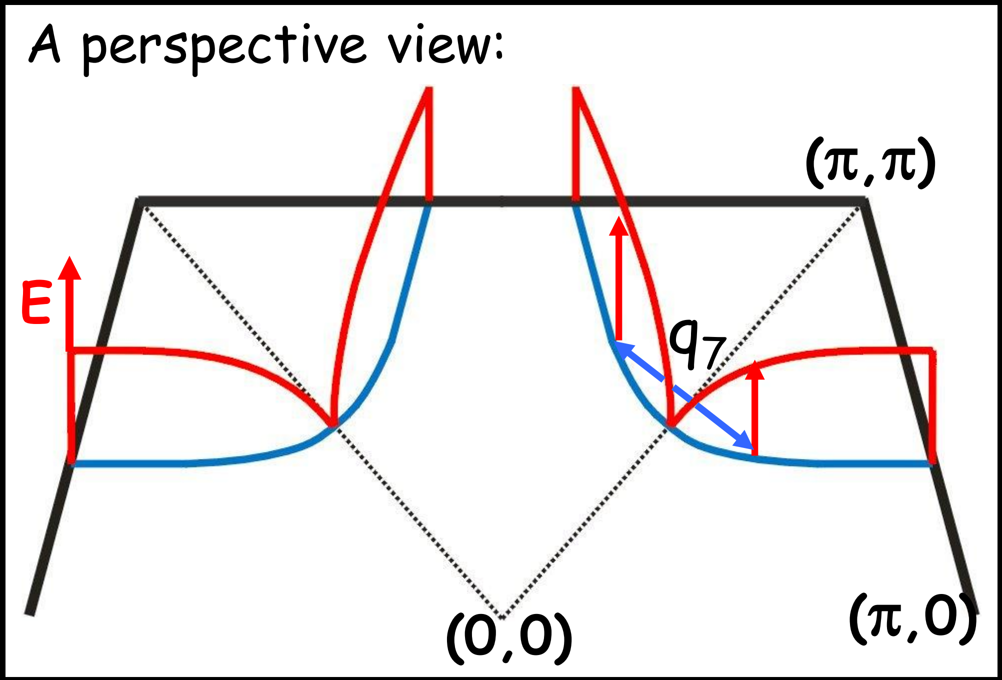

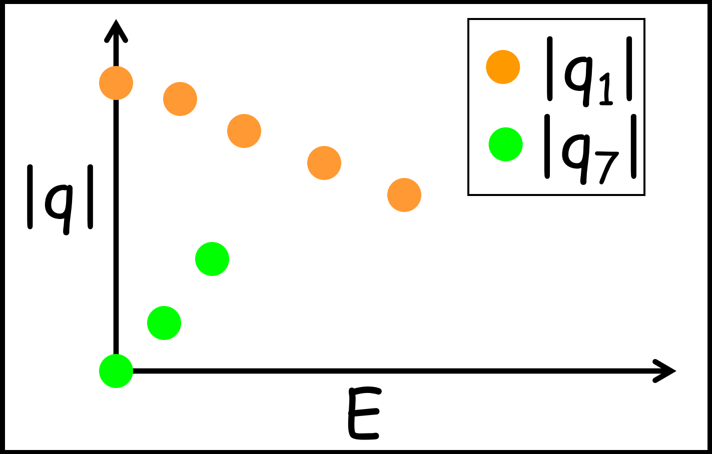

Expected energy dependence of $|\vec{q}_7|$

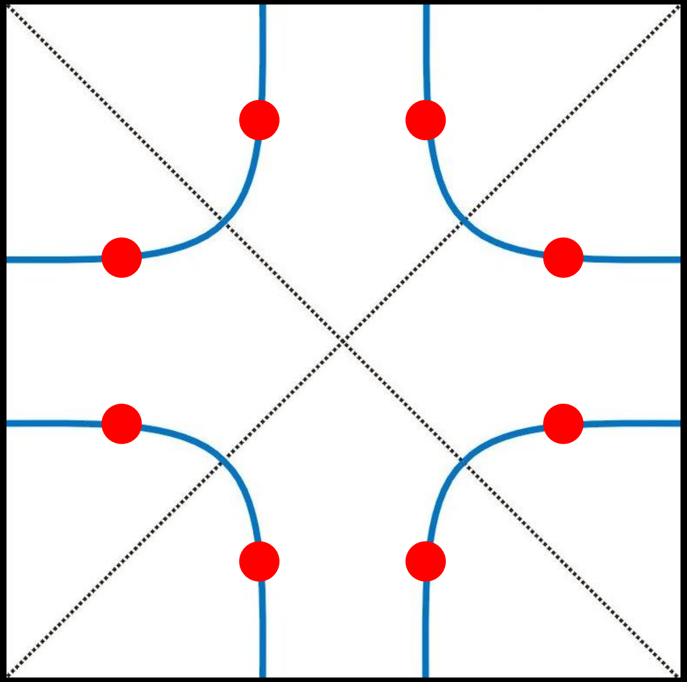

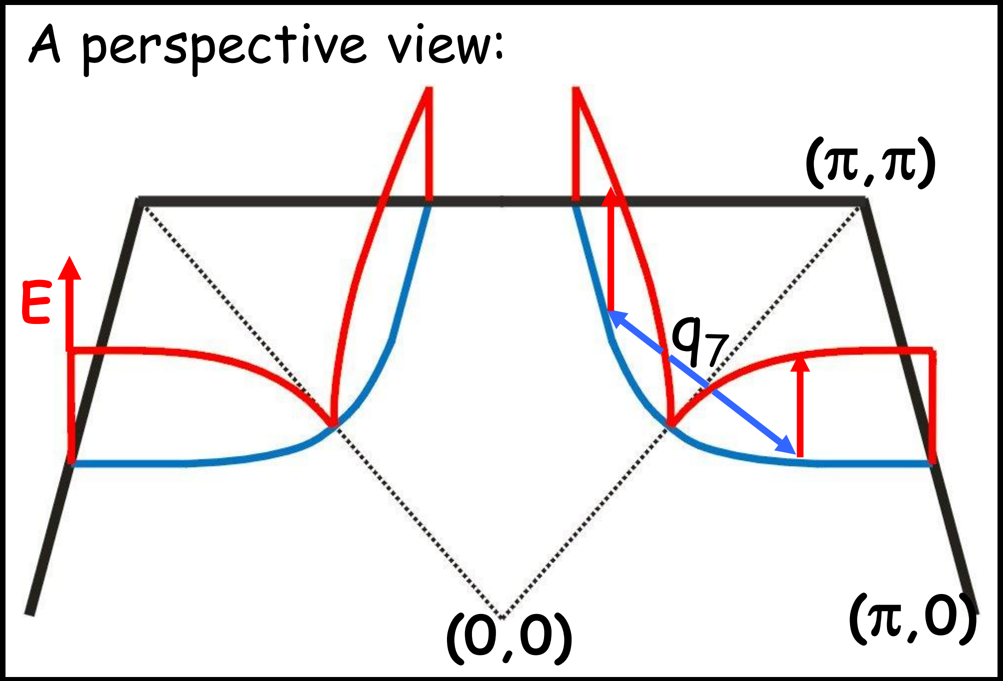

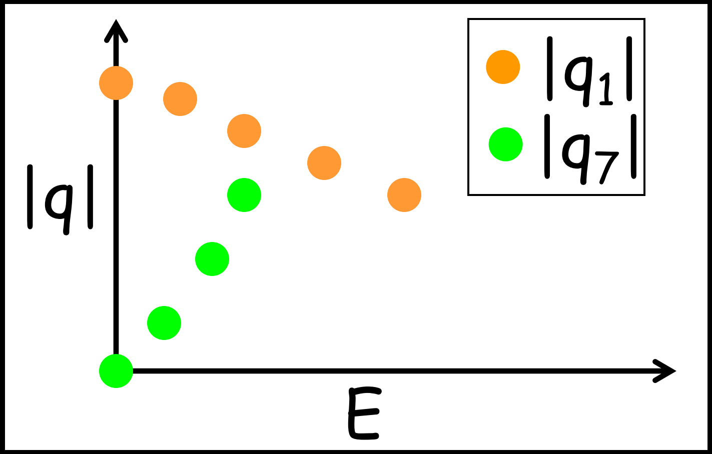

Expected energy dependence of $|\vec{q}_7|$

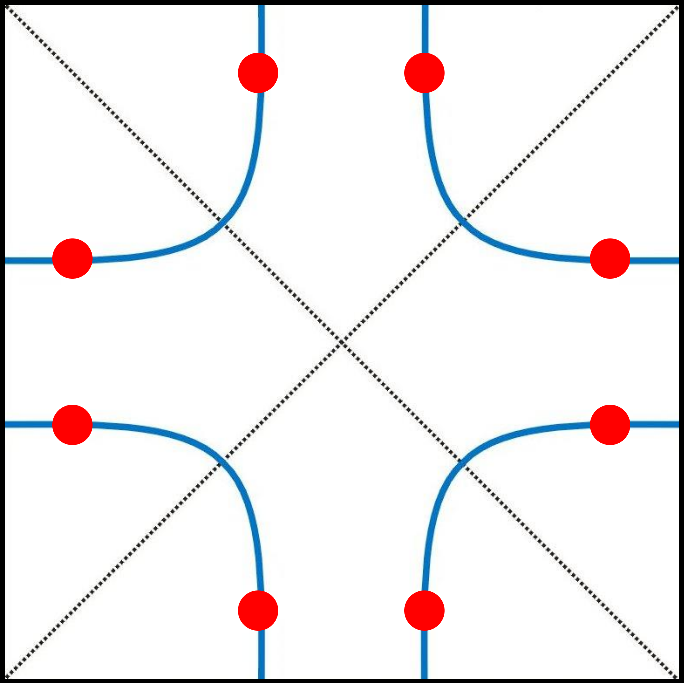

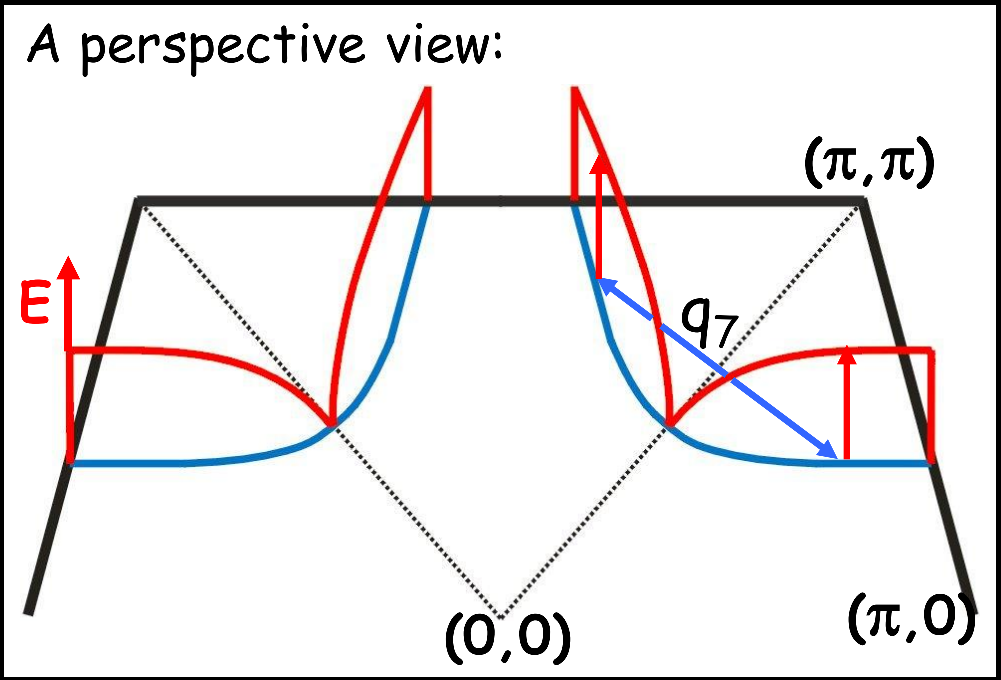

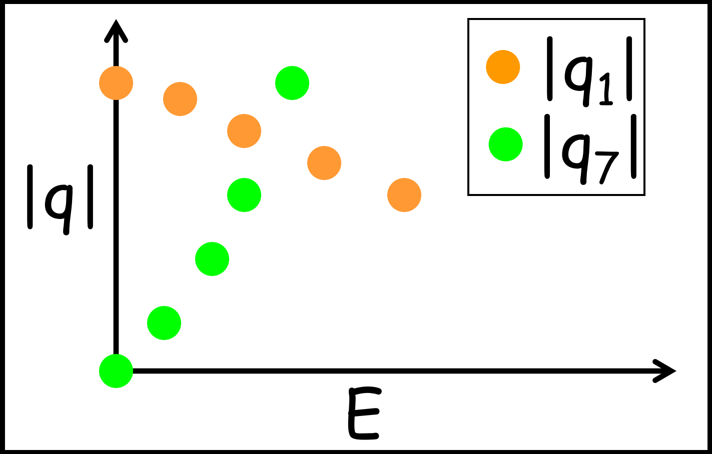

Expected energy dependence of 5 independent q_i's

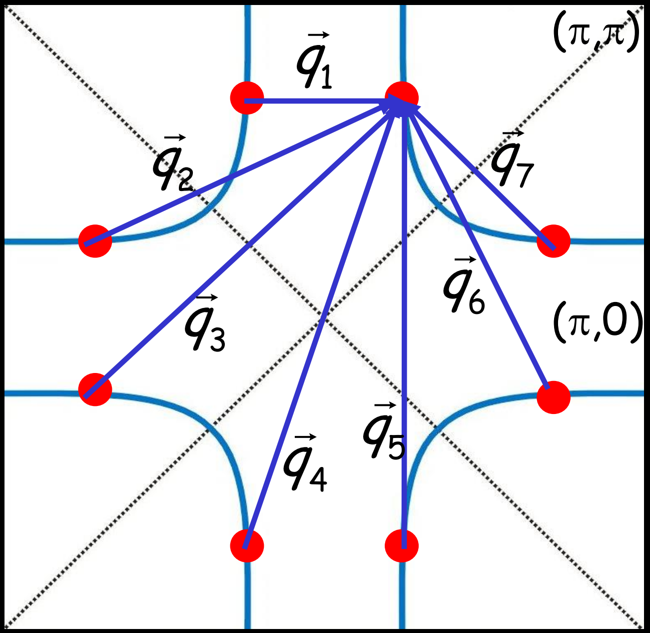

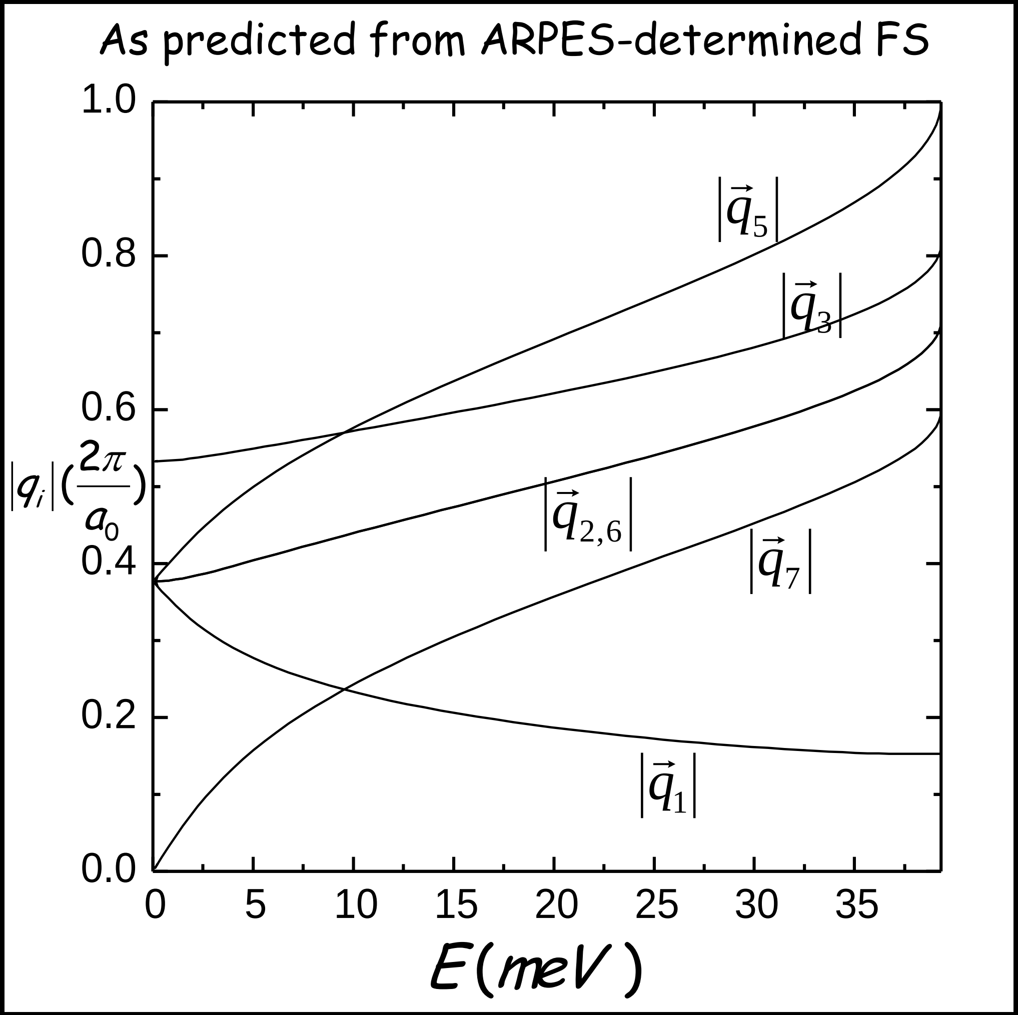

$Bi_2Sr_2CaCu_2O_{8+d}$ Data

topograph

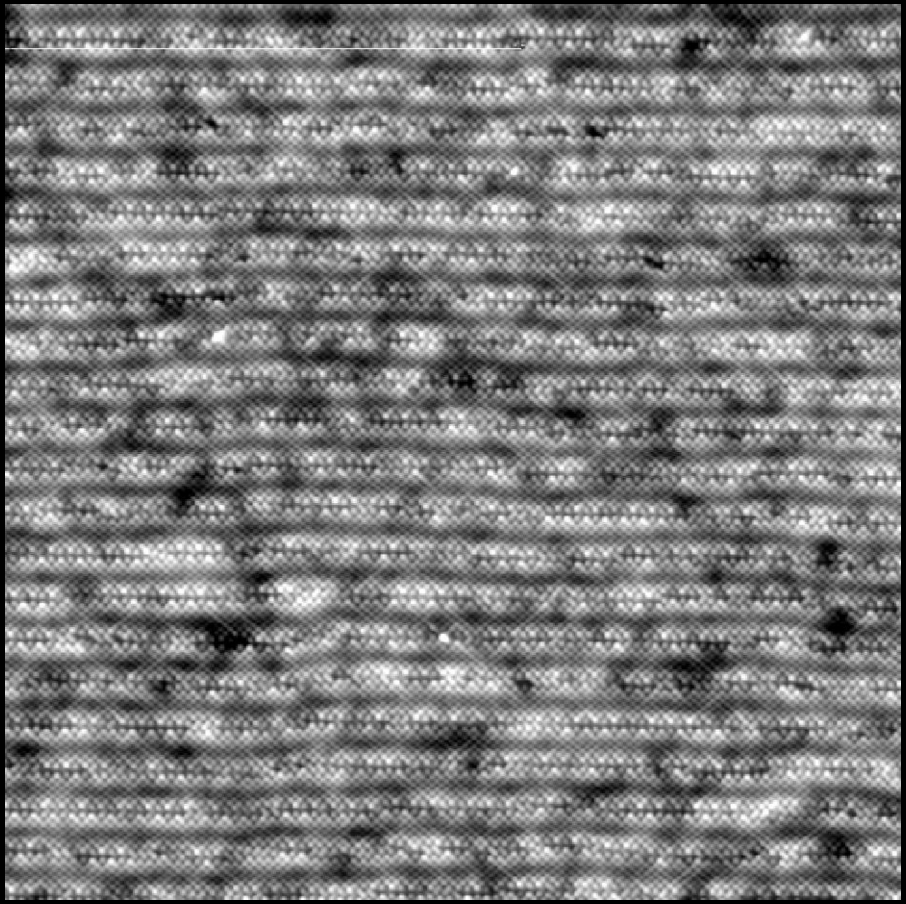

545 Å

Bi-2212
T_c=76 K
Δ~51meV

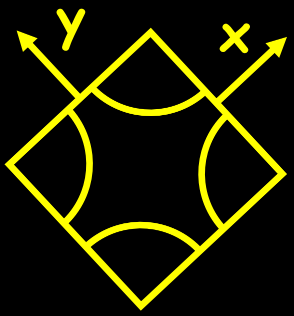

Imaging quasiparticle wavefunctions

energy (meV)

$g(\vec{r},E)$

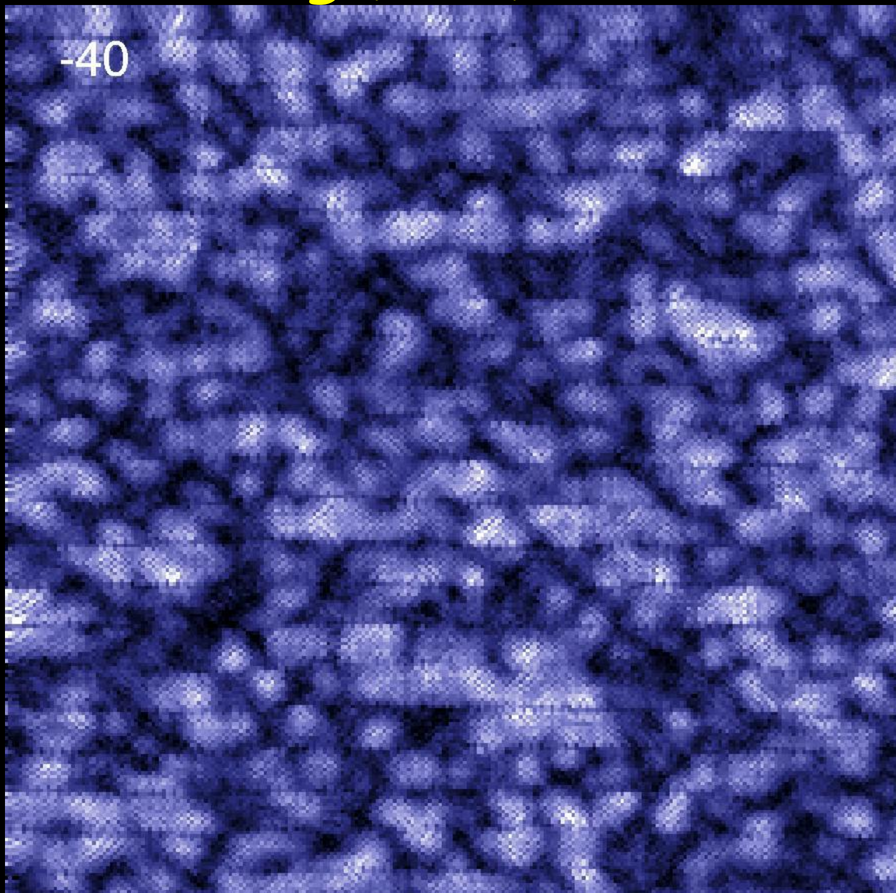

545 Å

FFT

$g(\vec{q},E) = \sqrt{P(\vec{q},E)}$

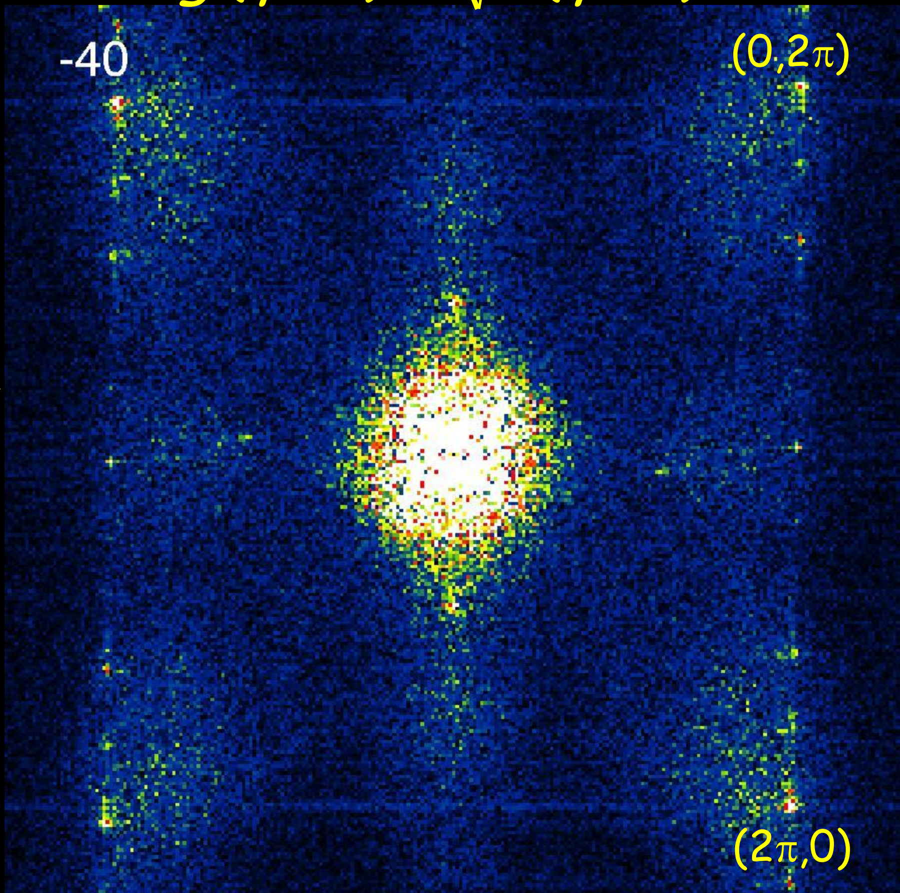

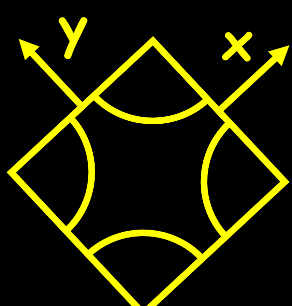

Bi-2212

T_c=76 K

Δ~51meV

Imaging quasiparticle wavefunctions

energy (meV)

$g(\vec{r},E)$

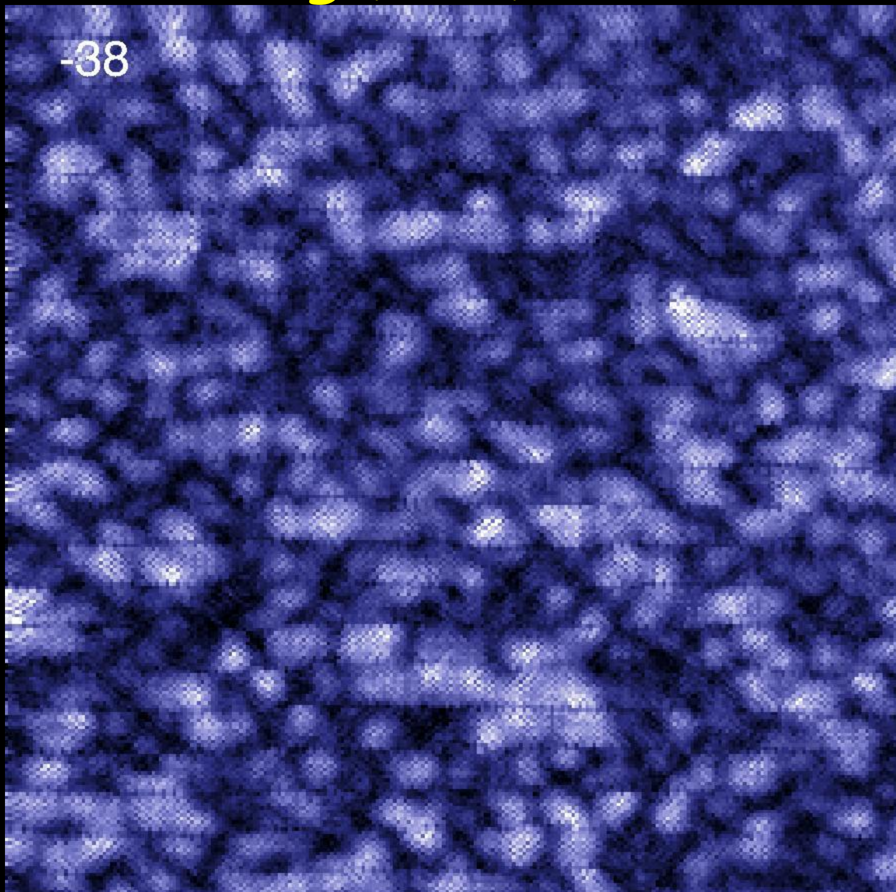

545 Å

FFT

$g(\vec{q},E) = \sqrt{P(\vec{q},E)}$

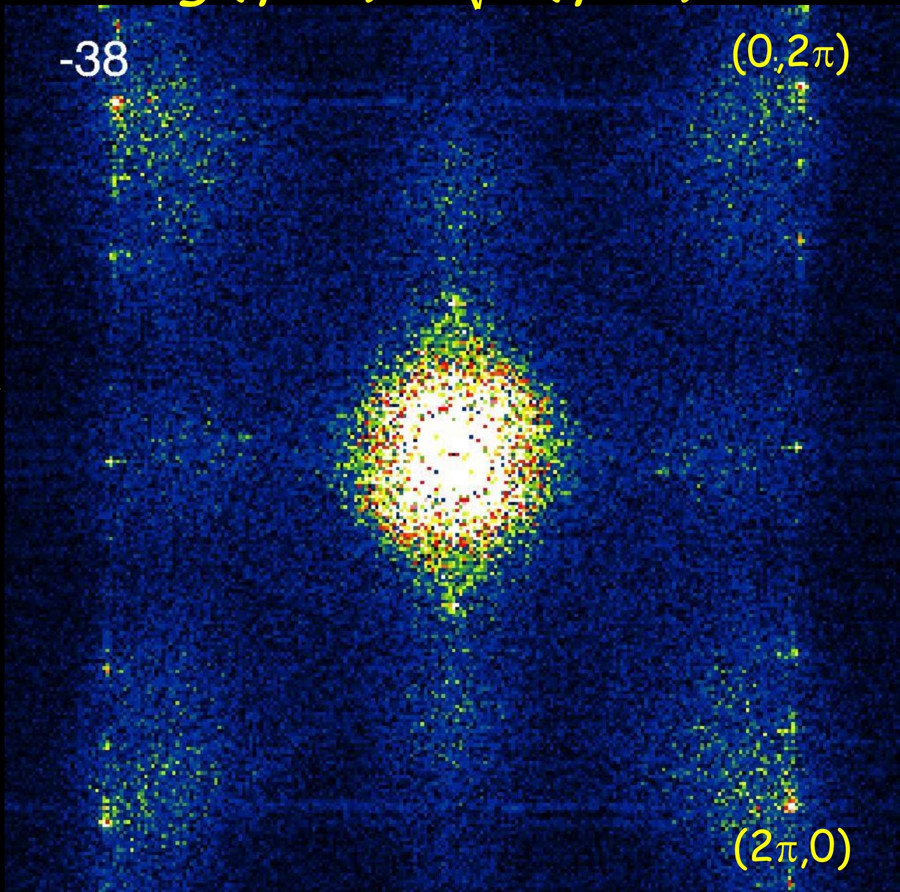

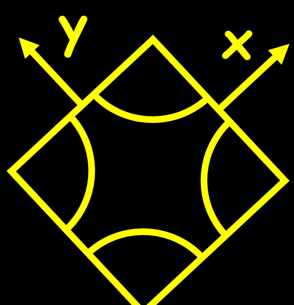

Bi-2212

T_c=76 K

Δ~51meV

Imaging quasiparticle wavefunctions

energy (meV)

$g(\vec{r},E)$

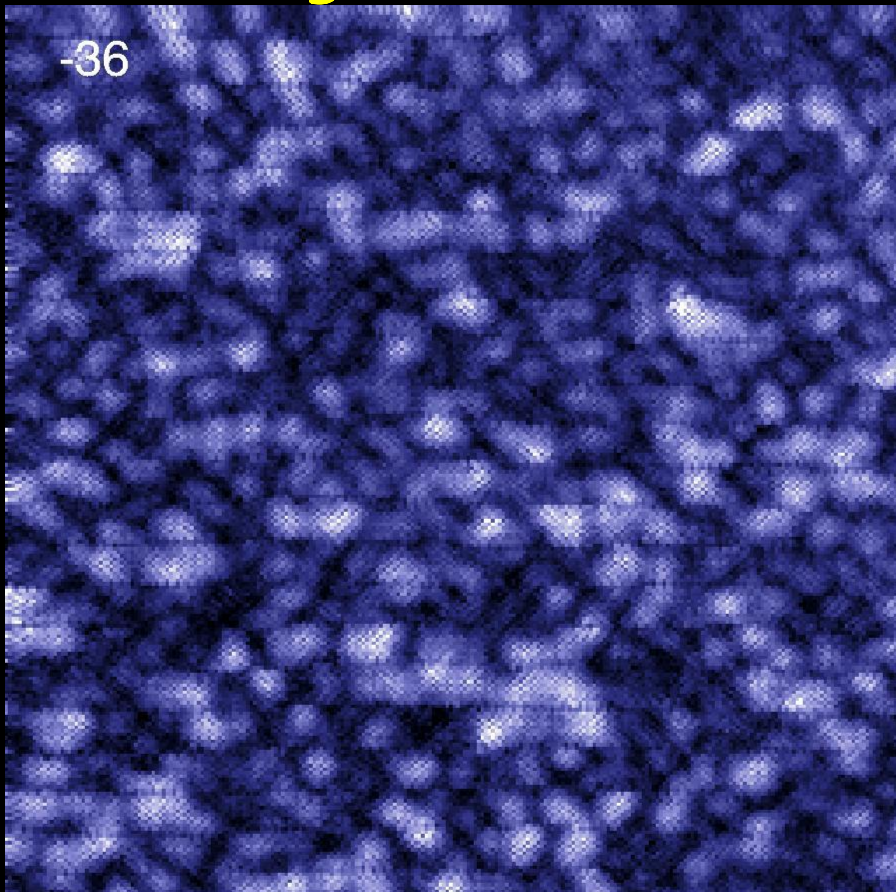

545 Å

FFT

$g(\vec{q},E)=\sqrt{P(\vec{q},E)}$

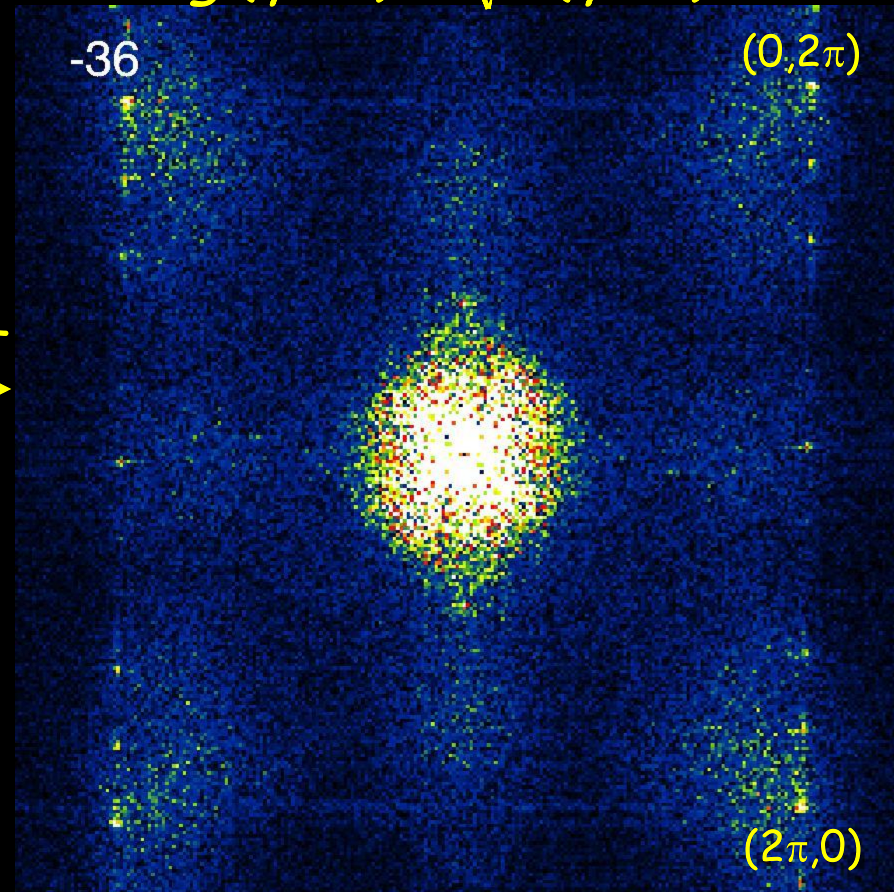

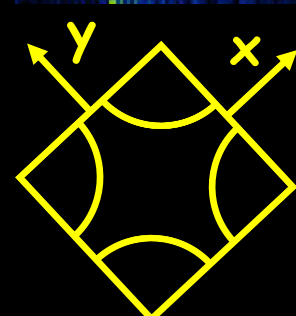

Bi-2212

T_c=76 K

Δ~51meV

Imaging quasiparticle wavefunctions

energy (meV)

$g(\vec{r},E)$

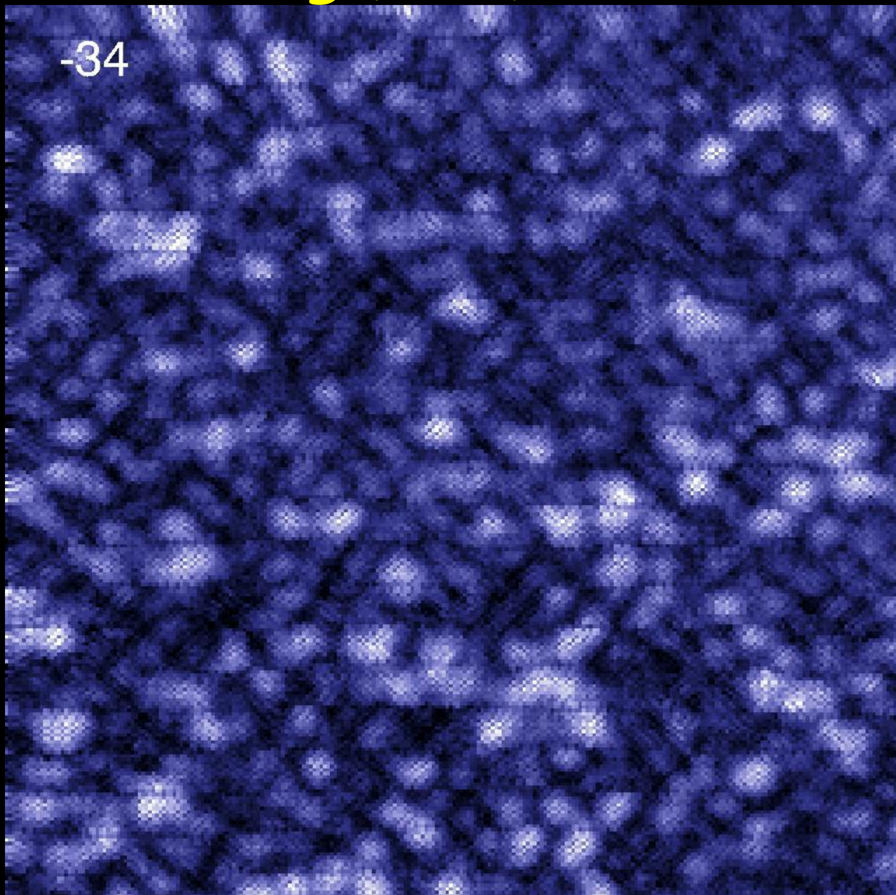

545 Å

FFT

$$g(\vec{q},E)=\sqrt{P(\vec{q},E)}$$

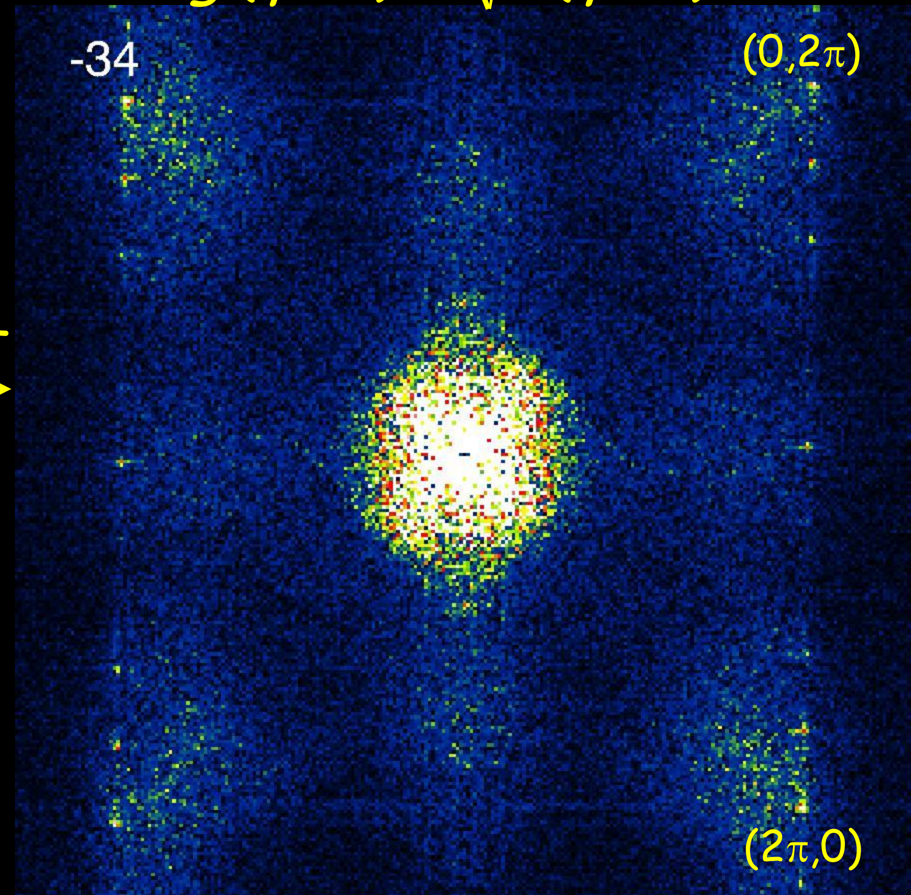

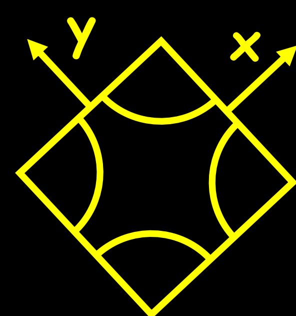

Bi-2212

T_c=76 K

Δ~51meV

Imaging quasiparticle wavefunctions

energy (meV)

$g(\vec{r},E)$

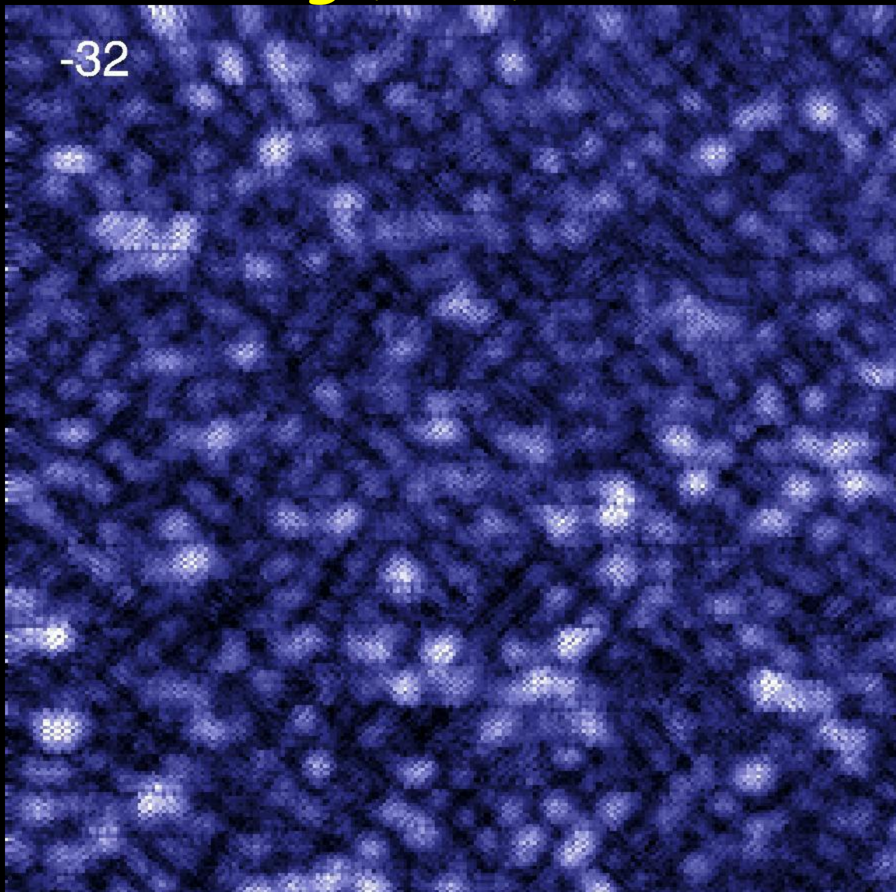

545 Å

FFT

$g(\vec{q},E)=\sqrt{P(\vec{q},E)}$

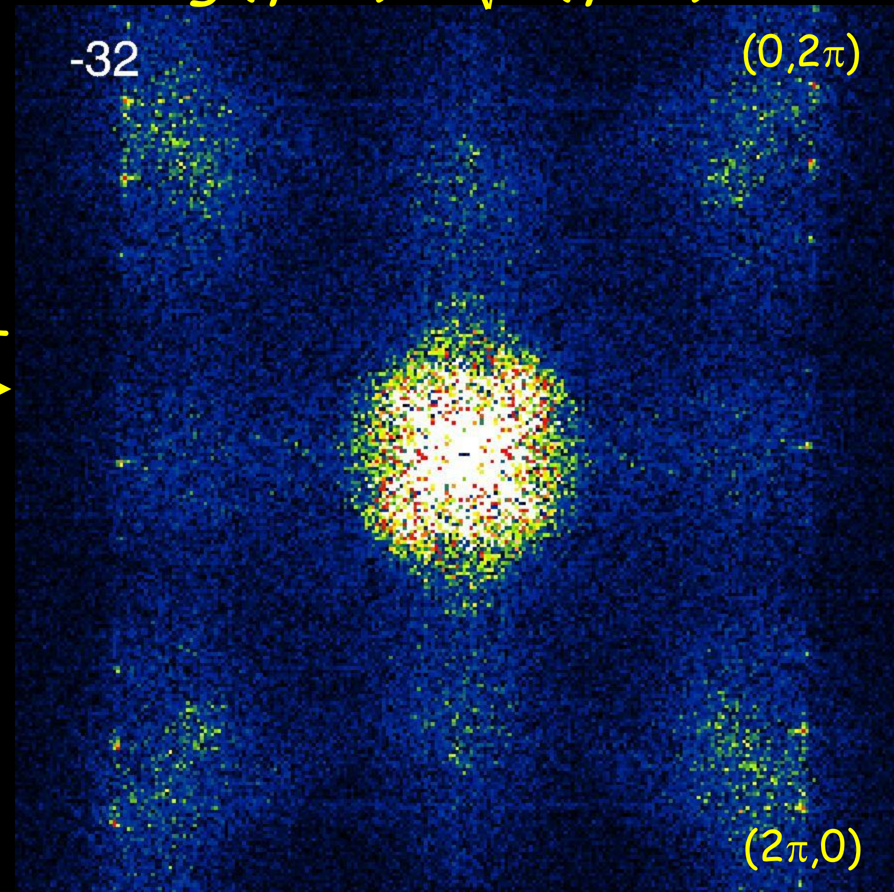

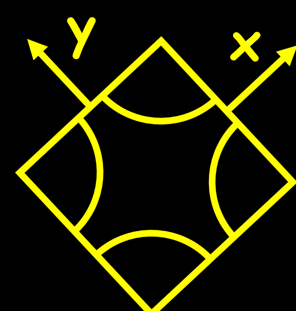

Bi-2212

T_c=76 K

Δ~51meV

Imaging quasiparticle wavefunctions

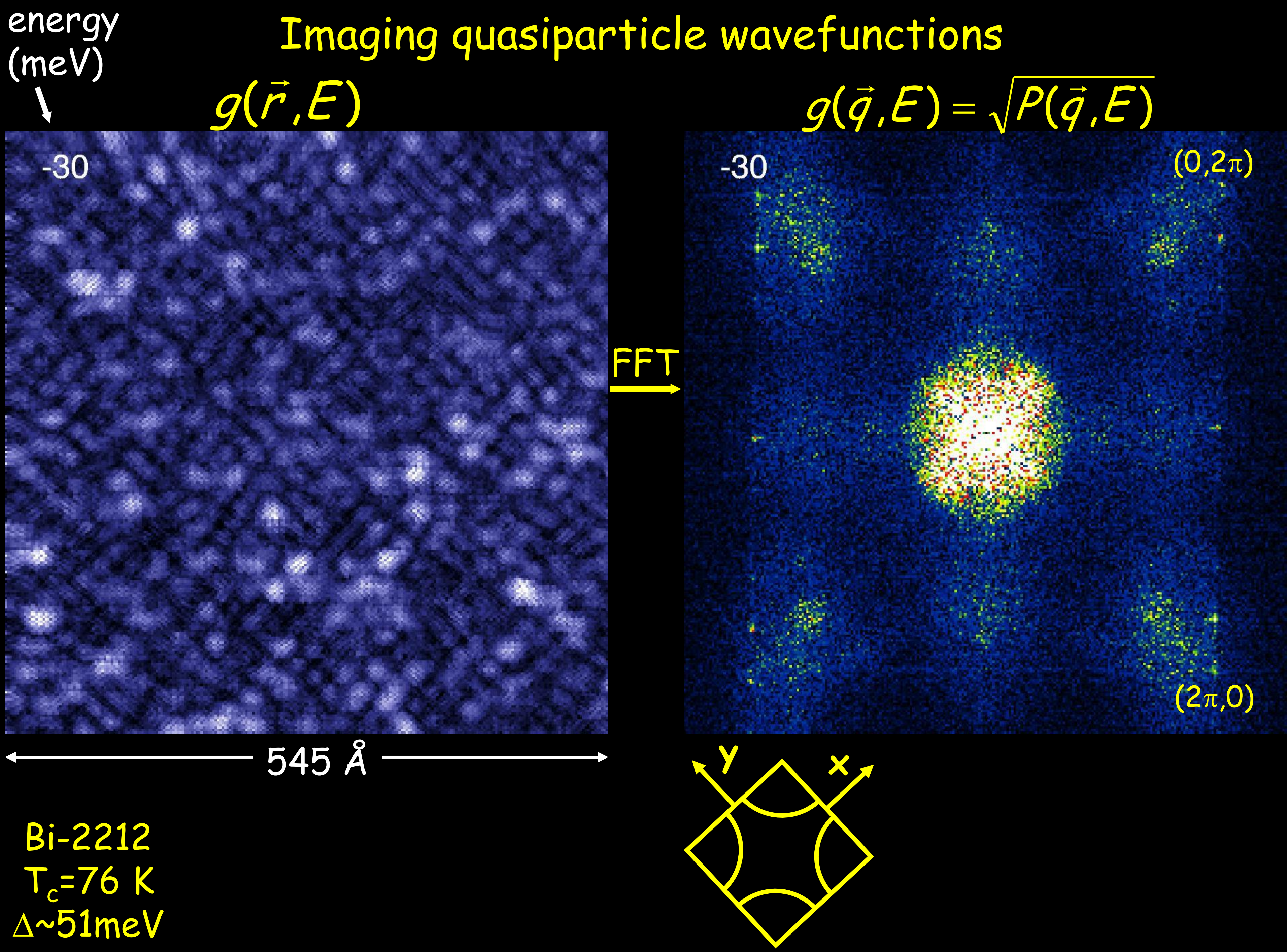

Bi-2212
T_c=76 K
Δ~51meV

Imaging quasiparticle wavefunctions

energy (meV)

$g(\vec{r},E)$

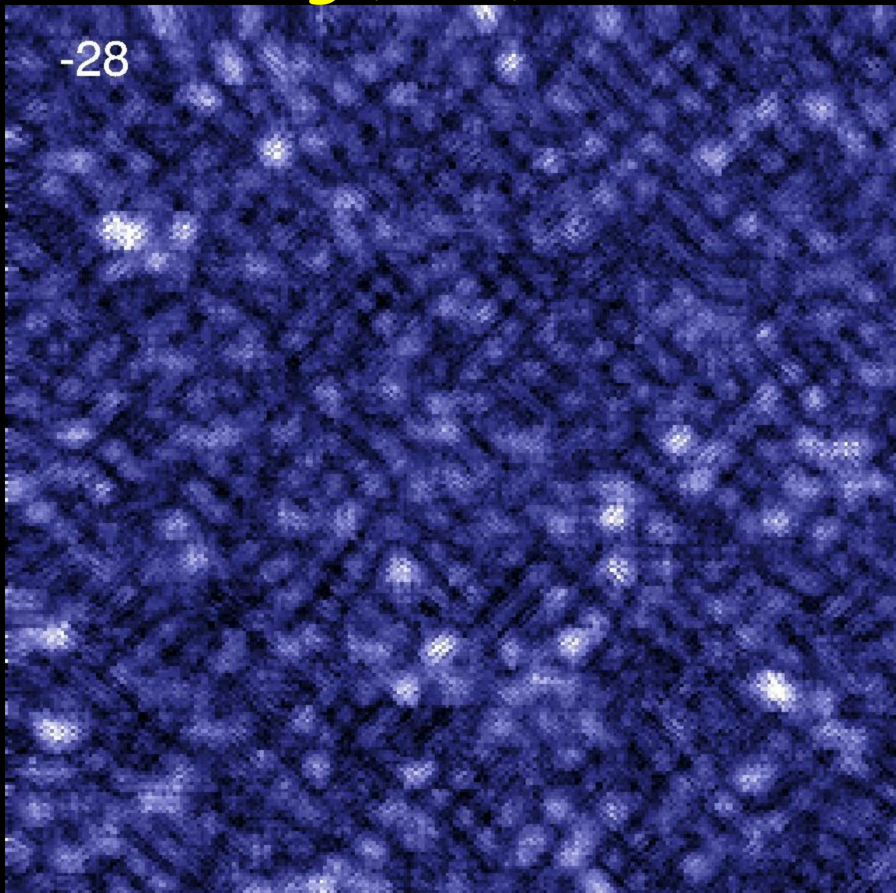

← 545 Å →

FFT →

$g(\vec{q},E)=\sqrt{P(\vec{q},E)}$

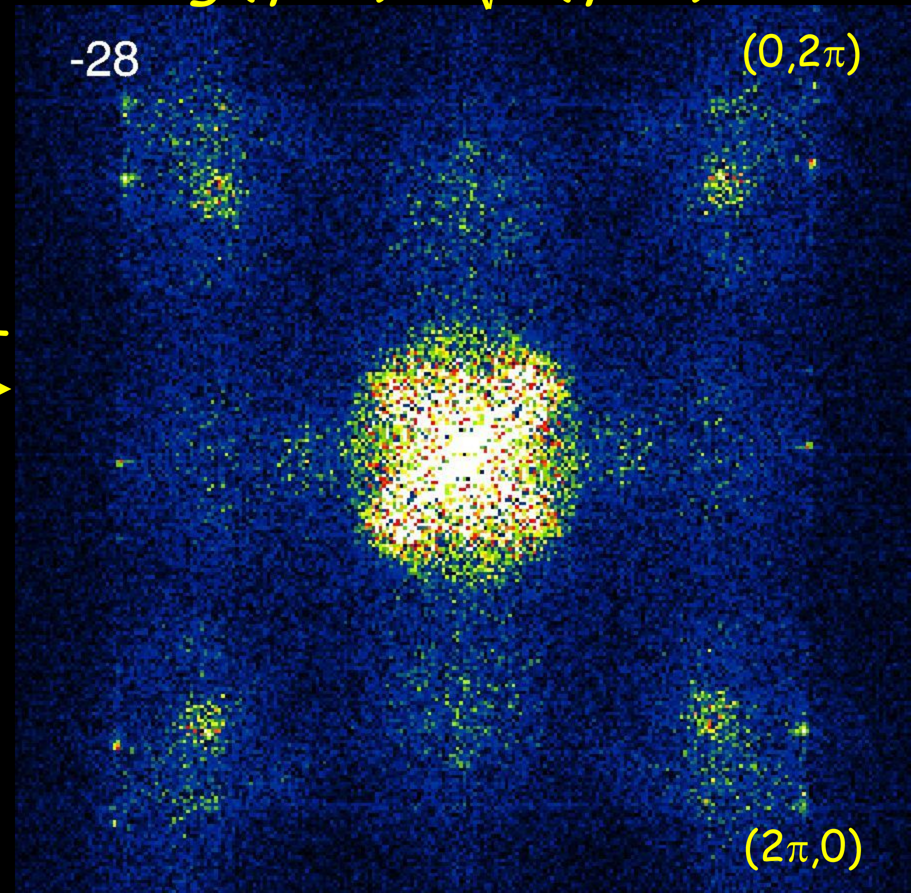

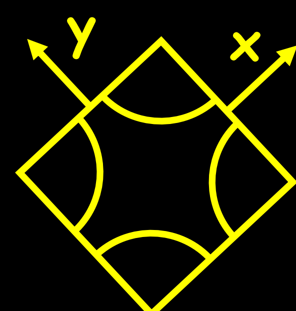

Bi-2212
T_c=76 K
Δ~51meV

Imaging quasiparticle wavefunctions

energy (meV)

$g(\vec{r},E)$

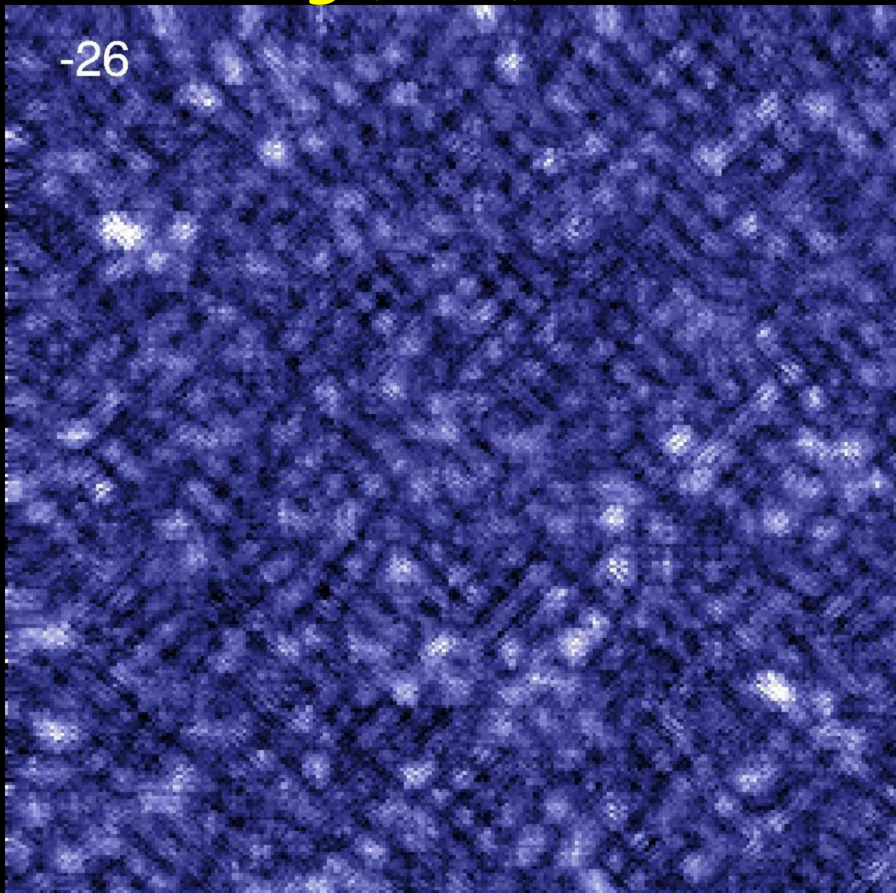

545 Å

FFT

$g(\vec{q},E)=\sqrt{P(\vec{q},E)}$

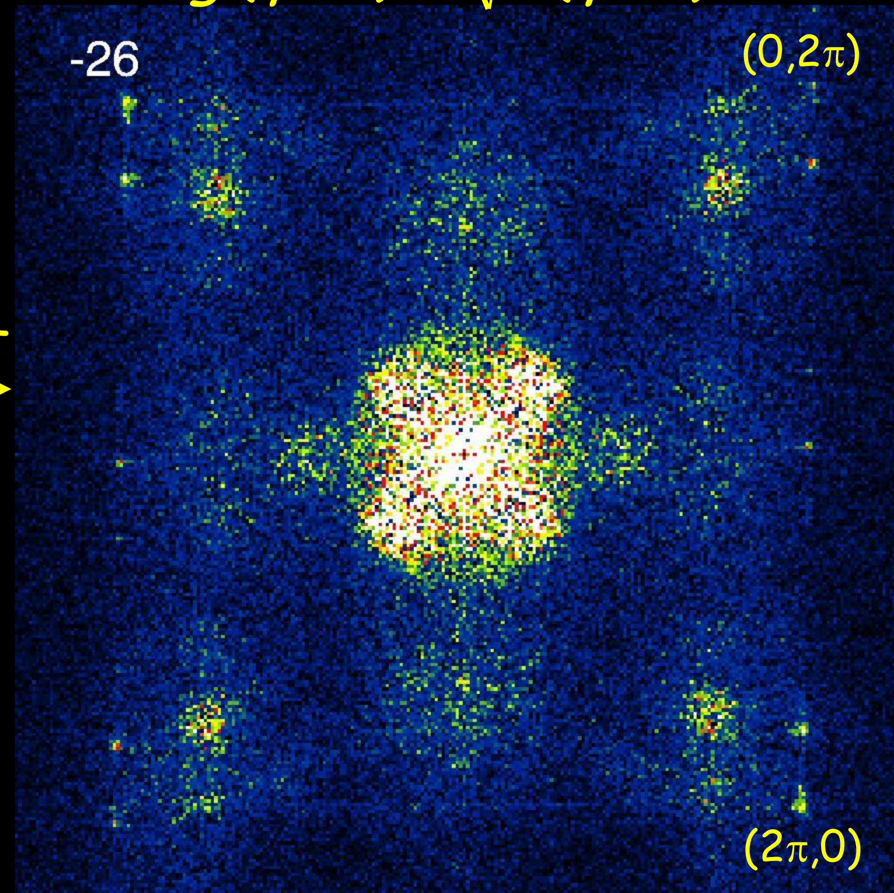

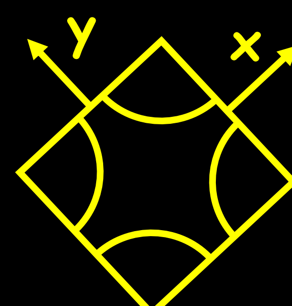

Bi-2212
T_c=76 K
Δ~51meV

Imaging quasiparticle wavefunctions

energy (meV)

$g(\vec{r},E)$

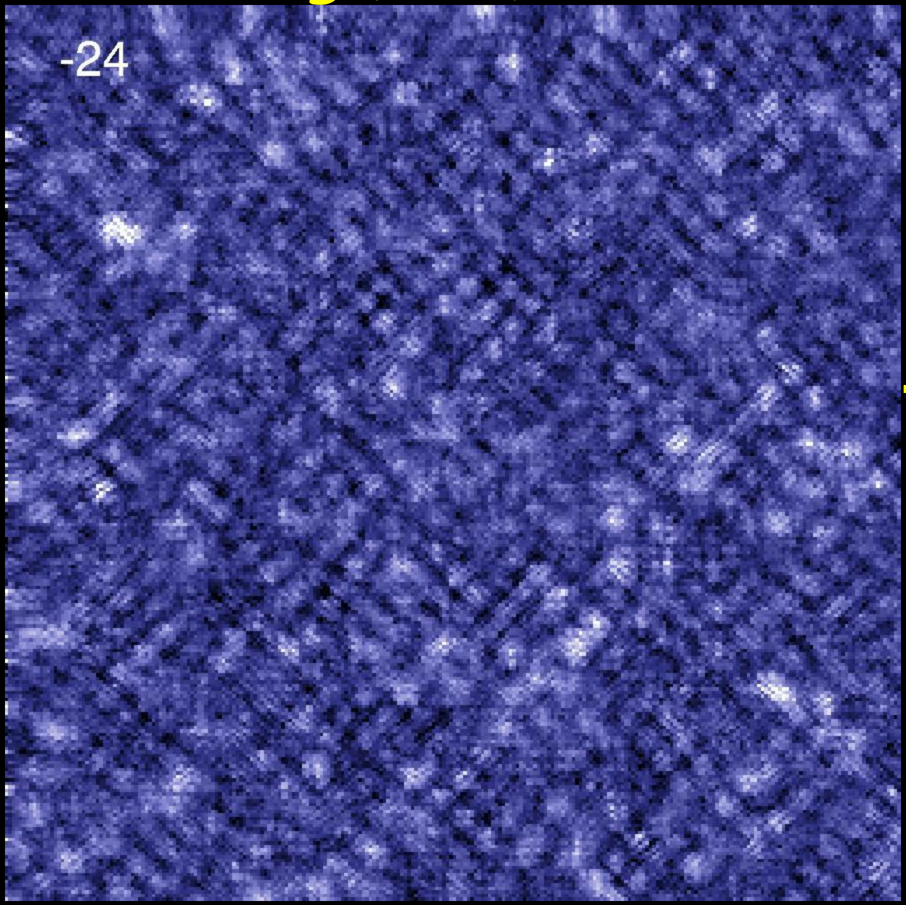

545 Å

FFT

$g(\vec{q},E)=\sqrt{P(\vec{q},E)}$

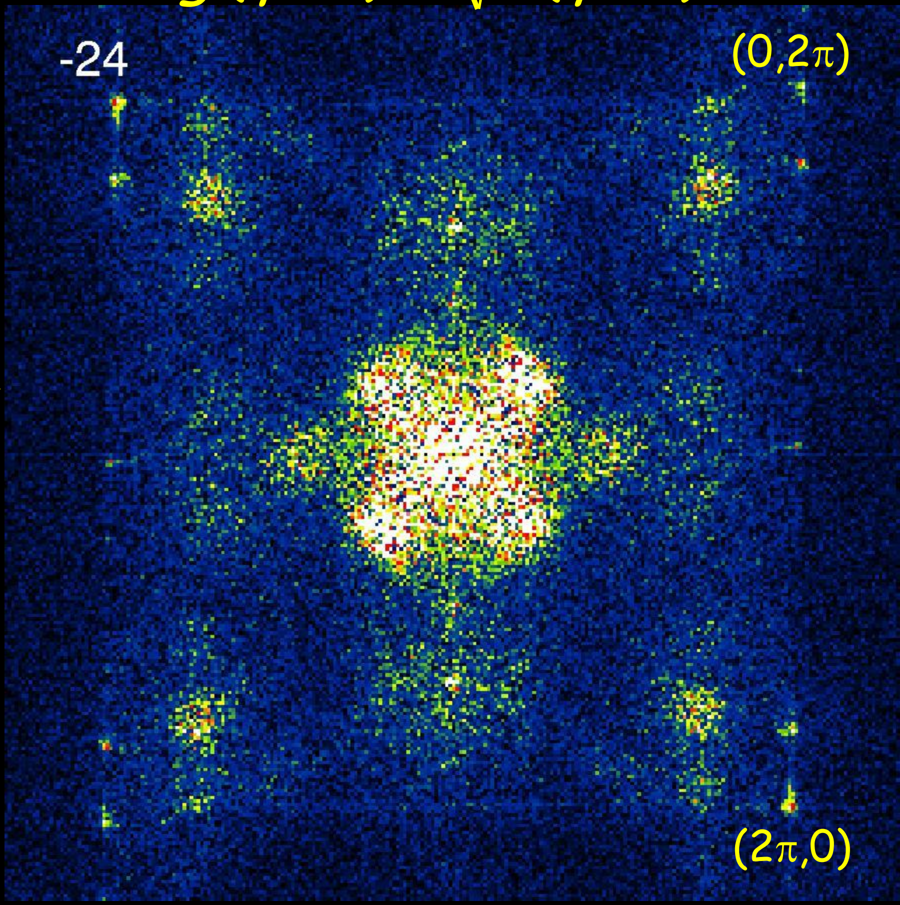

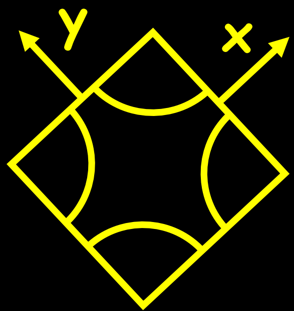

Bi-2212

T_c=76 K

Δ~51meV

Imaging quasiparticle wavefunctions

energy (meV)

$g(\vec{r},E)$

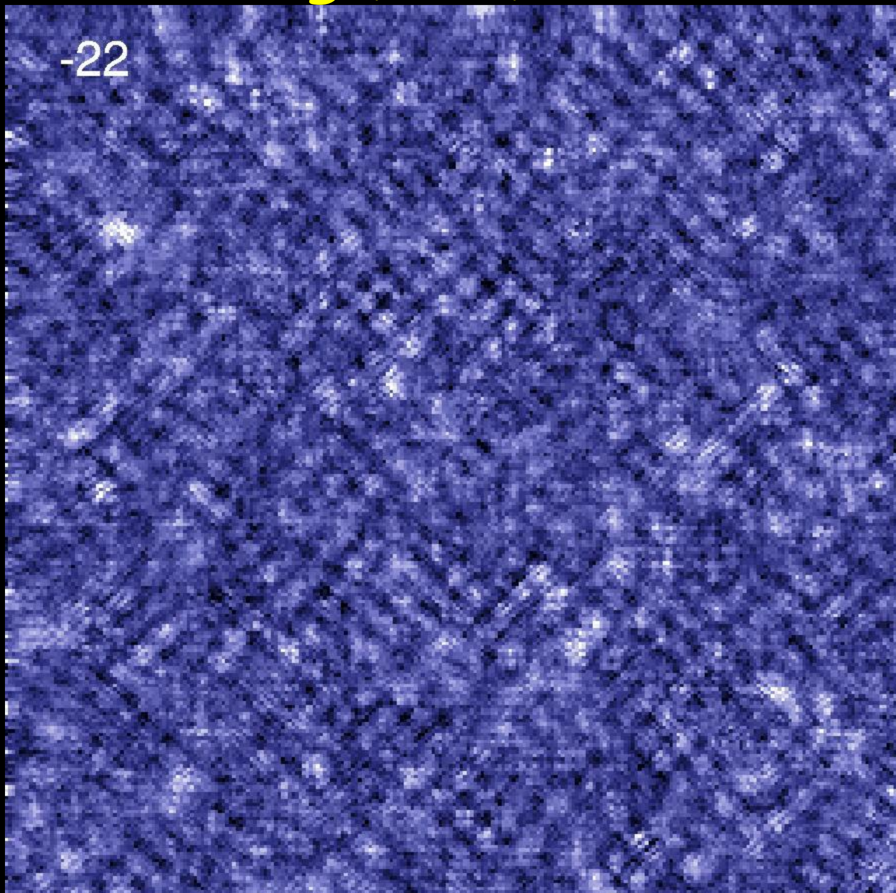

545 Å

FFT

$g(\vec{q},E)=\sqrt{P(\vec{q},E)}$

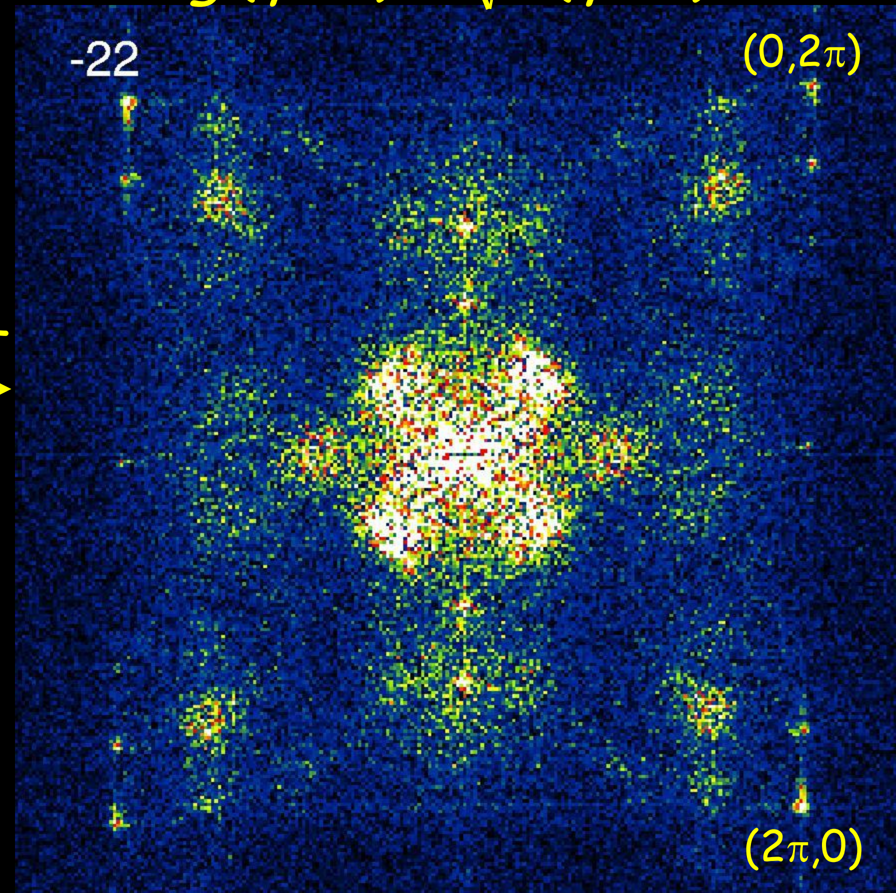

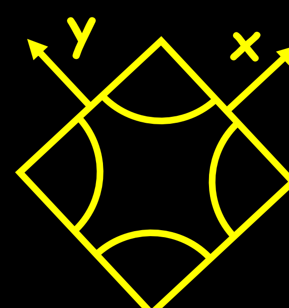

Bi-2212

T_c=76 K

Δ~51meV

Imaging quasiparticle wavefunctions

energy (meV)

$g(\vec{r},E)$

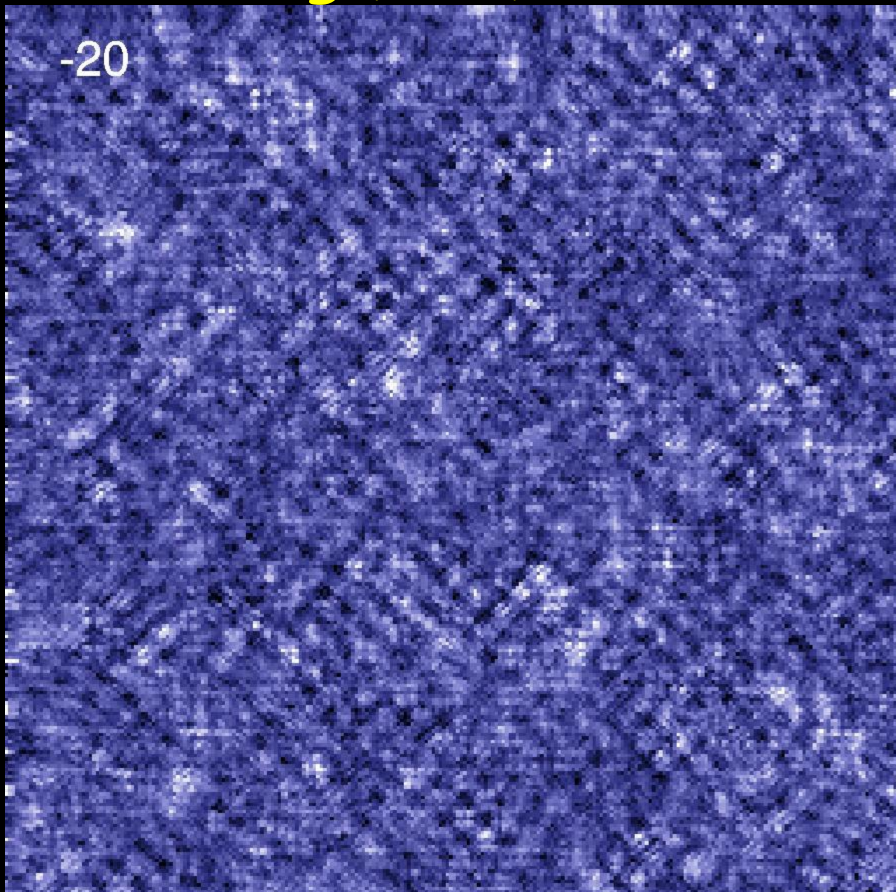

545 Å

FFT

$g(\vec{q},E)=\sqrt{P(\vec{q},E)}$

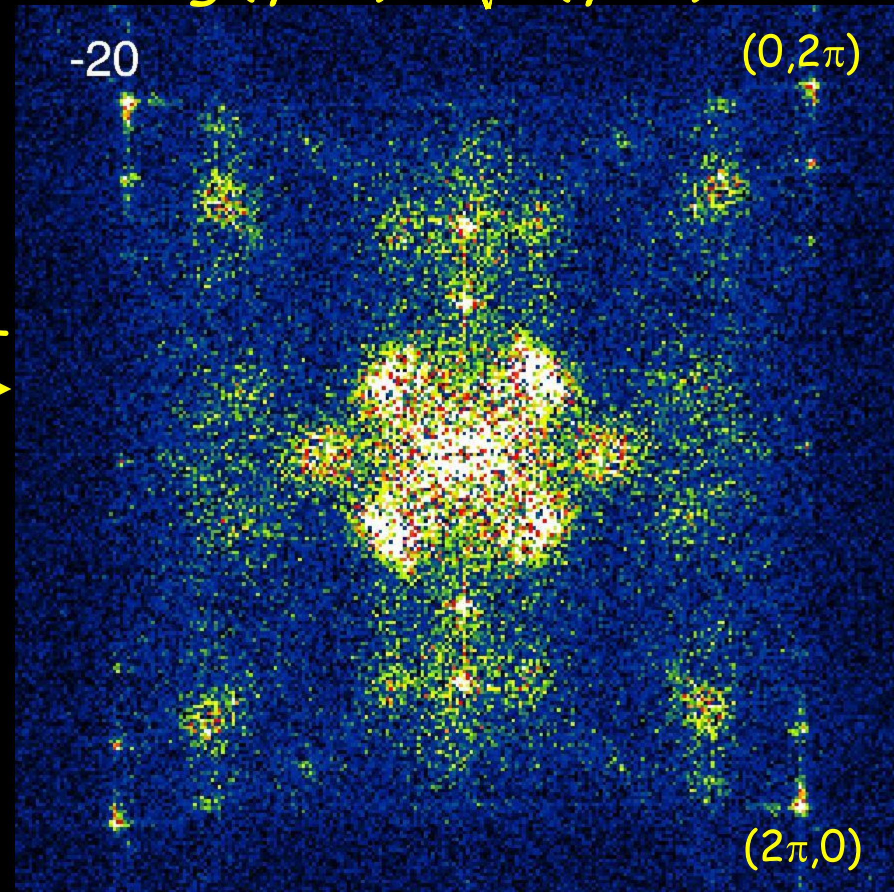

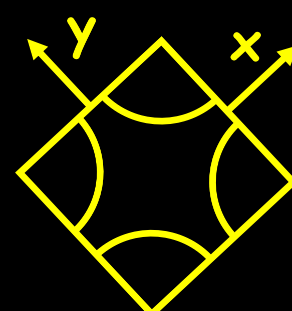

Bi-2212
T_c=76 K
Δ~51meV

Imaging quasiparticle wavefunctions

energy (meV)

$g(\vec{r},E)$

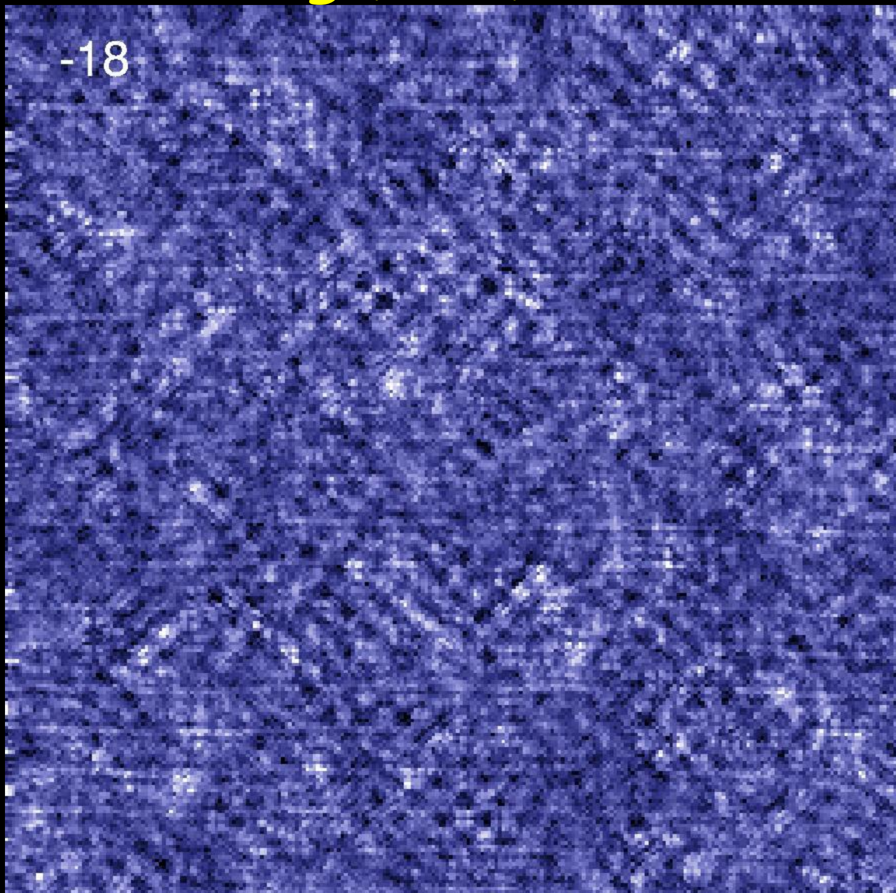

545 Å

FFT →

$g(\vec{q},E)=\sqrt{P(\vec{q},E)}$

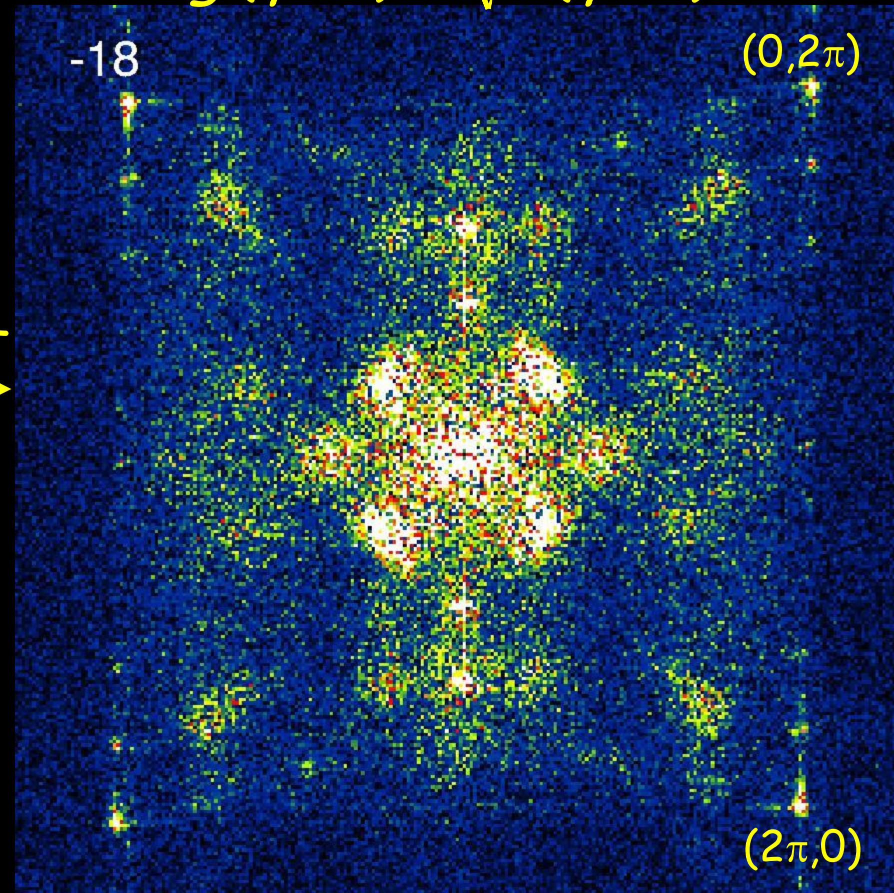

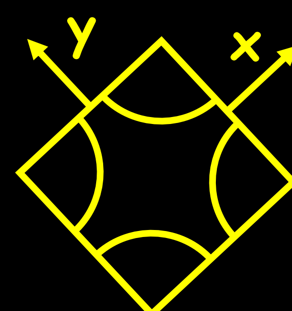

Bi-2212

T_c=76 K

Δ~51meV

Imaging quasiparticle wavefunctions

energy (meV)

$g(\vec{r},E)$

$g(\vec{q},E)=\sqrt{P(\vec{q},E)}$

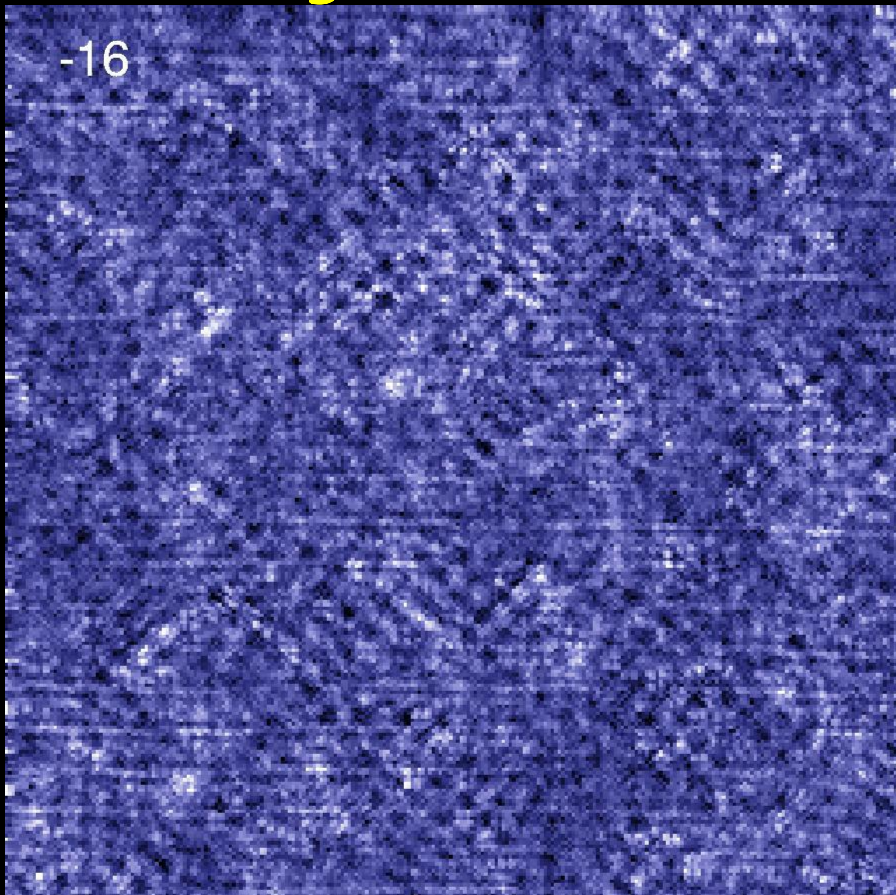

FFT

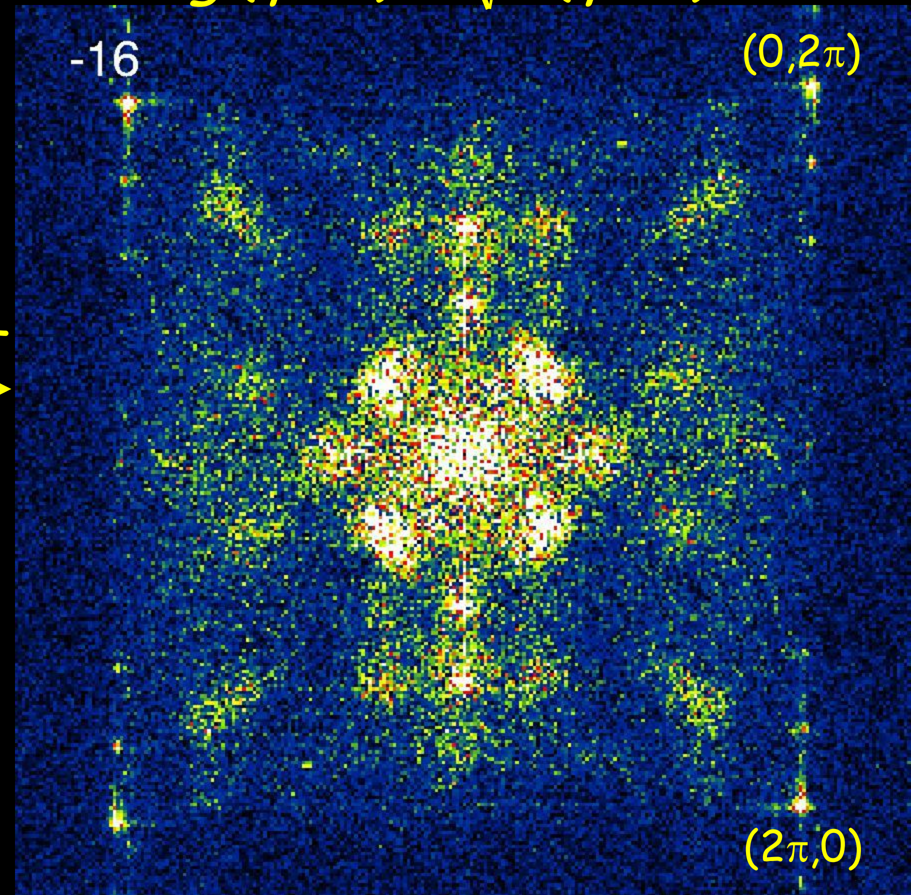

545 Å

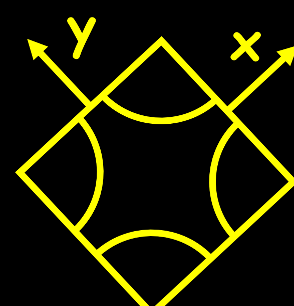

Bi-2212

T_c=76 K

Δ~51meV

Imaging quasiparticle wavefunctions

energy (meV)

$g(\vec{r},E)$

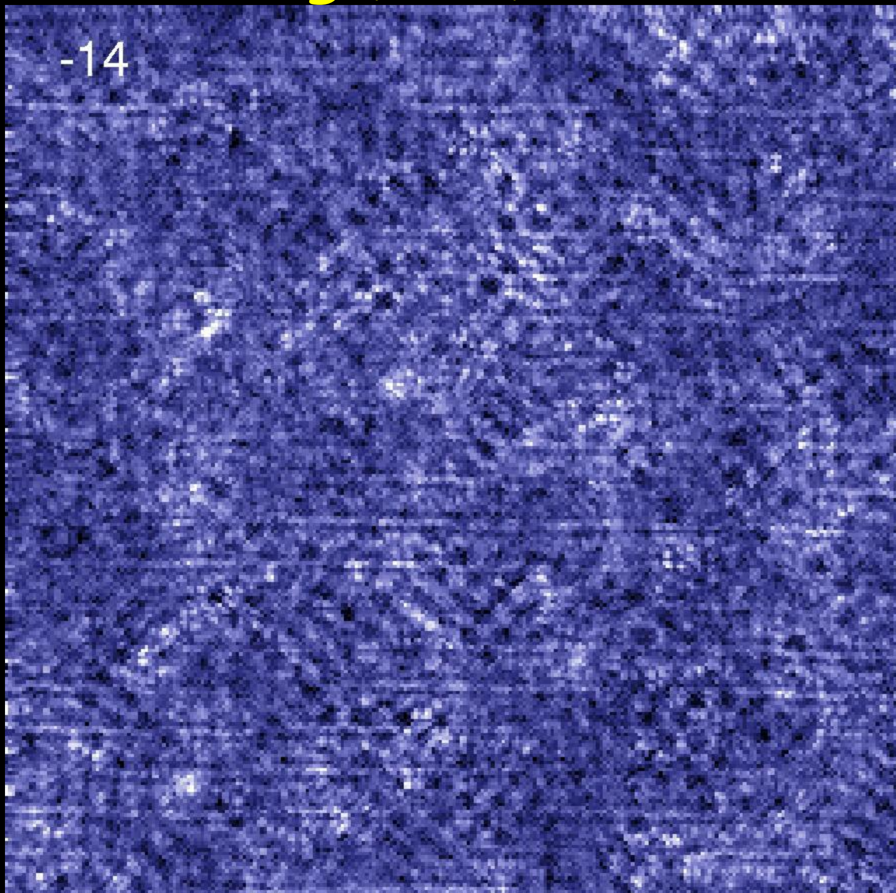

545 Å

FFT

$g(\vec{q},E) = \sqrt{P(\vec{q},E)}$

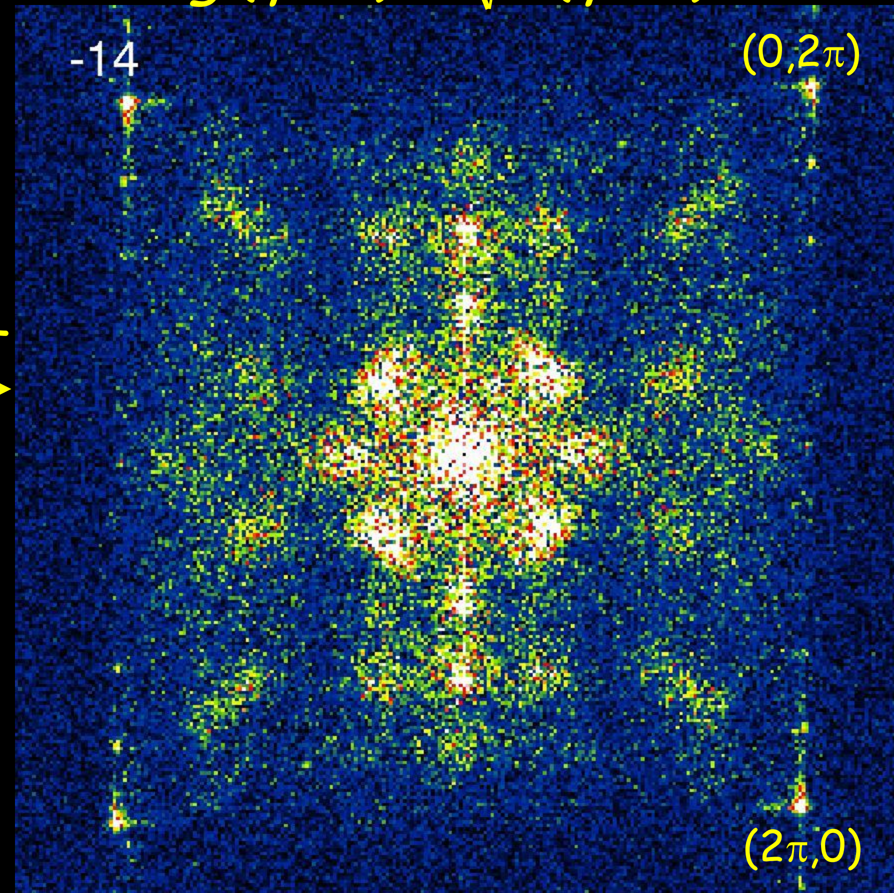

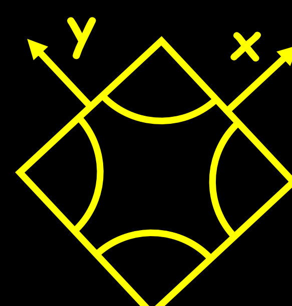

Bi-2212
T_c=76 K
Δ~51meV

Imaging quasiparticle wavefunctions

energy
(meV)

$g(\vec{r},E)$

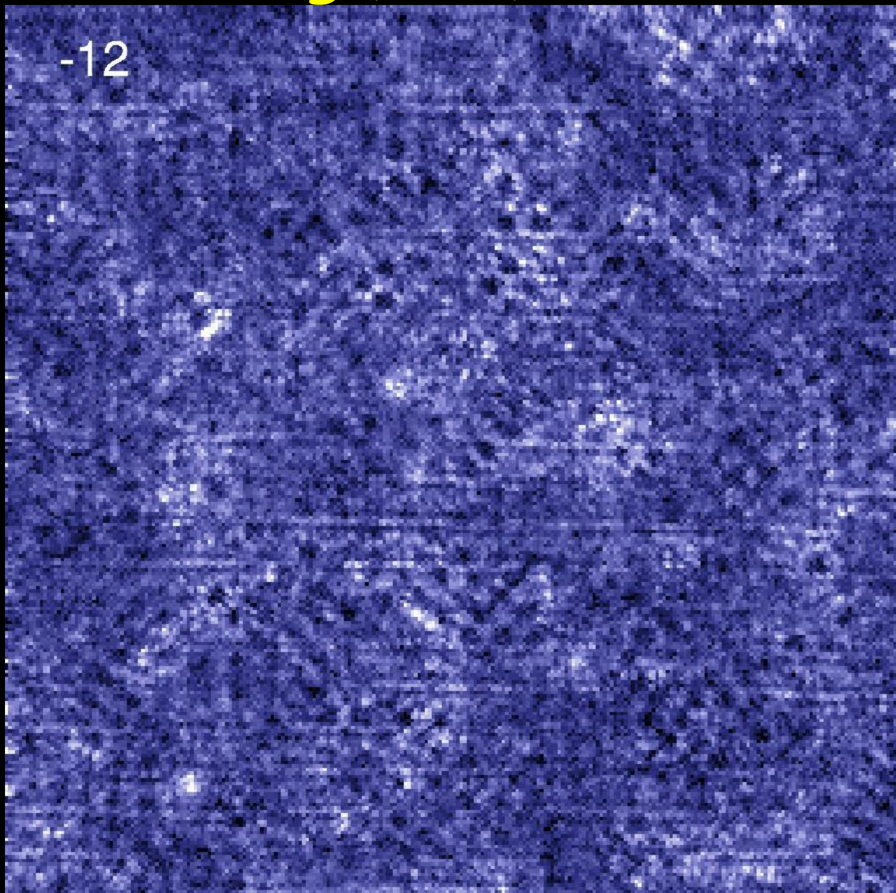

FFT

$g(\vec{q},E)=\sqrt{P(\vec{q},E)}$

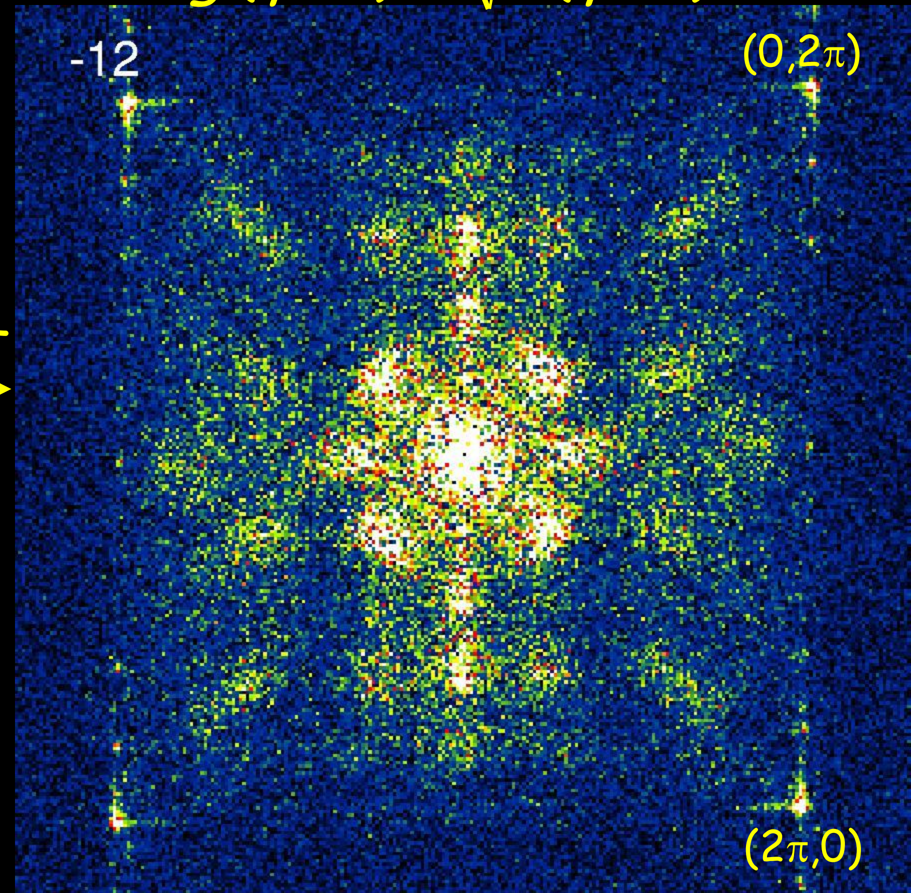

545 Å

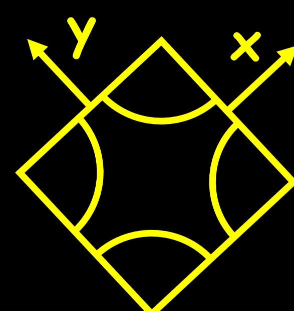

Bi-2212
T_c=76 K
Δ~51meV

Imaging quasiparticle wavefunctions

energy (meV)

$g(\vec{r},E)$

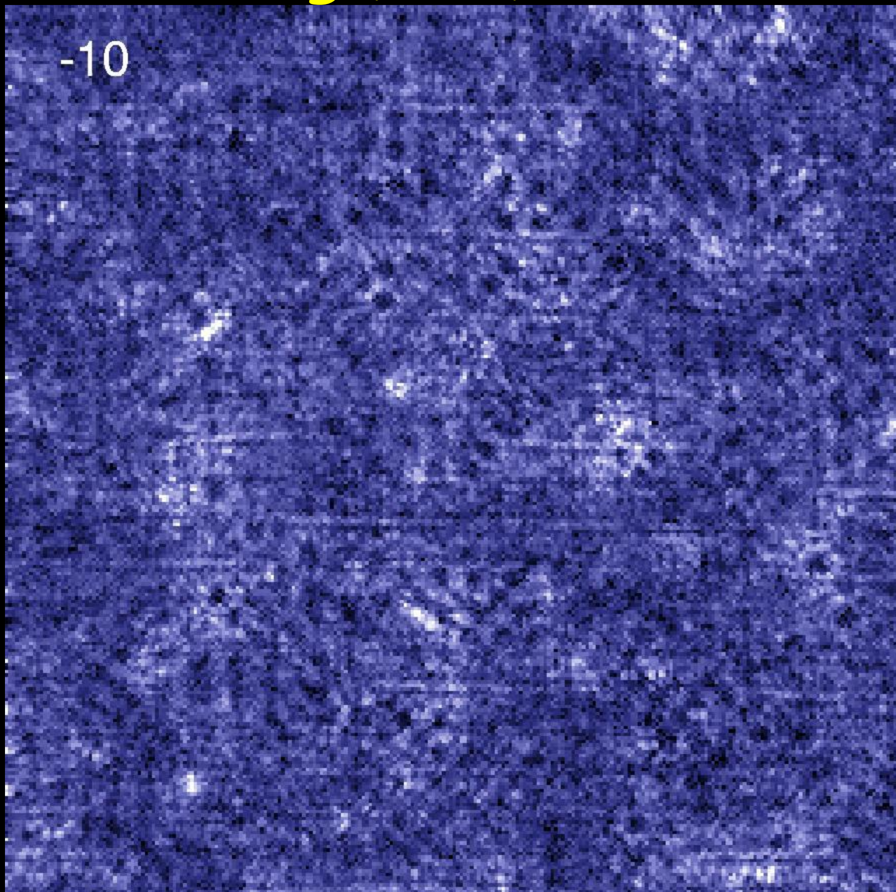

545 Å

FFT

$g(\vec{q},E)=\sqrt{P(\vec{q},E)}$

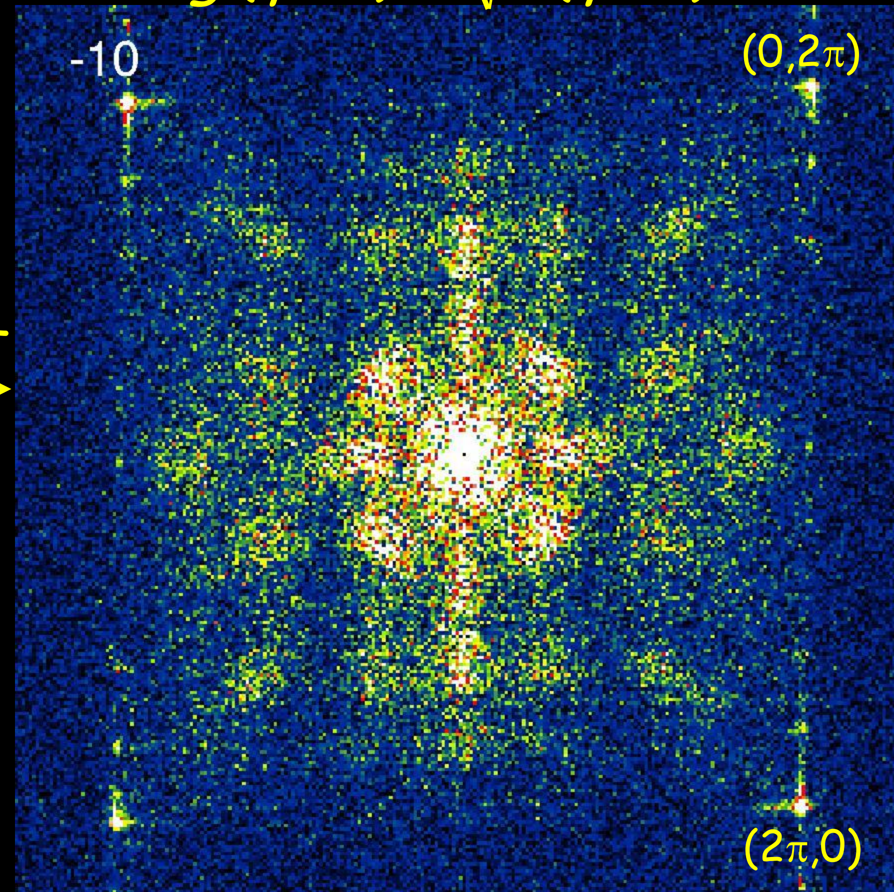

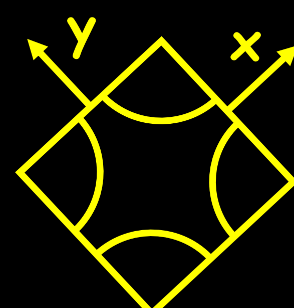

Bi-2212

T_c=76 K

Δ~51meV

Imaging quasiparticle wavefunctions

energy (meV)

$g(\vec{r},E)$

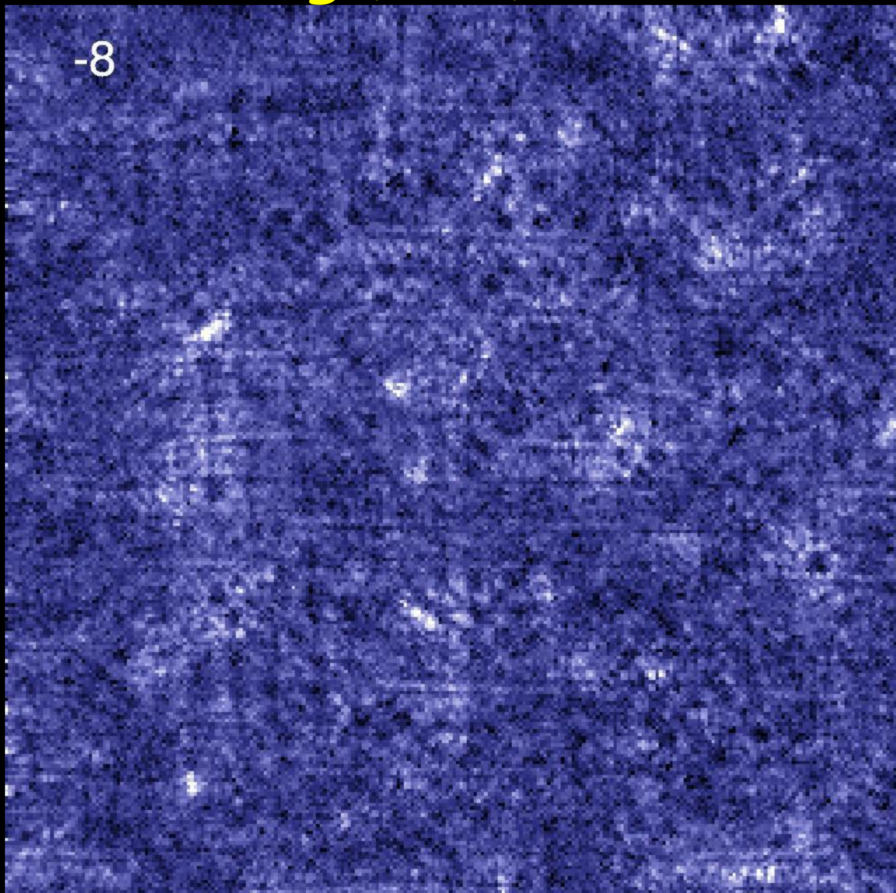

← 545 Å →

FFT →

$g(\vec{q},E)=\sqrt{P(\vec{q},E)}$

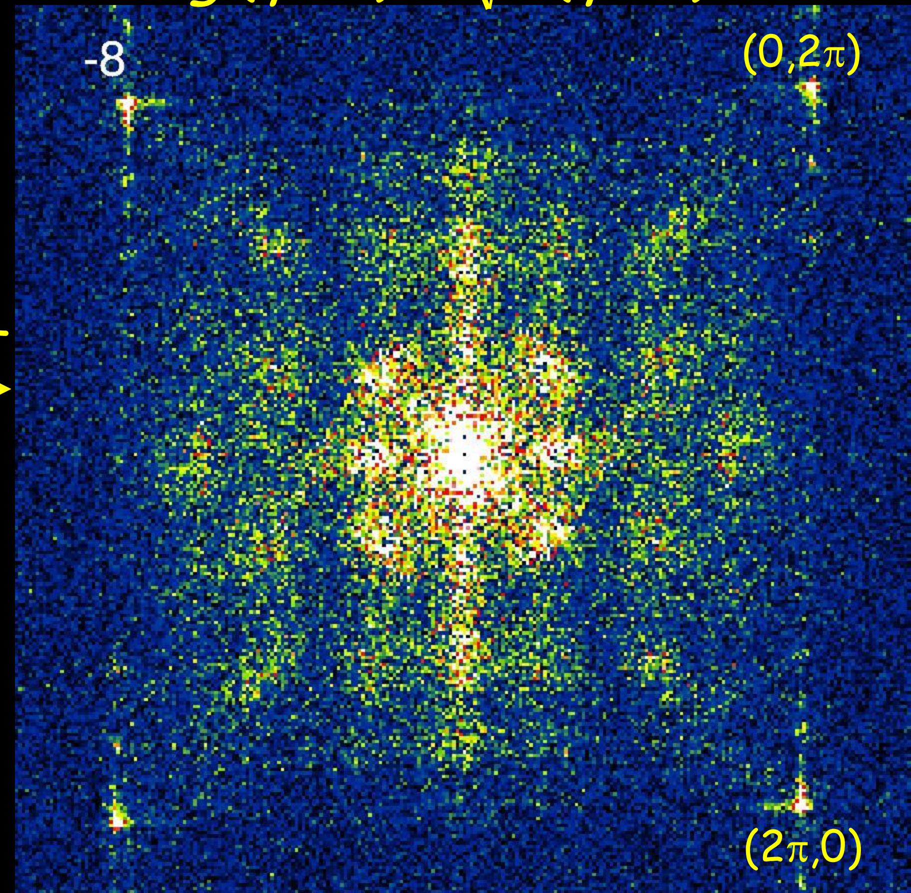

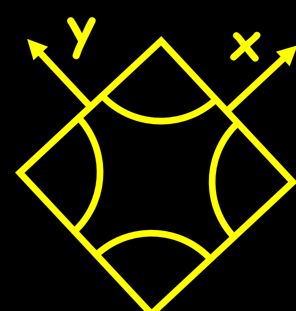

Bi-2212
T_c=76 K
Δ~51meV

Imaging quasiparticle wavefunctions

energy (meV)

$g(\vec{r},E)$

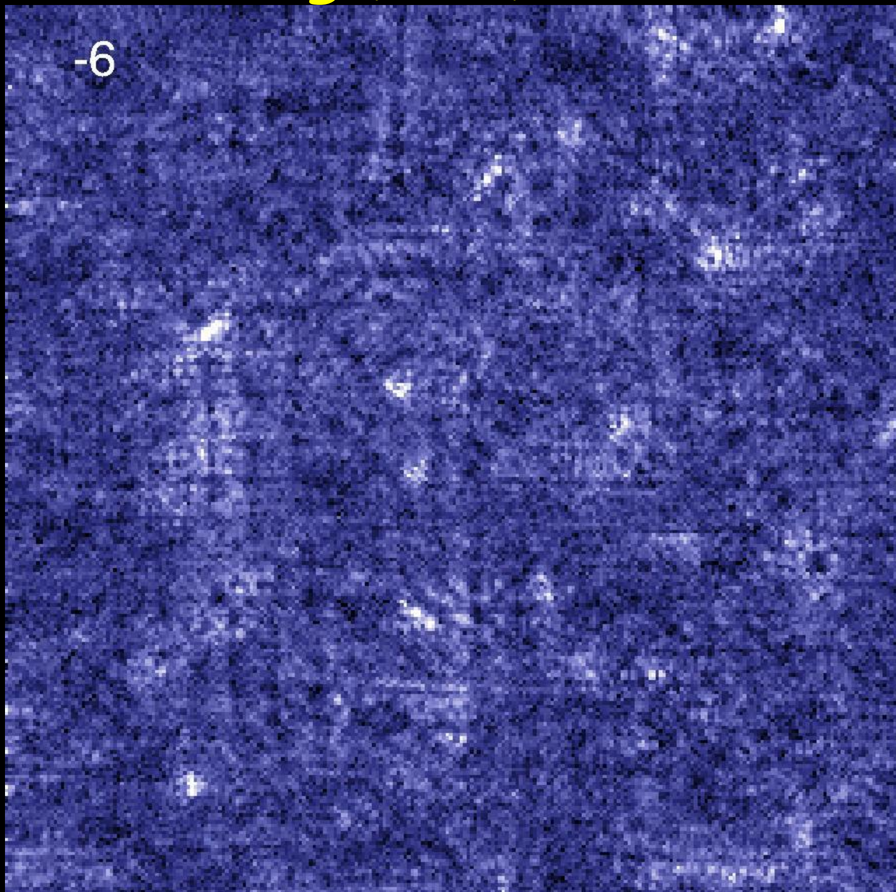

← 545 Å →

FFT →

$g(\vec{q},E)=\sqrt{P(\vec{q},E)}$

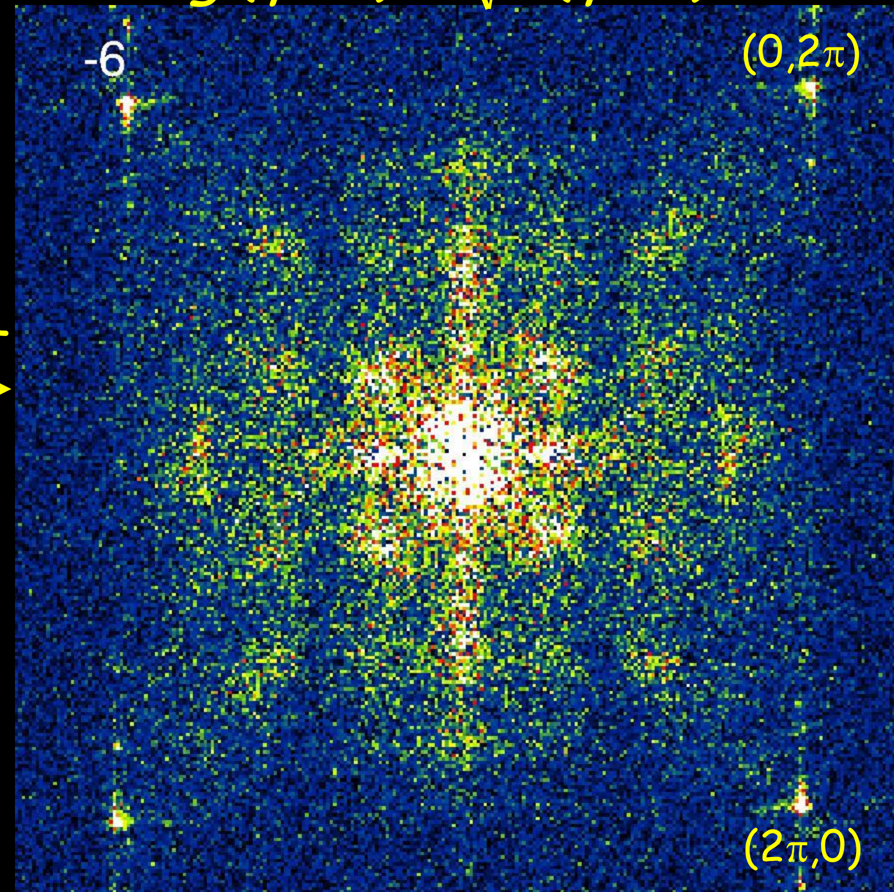

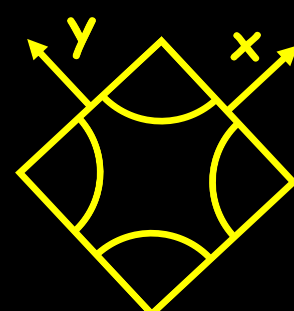

Bi-2212
T_c=76 K
Δ~51meV

Imaging quasiparticle wavefunctions

energy (meV)

$g(\vec{r},E)$

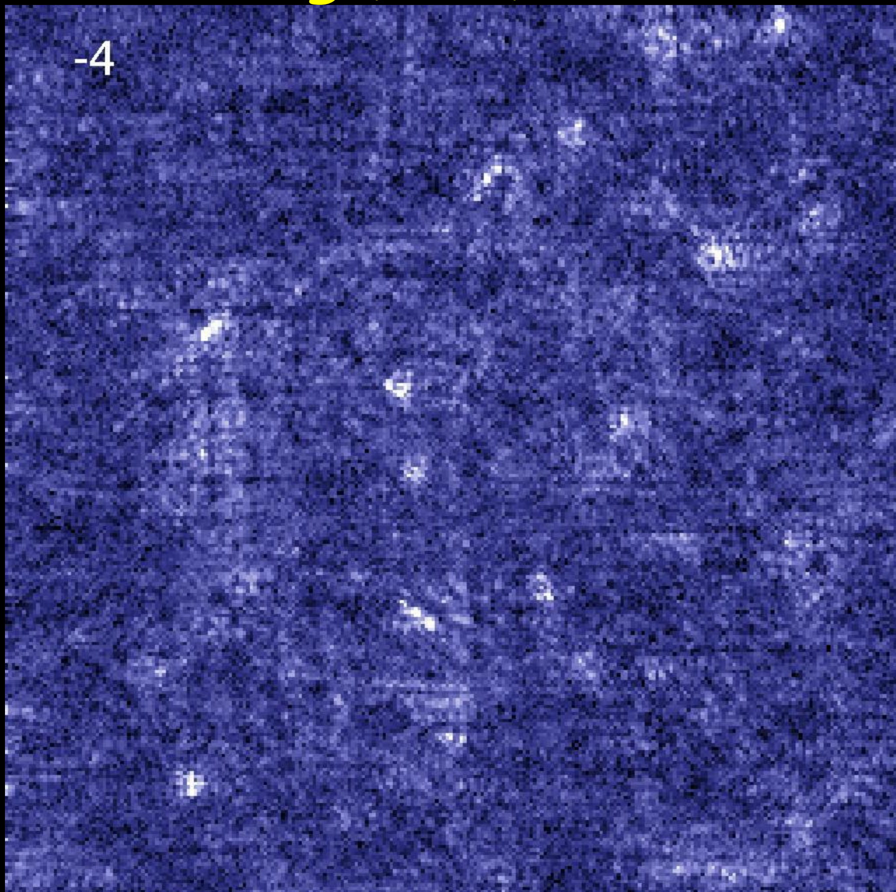

545 Å

FFT

$g(\vec{q},E) = \sqrt{P(\vec{q},E)}$

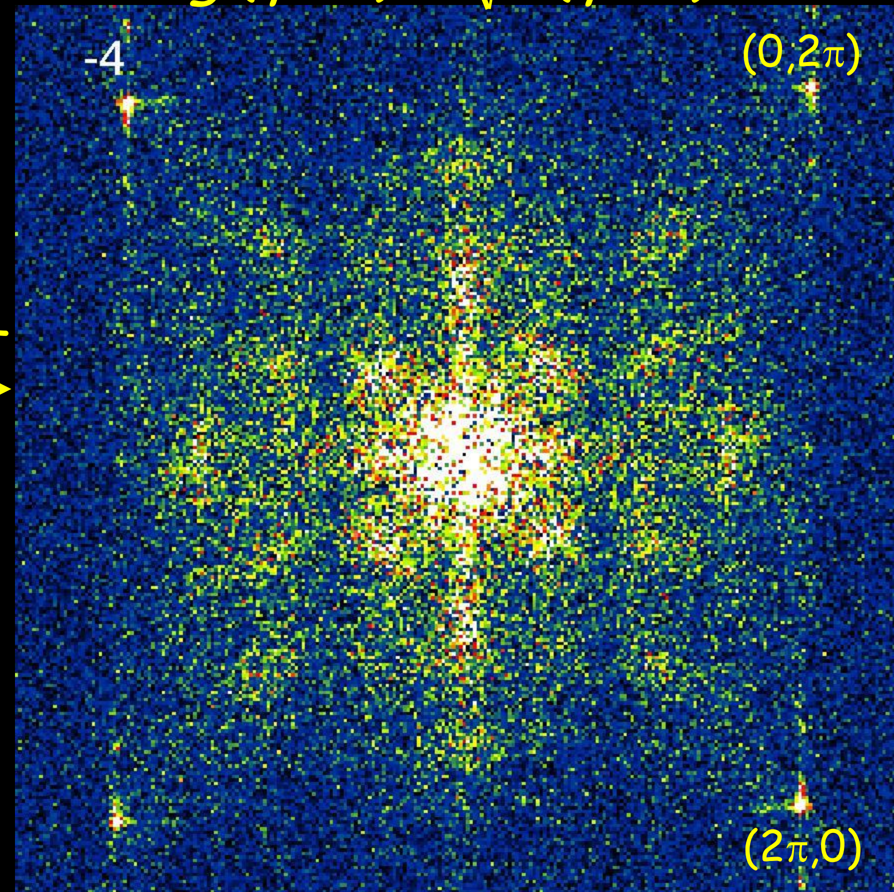

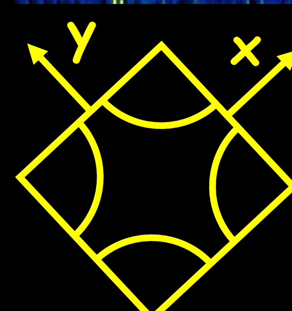

Bi-2212

T_c=76 K

Δ~51meV

Imaging quasiparticle wavefunctions

energy (meV)

$g(\vec{r},E)$

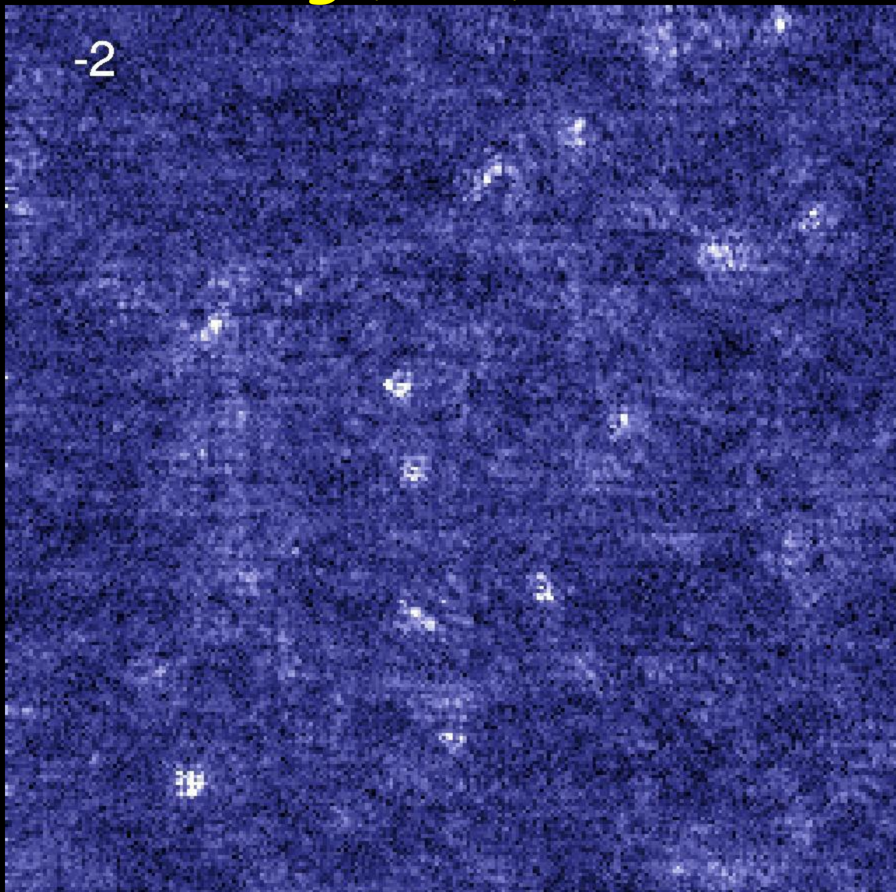

545 Å

FFT

$g(\vec{q},E)=\sqrt{P(\vec{q},E)}$

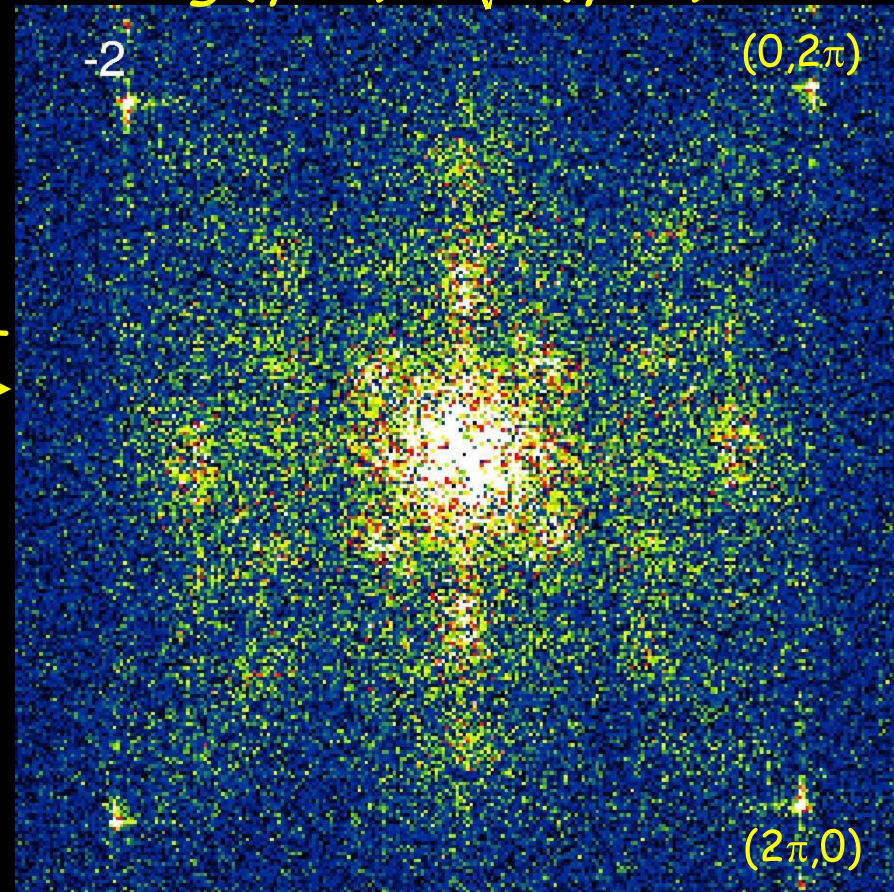

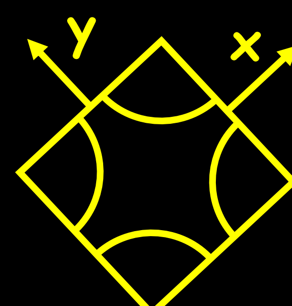

Bi-2212
T_c=76 K
Δ~51meV

Imaging quasiparticle wavefunctions

energy (meV)

$g(\vec{r},E)$

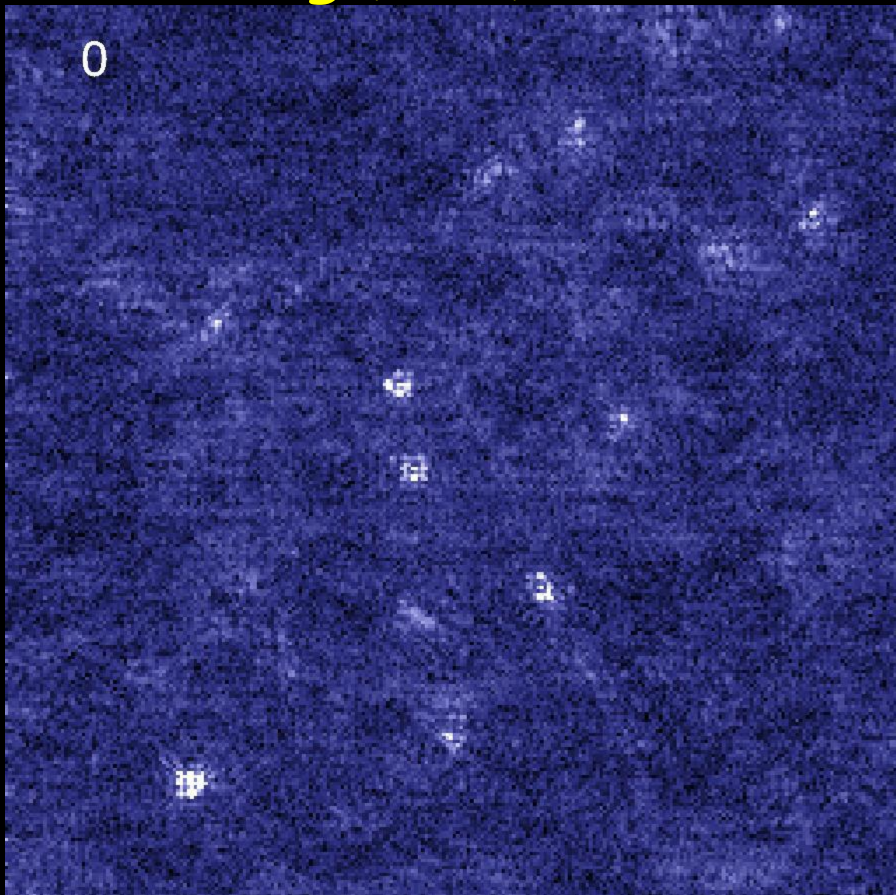

545 Å

FFT

$g(\vec{q},E)=\sqrt{P(\vec{q},E)}$

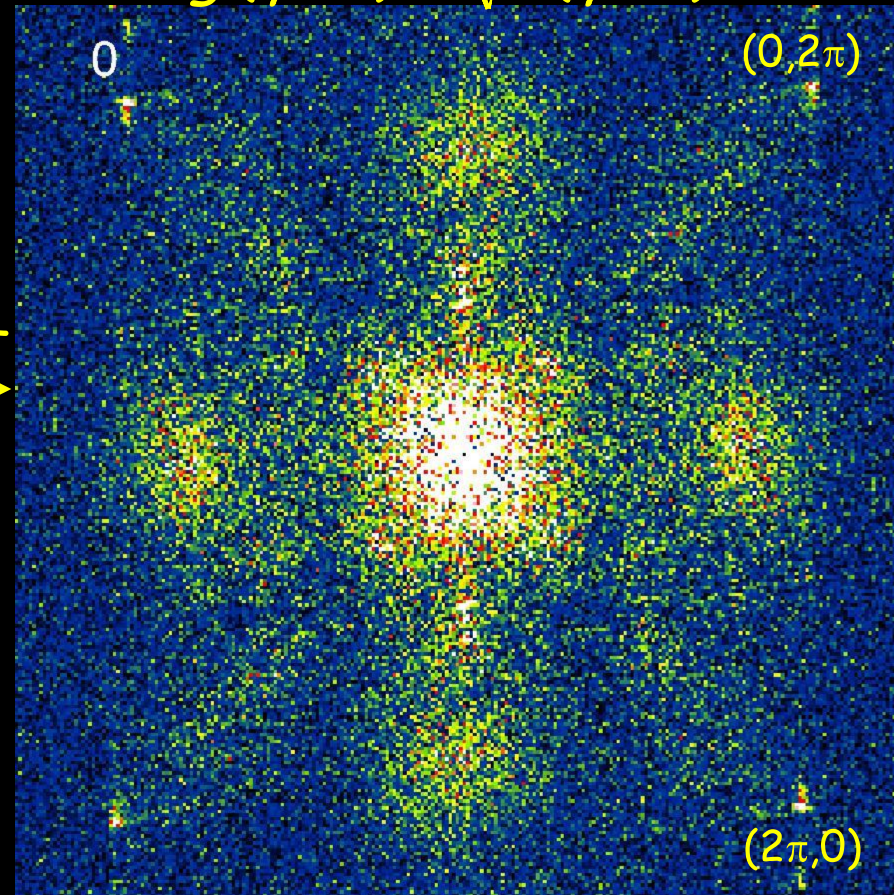

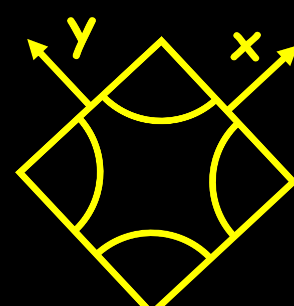

Bi-2212

T_c=76 K

Δ~51meV

Measuring the dispersion of the $q_i(E)$

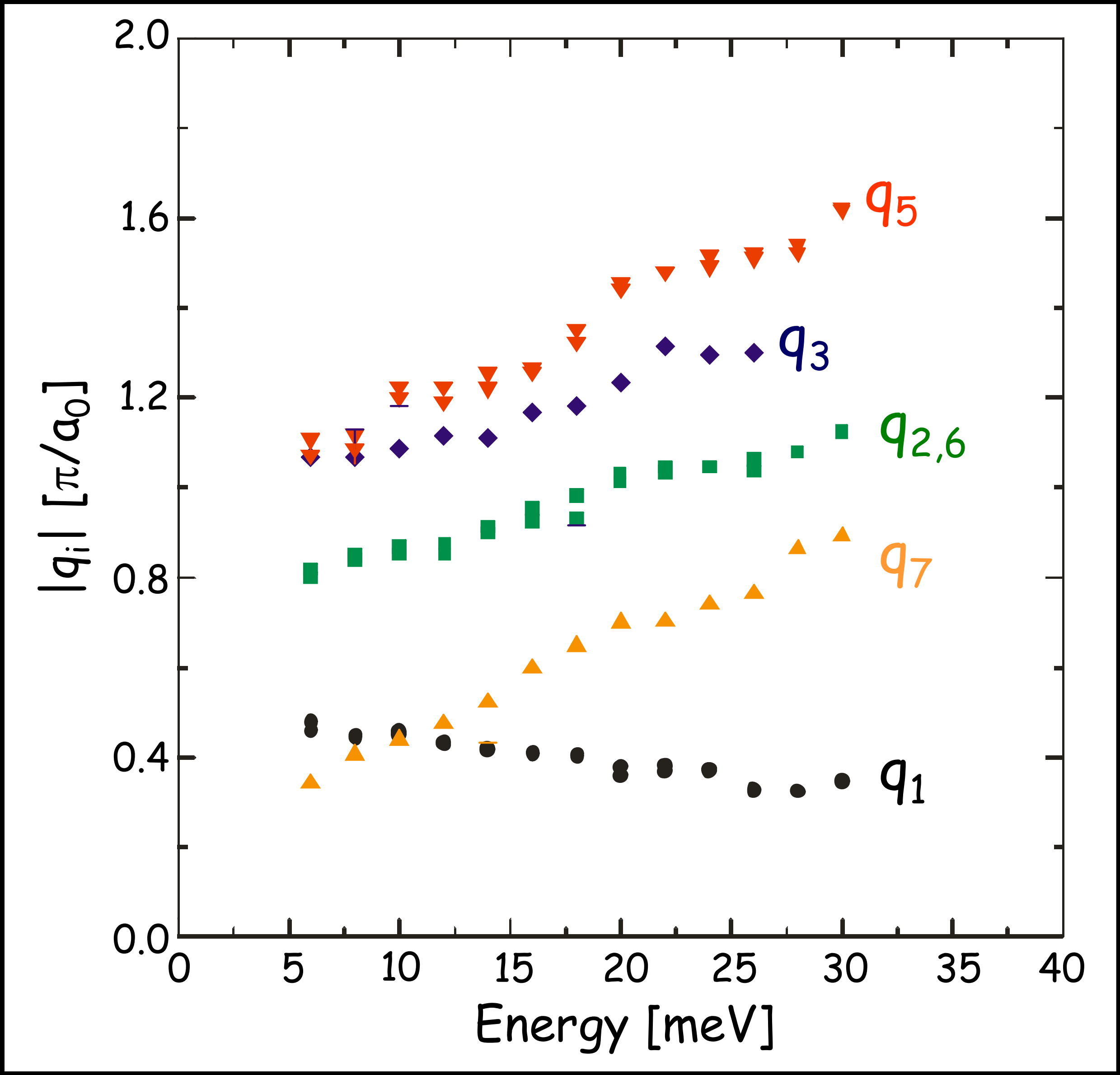

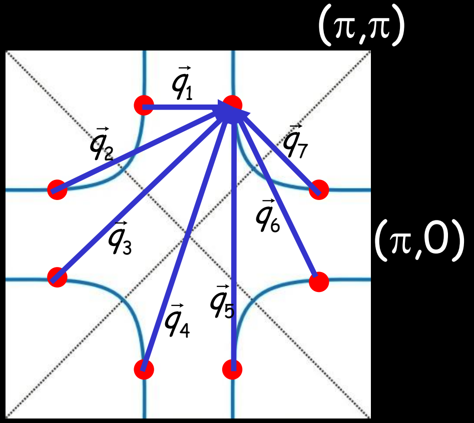

McElroy, Nature, 222, 592 (2003)

ARPES & STM: Fermi surface comparison

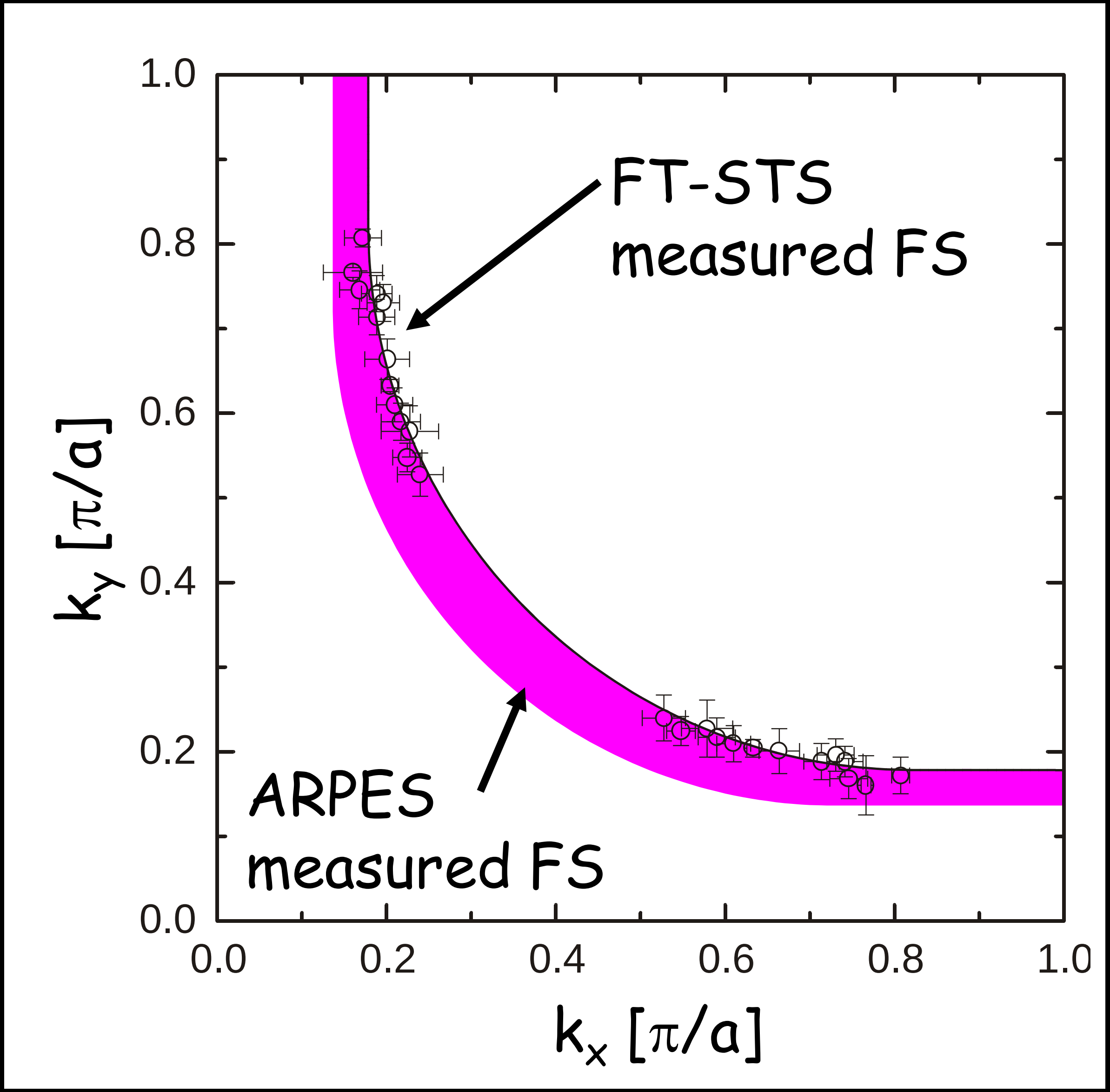

McElroy, Nature, 222, 592 (2003)

QPI persists to > 1.5*T_c

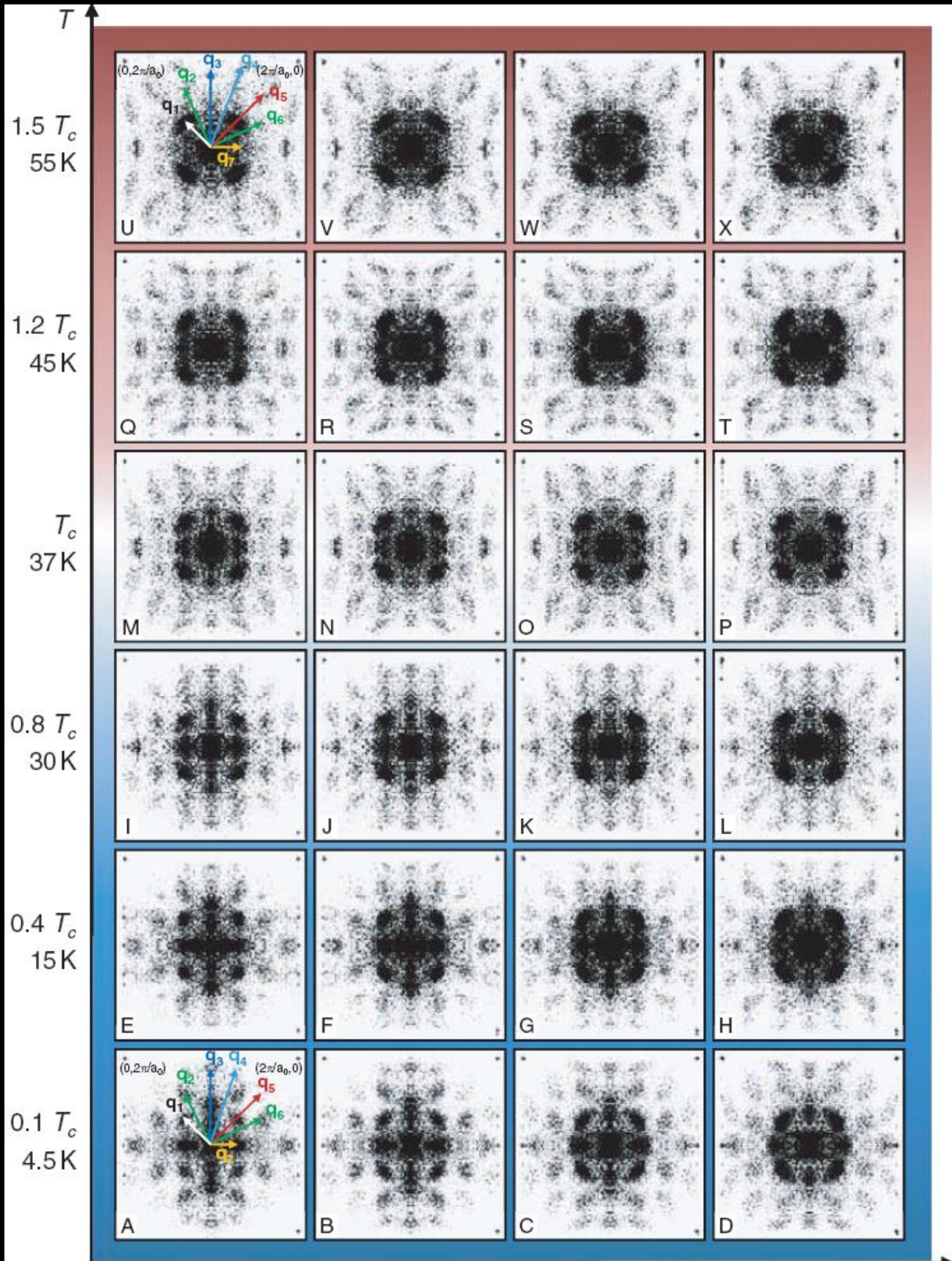

Motivation: QPI is p-h symmetric.
Claim: no state other than superconductivity is p-h symmetric.
Therefore, QPI is marker for SC.

Dy-BSCCO
T_c ~ 37 K

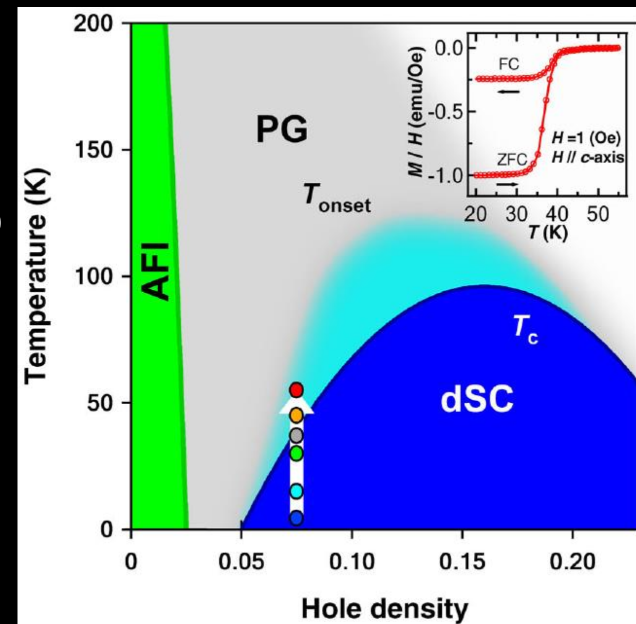

Caveat: these are Z maps
→ they assume p-h symmetry

Lee, … Davis, Science 325, 1099 (2009)

nesting wavelength vs. local *and* global Δ

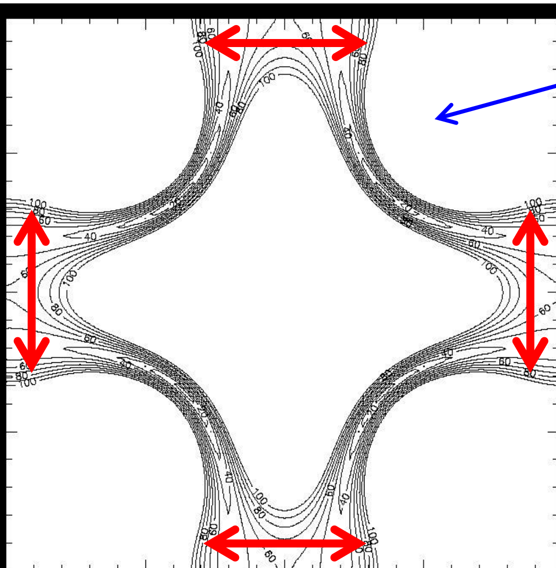

- hole pocket expands with doping
- nesting wavevector decreases with doping

→ nesting wavevector increases with PG

- pseudogap also decreases with doping

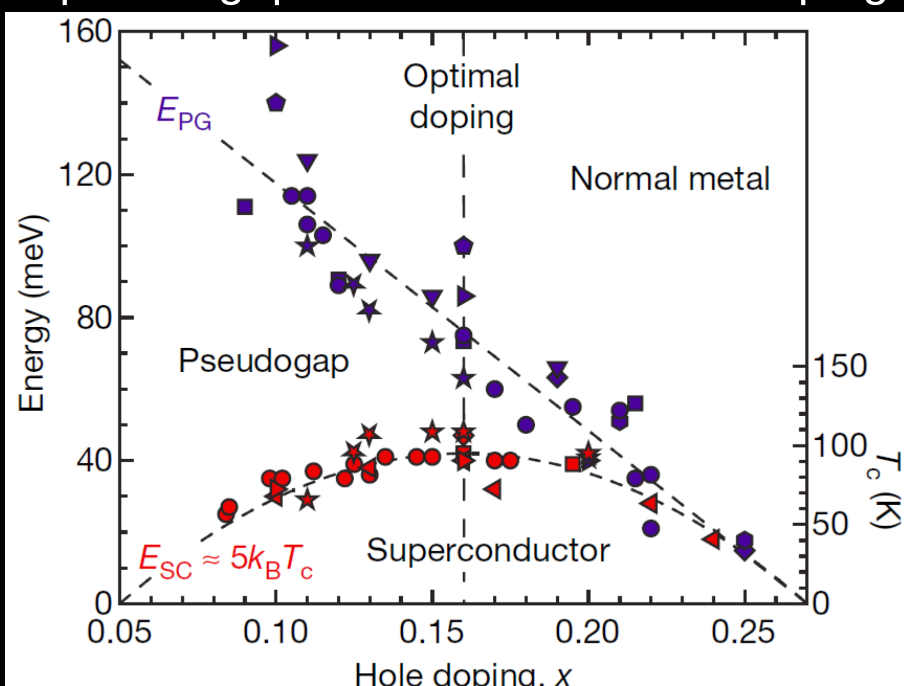

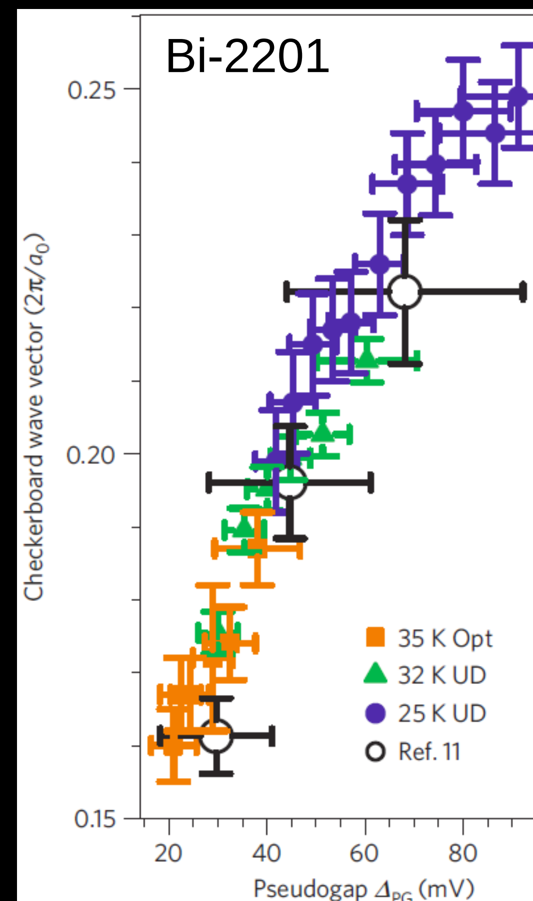

Wise, Hudson, Nat Phys 5, 213 (2009)

Spatial vs. Momentum Resolution

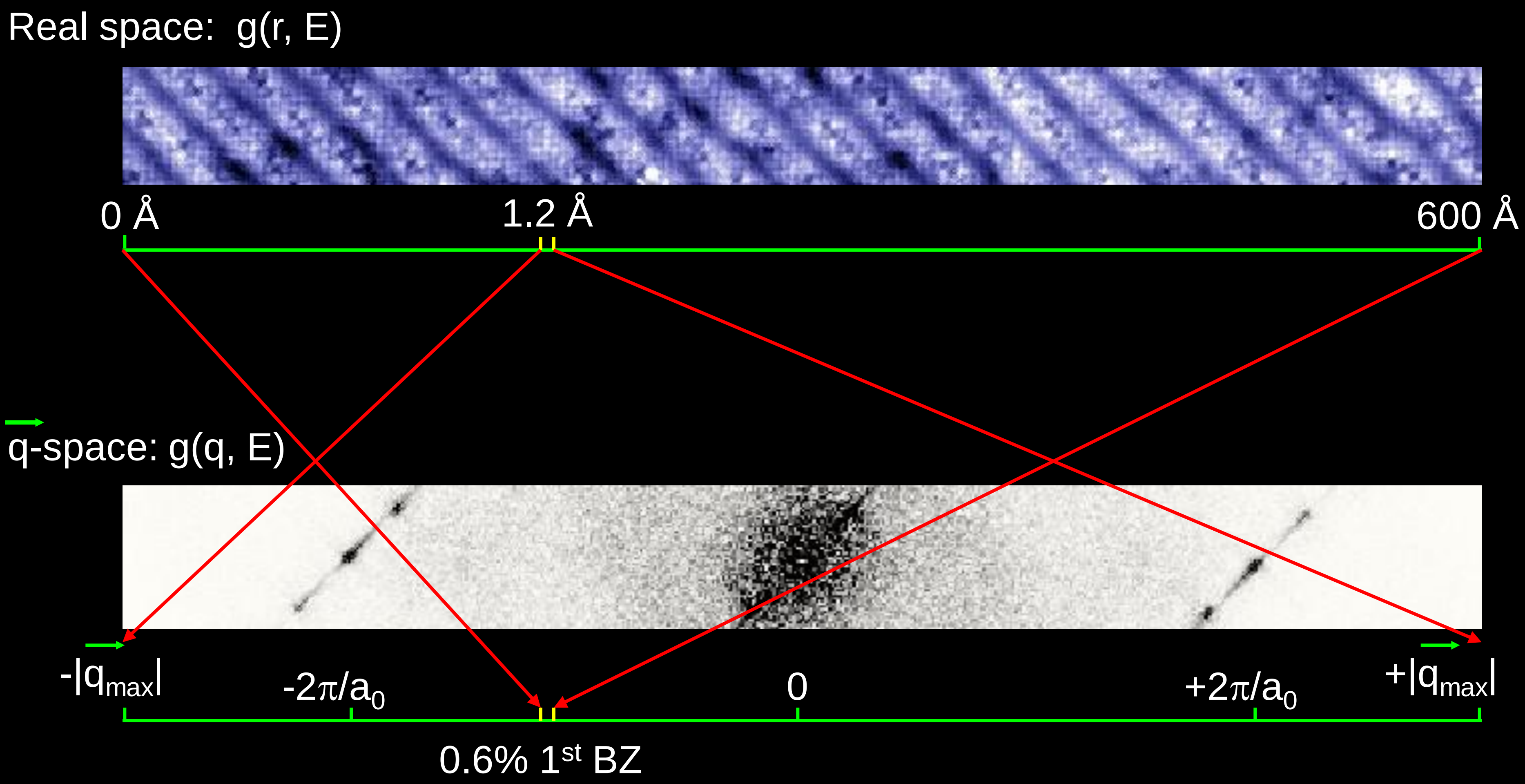

Superconductivity Tunneling Milestones

1960: gap measurement (Pb)

1965: boson energies & coupling (Pb)

1985: charge density wave ($TaSe_2$)

1989: vortex lattice ($NbSe_2$)

1997: single atom impurities (Nb)

2002: quasiparticle interference
→ band structure & gap symmetry (BSCCO)

2009: phase-sensitive gap measurement (Na-CCOC)

2010: intra-unit-cell structure (BSCCO)

1989: Vortex imaging

Vortex core states (conventional superconductors): $\epsilon_0 \sim \Delta_\infty^2 / E_F$

Caroli, deGennes, Matricon, Phys. Lett. 9, 307 (1964)

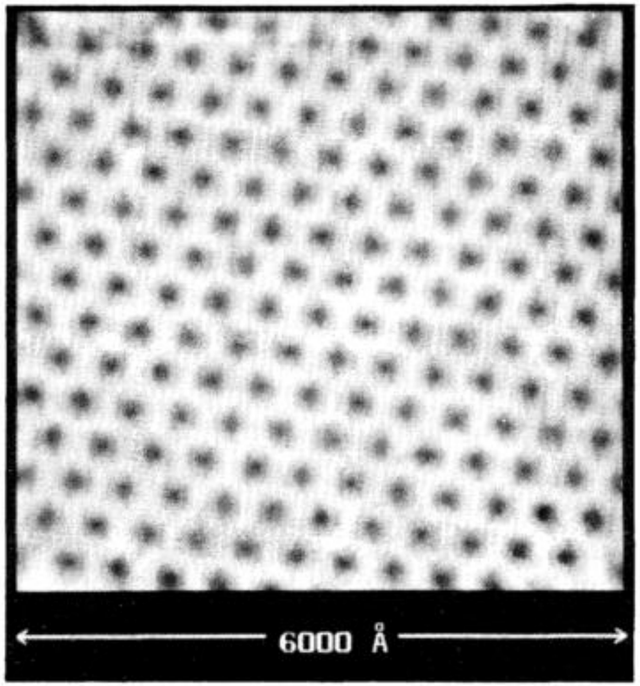

FIG. 2. Abrikosov flux lattice produced by a 1-T magnetic field in $NbSe_2$ at 1.8 K. The scan range is about 6000 Å. The gray scale corresponds to dI/dV ranging from approximately 1×10^{-8} mho (black) to 1.5×10^{-9} mho (white).

Typical: ϵ_F ~ 5 eV, Δ_∞ ~ 1.5 meV } $\epsilon_0 < 1\ \mu$V

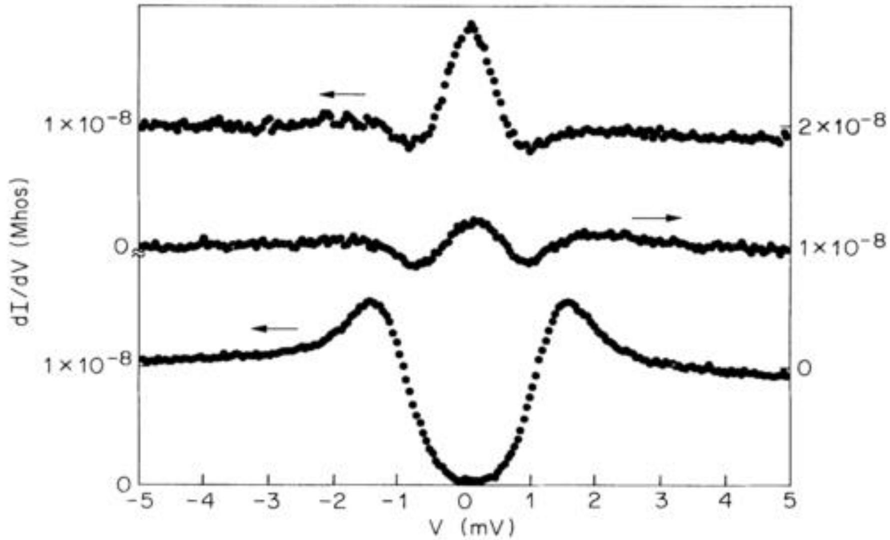

FIG. 3. dI/dV vs V for $NbSe_2$ at 1.85 K and a 0.02-T field, taken at three positions: on a vortex, about 75 Å from a vortex, and 2000 Å from a vortex. The zero of each successive curve is shifted up by one quarter of the vertical scale.

Hess, PRL 62, 214 (1989)

Vortices in cuprates

YBCO

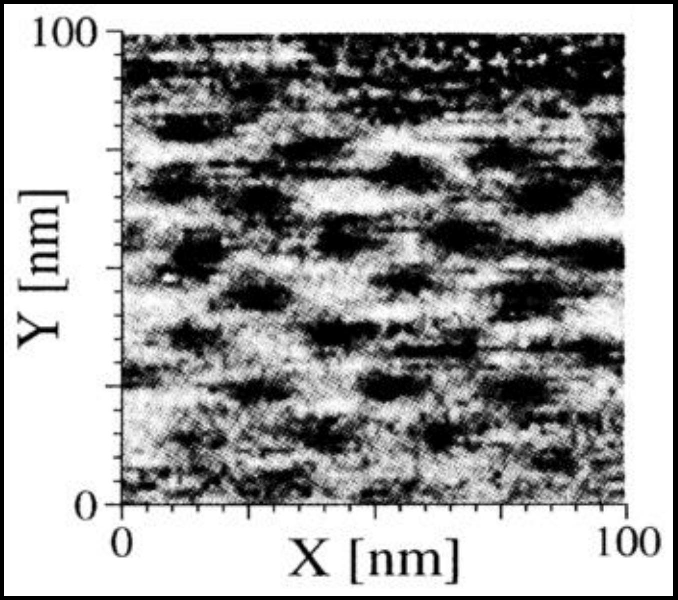

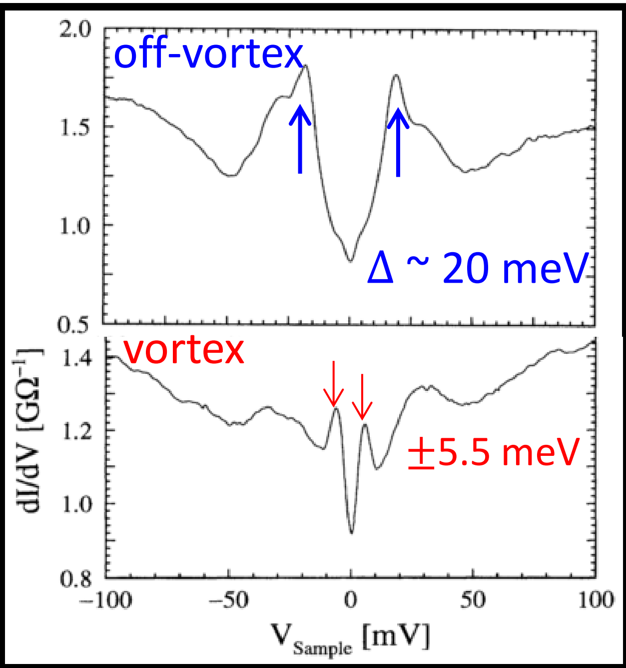

Maggio-Aprile PRL 75, 2754 (1995)

BSCCO

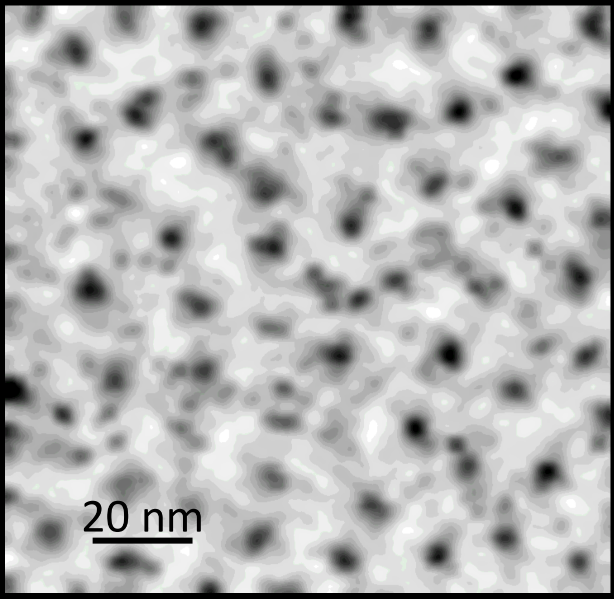

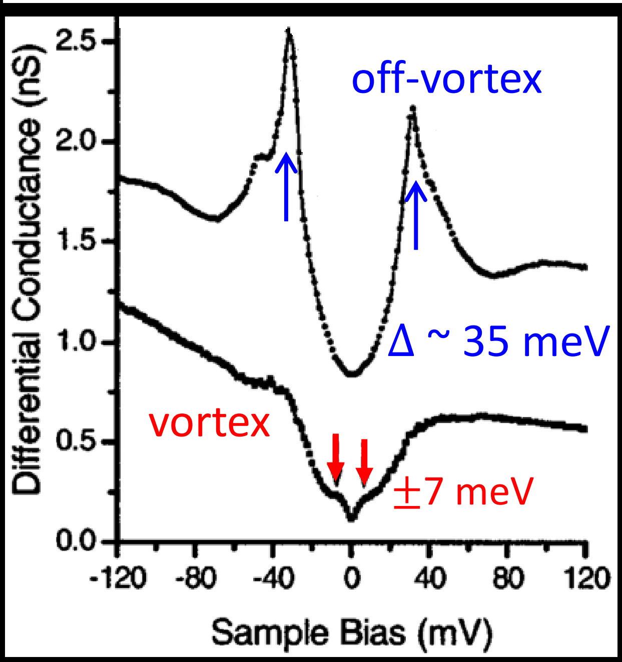

Pan, PRL 85, 1536 (2000)

Vortex pinning force measurement

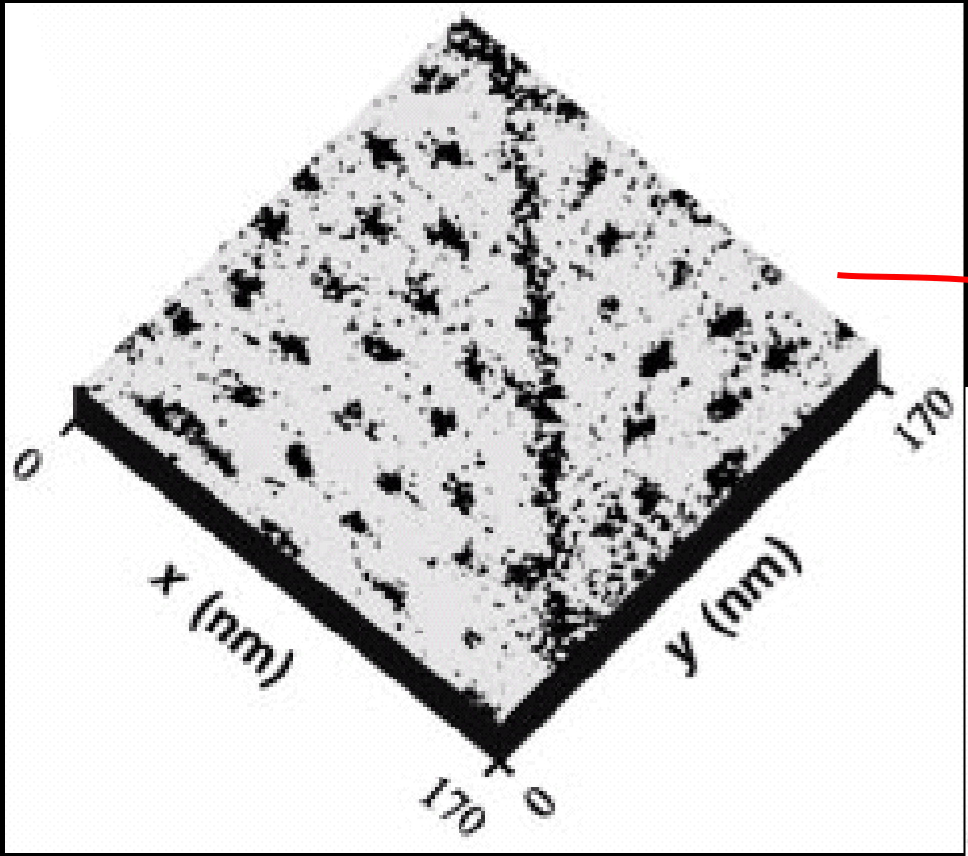

Maggio-Aprile, Nature 390, 487 (1997)

reduce field from
3 Tesla to 1.5 Tesla

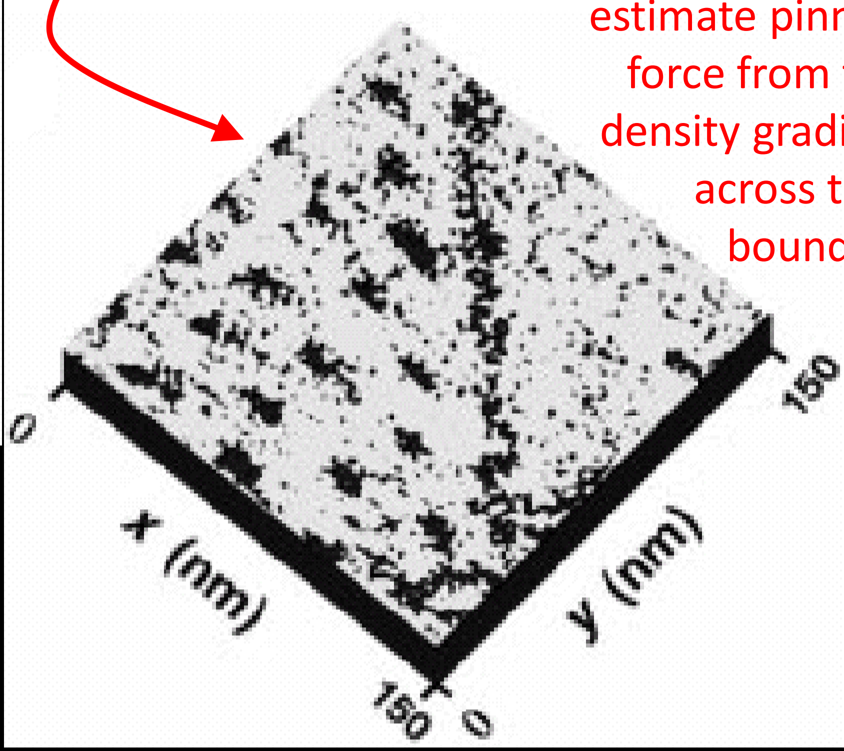

estimate pinning
force from flux
density gradient
across twin
boundary

Vortex pinning possibilities

(1) no strong pinners
inter-vortex forces dominate
→ lattice formation

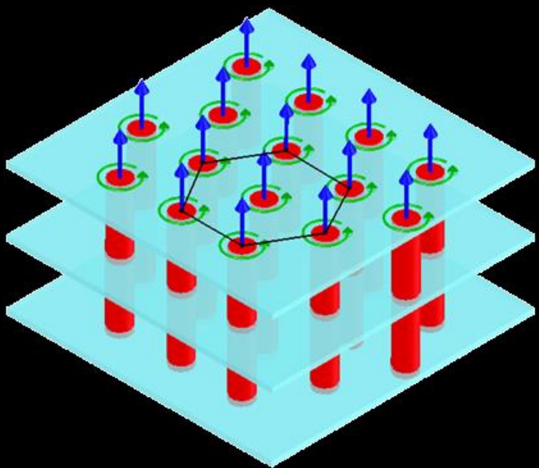

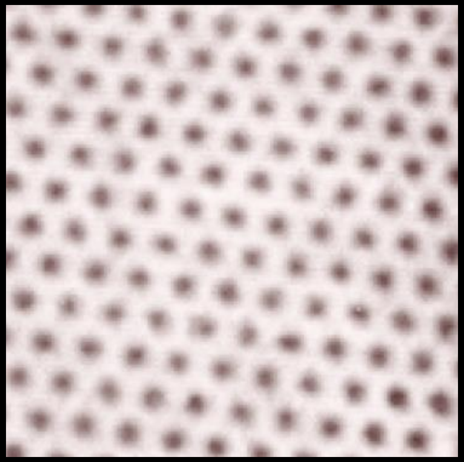

$NbSe_2$

(2) strong pinners exist
low anisotropy
→ vortices bend slightly
to accommodate pinners

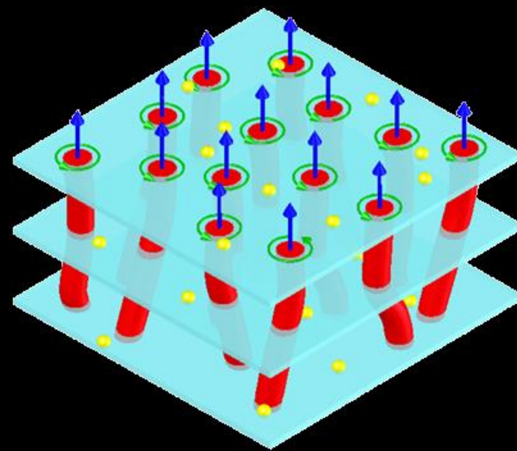

ideal case
for applications

(3) strong pinners exist
high anisotropy
→ vortices pancake
each pancake pins independently

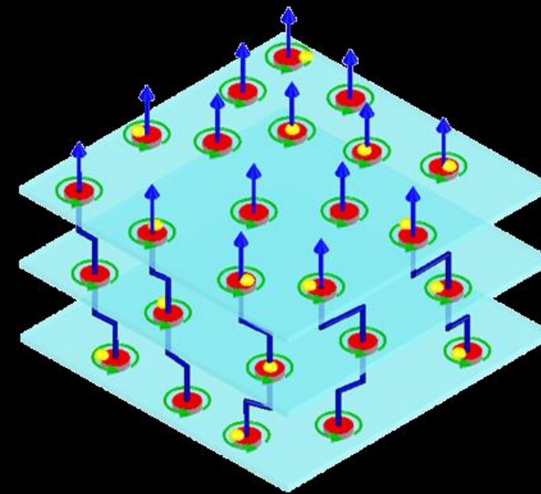

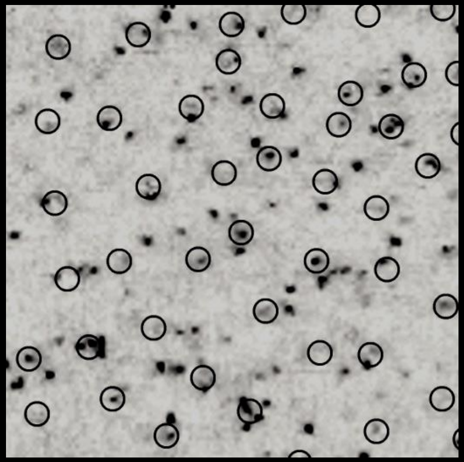

$Bi_2Sr_2CaCu_2O_8$

Are Vortices Pinned to Surface Impurities?

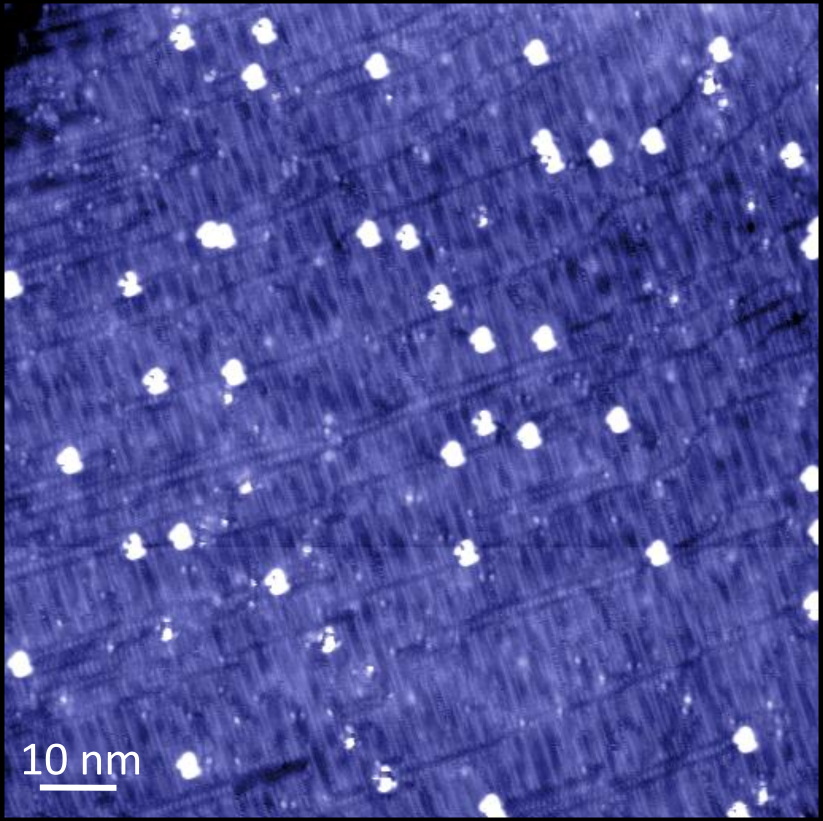

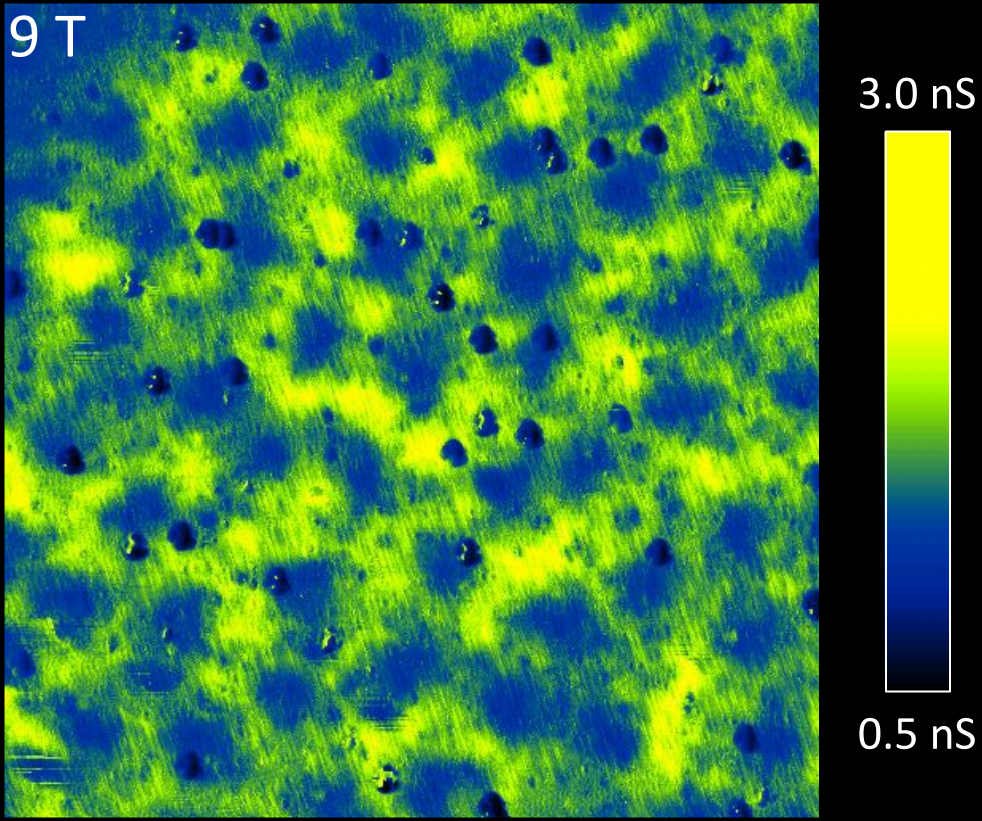

Are Vortices Pinned to Surface Impurities?

Raw Data   Idealized Data

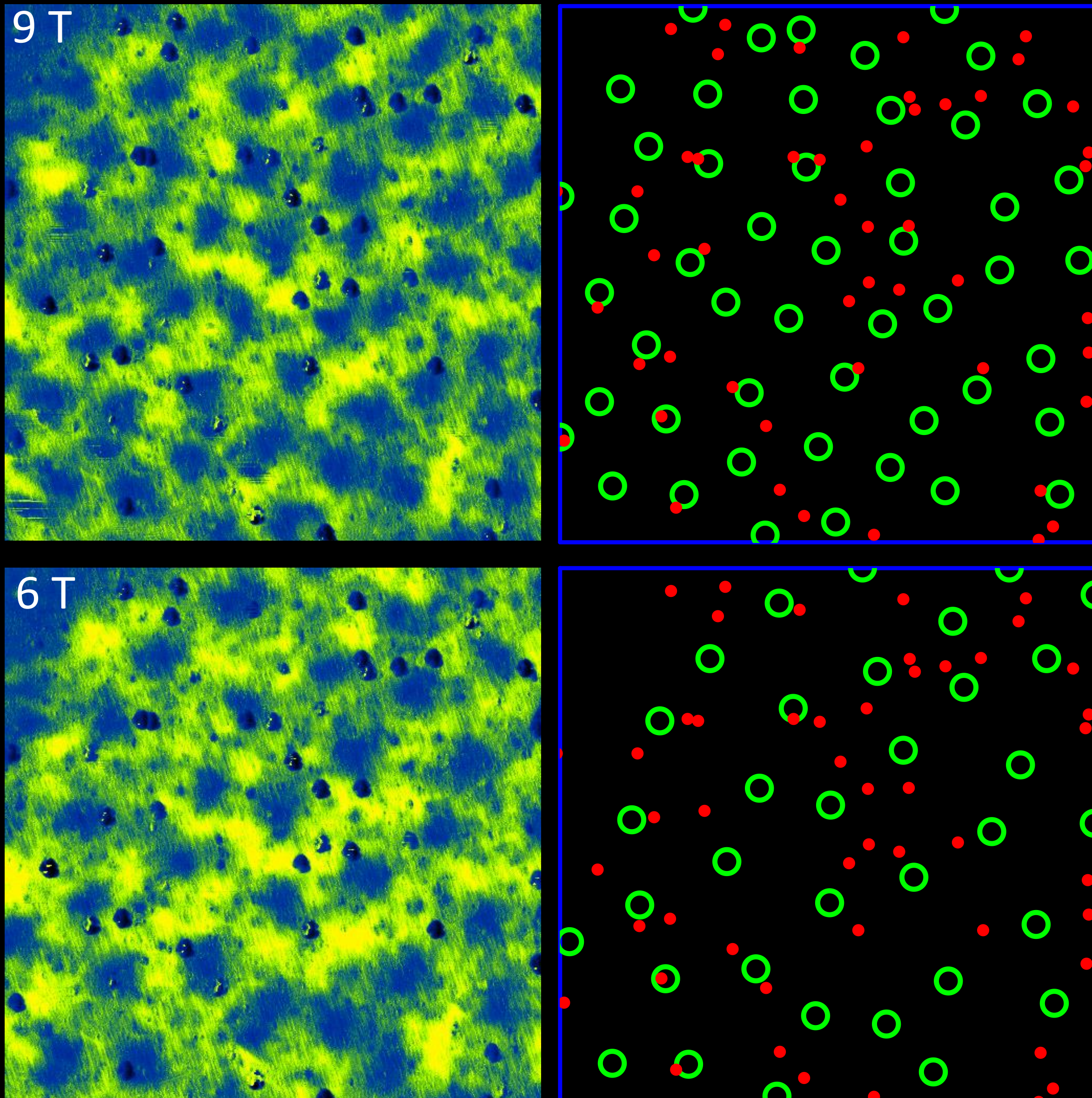

○ vortex, radius ξ_0 = 2.76 nm

• impurity

→Vortices are <u>not</u> pinned to visible surface impurities

Vortex pinning possibilities

(1) no strong pinners
inter-vortex forces dominate
→ lattice formation

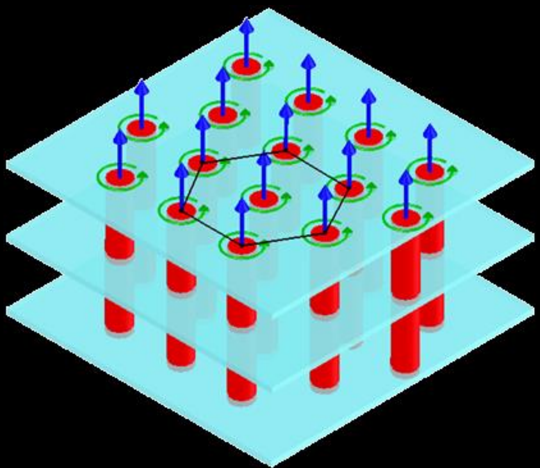

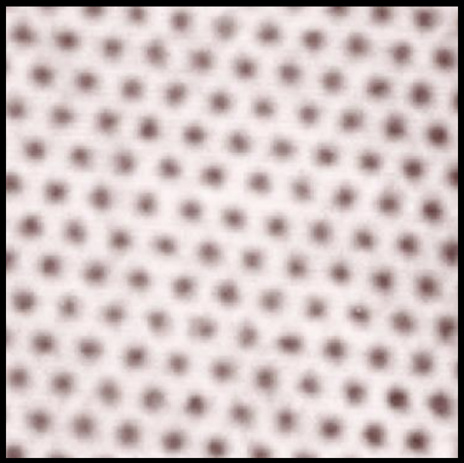

$NbSe_2$

(2) strong pinners exist
low anisotropy
→ vortices bend slightly
to accommodate pinners

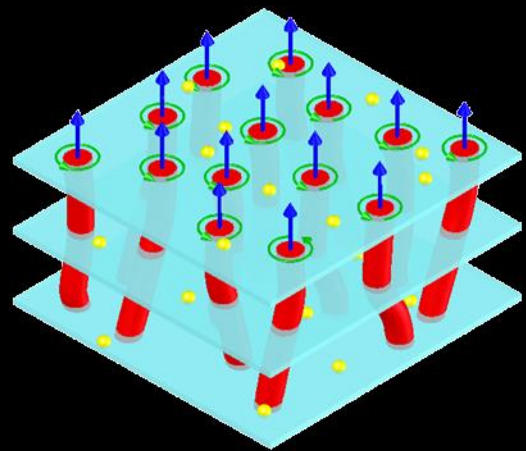

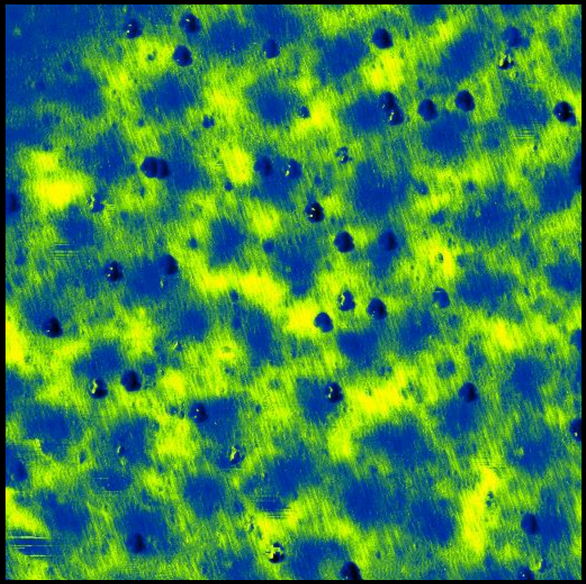

$Ba(Co_xFe_{1-x})_2As_2$

(3) strong pinners exist
high anisotropy
→ vortices pancake
each pancake pins independently

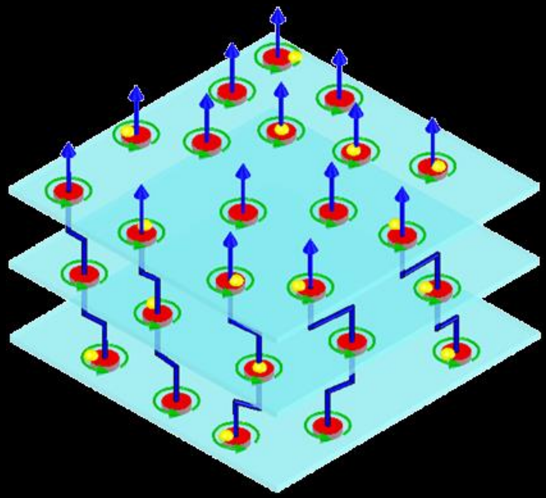

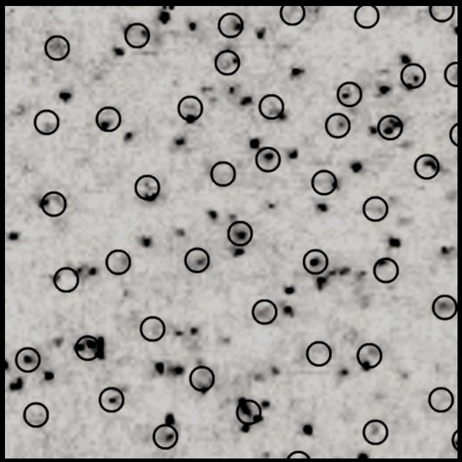

$Bi_2Sr_2CaCu_2O_8$

Next up: vortices as a window to the “normal” state…